# Sensorimotor hand representation following altered input




Daan Berend Wesselink

Balliol College

University of Oxford

A thesis submitted for the degree of

*Doctor of Philosophy*

Trinity 2019

# Sensorimotor hand representation following altered input

**Daan Berend Wesselink**

Trinity Term 2019 Balliol College

*A thesis submitted in partial fulfilment of the requirements of the University of Oxford for the degree of Doctor of Philosophy.*

## Thesis Abstract

This thesis investigates to what extent cortical representation of the human hand is affected by differences in tactile experience. Using functional magnetic resonance imaging as well as questionnaires, psychophysics and other imaging techniques, the included experiments aim to develop a better understanding of plasticity of the primary somatosensory cortex. In the first experiment, a diverse group of upper-limb amputees is shown to have maintained representation of their missing hand. As such, preservation of hand representation appears not to depend on continuous somatosensory inputs or even vivid phantom limb sensations. In contrast, congenital one-handers do not represent a hand they do not have. Together, this suggests hand representation is preserved in all amputees, but does require some prior hand experience. Then, congenitally blind individuals are shown to have typical hand representation in the primary somatosensory cortex. This suggests that the subtle differences in behaviour due to tactile skill acquisition (e.g. Braille reading) does not continue to shape low-level sensory areas in adulthood. In contrast, two individuals who have acquired starkly different limb behaviour from birth, professional foot painters, are shown to show different foot representation from controls. Unlike in controls, foot painters' S1 foot area contains organised toe clusters, marking the scope of early-life sensorimotor plasticity. Finally, the immediate effects of input loss are modelled using healthy controls who received a brief anaesthetic block of the afferent input from one digit. The rapid plasticity that was observed simultaneously with preservation of inter-digit relationships may help resolve apparent discrepancies between studies indicating sensorimotor representational change and long-term stability observed in amputees. Together, these studies stress the importance of early-life behaviour in shaping the primary somatosensory cortex and how later in life, the scope of sensorimotor plasticity is much more limited than previously thought.

*This thesis contains approximately 37,000 words*

# Acknowledgements

This thesis would not have existed without Tamar. Thanks for being embarrassingly generous with your praise and ruthlessly generous with criticism. I'll be forever grateful you took me into your lab from a place you probably still can't pronounce. It was a delight to be one of your first. You have shown me how to do science and I owe you so many drinks. I may even like dogs now.

Thanks to everyone who volunteered for the experiments in this thesis. You withstood blindfolds, injections, toe tickling, or jam-packed testing slots like champions. Many of you will never read this and could not be further removed from academia, which makes me even more grateful for your patience to help science.

A big thanks to Jörn Diedrichsen and Saad Jbabdi. You are true computational wizards. In your offices, I wish I could stay a student forever.

Fiona, I don't know how to thank you enough. In a long-past era, you introduced me to FMRIB and truly welcomed me. We should have seen you out. Thank god you're brilliant and a fighter. Now your projects are out, I hope you'll think of Oxford as the place we had a garden one summer. I will.

My grannies, thanks for always reminding me to bring a coat and turning every social event into a party. Sanne, thanks for being every poster session's good/bad cop to my bad/good cop. Please stop breaking everything. Harry, thanks for always having a floor for me and sticking it out until all our projects were finished. Please stop being from Brisbane.

Dinant, thanks for putting the glad in Gladstone and every time since. It was an honour going through all the real and fictional drama with you. Let there always be sequels, the Guardian and an abundance of pancakes.

Zeena, thanks for entertaining me when there's no internet, and when there is. You are nothing like a coconut.

Roni, thanks for starting together with me. You are generous beyond compare and a soldier in every good way. And obviously a scientist. I'm proud to have sat near your desk across the many moves.

Cats and Camels of Balliol, thanks for port and music, late night musings and making me wear a tie every now and then. How can so many amazing people belong to one small manor?

Plasticity Oxford, thanks for all your many great insights and hilarious lunches. You even welcome me back from afar. I hope we grow up to be the old guard together. Keep going wild!

Plasticity London, thanks for turning the big city into a small town. You've given me so much to cherish in very little time, the Holy moments and the ungodly ones. Keep the wheel turning!

Jeroen and Noa, thank you even though you're too far away. It is time you two meet. And past time for us to meet again, for that matter.

Papa, mama en de rest, bedankt voor alle steun en aanmoediging. De laatste loodjes waren anders niet gelukt. Al ga ik van ver naar verder weg, ik houd jullie dichtbij me. En ik kom terug.

And most importantly, my liefje Helen. You inspired me to finish every piece of work except for the most special of projects. As much as my late nights were fueled by your evenings, it's time for your days to be mine.

# Contents


**1 Introduction** **1**

1.1 Introduction . . . 2
1.2 Plasticity in the visual cortex . . . 3
1.3 Organisation in the somatosensory cortex . . . 6
1.3.1 Somatotopy . . . 6
1.3.2 Beyond somatotopy . . . 8
1.4 The sensorimotor system . . . 11
1.5 Plasticity in the somatosensory cortex . . . 13
1.5.1 Alternative development . . . 13
1.5.2 Reorganisation . . . 14
1.6 Aims of this thesis . . . 17

**2 General methodology** **20**

2.1 Introduction . . . 21
2.2 Univariate versus multivariate analysis . . . 21
2.2.1 Comparison between modalities . . . 23
2.3 Representational similarity analysis . . . 23
2.4 Visualisation . . . 25

**3 Acquired versus congenital hand-loss** **28**

3.1 Abstract . . . 29
3.2 Introduction . . . 29
3.3 Methods . . . 31
3.3.1 Participants . . . 31
3.3.2 Experimental procedures . . . 32
3.3.3 MRI acquisition . . . 36
3.3.4 MRI analysis . . . 36
3.3.5 Statistical analysis . . . 39

3.4 Results . . . 41
3.4.1 Acquired amputees . . . 41
3.4.2 Phantom sensations . . . 46
3.4.3 Congenital one-handers . . . 48
3.5 Discussion . . . 51

**4 Congenital blindness** **57**
4.1 Abstract . . . 58
4.2 Introduction . . . 59
4.3 Methods . . . 63
4.3.1 Participants . . . 63
4.3.2 Behavioural task & analysis . . . 64
4.3.3 fMRI task . . . 64
4.3.4 MRI acquisition, pre-processing, and low level analysis . . . 66
4.3.5 fMRI analysis . . . 69
4.3.6 Statistical analysis . . . 71
4.4 Results . . . 71
4.4.1 Increased tactile acuity in anophthalmic individuals . . . 71
4.4.2 Hand representations in S1 is similar in anophthalmic individuals and sighted controls . . . 72
4.4.3 Finger-specific information in the occipitotemporal cortex of anophthalmic individuals . . . 76
4.5 Discussion . . . 79

**5 Extreme foot behaviour** **86**
5.1 Abstract . . . 87
5.2 Introduction . . . 87
5.3 Methods . . . 89
5.3.1 Participants . . . 89
5.3.2 Experimental procedures . . . 89
5.3.3 MRI acquisition . . . 91
5.3.4 MRI analysis . . . 92
5.3.5 Behavioural analysis . . . 95
5.3.6 Statistical analysis . . . 98
5.4 Results . . . 99
5.4.1 Hand-like foot use in artists' daily life . . . 99
5.4.2 Somatotopic toe selectivity in artists but not controls . . . 100

5.4.3 Somatotopic toe overlap in artists but not controls . . . . . 101
5.4.4 'Hand-like' inter-toe activity patterns in the foot area of artists 101
5.4.5 Hand-like inter-toe activity patterns in the hand area of artists 106
5.4.6 Greater correlation between toe representation and toe kinematics in artists . . . . . 108
5.4.7 Enhanced tactile perception for the toes of artists . . . . . 109
5.5 Discussion . . . . . 110
5.5.1 Complexity in bodily experience . . . . . 110
5.5.2 Latent genetic template . . . . . 111
5.5.3 Bodily experience in the critical period . . . . . 112
5.5.4 Foot representation in the hand area . . . . . 113
5.5.5 Conclusions . . . . . 114

**6 Localised input loss** **116**
6.1 Abstract . . . . . 117
6.2 Introduction . . . . . 117
6.3 Methods . . . . . 118
6.3.1 Participants . . . . . 118
6.3.2 Experimental procedures . . . . . 119
6.3.3 MRI acquisition, pre-processing and low-level analysis . . . . . 122
6.3.4 fMRI analysis . . . . . 124
6.4 Preliminary Results & Discussion . . . . . 127

**7 Discussion** **132**
7.1 Overview . . . . . 133
7.2 Persistence and plasticity . . . . . 133
7.3 Spatiotemporal detail of representations . . . . . 136
7.4 Future directions . . . . . 138

**Personal contributions** **142**

**A Supplementary figures and tables** **143**

**References** **152**

# List of Figures


1.1 Somatotopy in the primary somatosensory cortex . . . . . 7

2.1 Overview of Representational Similarity Analysis . . . . . 26

3.1 Similar representation in primary somatosensory cortex (SI) for amputees' missing hand and controls' nondominant hand, but not for congenital one-handers' missing hand . . . . . 43
3.2 Similar representation in primary motor cortex (M1) for amputees' missing hand and controls' nondominant hand, but not for the congenital one-handers' missing hand. . . . . 45
3.3 Kinaesthetic sensations during individuated phantom hand movements in amputees correlate with typicality in the missing hand's primary somatosensory cortex (SI). . . . . 47
3.4 Similar ipsilateral hand representation in primary somatosensory cortex (SI) for amputees' and controls' intact hand. . . . . 50

4.1 Tactile thresholds in anophthalmic individuals and sighted controls . 72
4.2 Hand representation in primary somatosensory cortex (S1) . . . . . 75
4.3 Individual finger maps for sighted controls . . . . . 76
4.4 Hand representation in area hMT+ . . . . . 78

5.1 Validation of kinematic task performance . . . . . 96
5.2 Assessment of hand-like foot use in the artist; Questionnaires . . . . . 100
5.3 Toe maps in the foot area. . . . . 102
5.4 Individual toe maps in the foot area. . . . . 103
5.5 Whole brain toe activity in artists vs controls . . . . . 104
5.6 Toe activity patterns in the foot area, using representational similarity analysis. . . . . 105
5.7 Toe activity patterns in the hand area, using representational similarity analysis. . . . . 107

5.8 Assessment of hand-like foot use in the artist; Kinematics . . . . . 109

6.1 Experimental timeline . . . . . 119
6.2 Univariate analysis . . . . . 129
6.3 Global rescaling of hand representation in the SI hand area . . . . . 131

S1 Individual selectivity graphs in foot area . . . . . 149
S2 Stabilising foot representation . . . . . 150

# Chapter 1

# Introduction

## 1.1 Introduction

An orderly representation of the body and the world is essential for the brain's ability to store and read out information and perform computations efficiently. Brain areas in the sensorimotor system are rich with maps of our various body parts, activated during touch or movement. Although many ways of organising such body maps can be imagined, they are often remarkably similar from one person's brain to the next. A large question in the field is how such structured representations come about and how they remain stable. To what degree are we born with highly specific innate body representations versus loose frameworks that require fine-tuning and upkeep during our lifetime? To what degree does our brain use its ability to adapt when the maps it has developed no longer represent the body well? And if the brain frequently updates its representations based on input, what happens when that is dramatically altered?

In order to comment on the above questions, this thesis focuses on the primary somatosensory cortex, because it contains representations that are both detailed and easily accessible. Certain key concepts and phenomena, however, have been studied initially in the visual system. I will briefly these concepts focussing on plasticity in the early visual cortex, as a model for somatosensory plasticity. This will focus on visual processing, but altered sensorimotor representations in the occipitotemporal cortex due to blindness will be discussed in chapter 4. Next, because it is necessary to understand how the somatosensory brain typically manifests itself in order to see what changes, I will summarise our current understanding of the primary somatosensory cortex and, in humans, its hand area. Finally, I will review previous studies specifically examining the role of experience on the organisation of the somatosensory cortex.

## 1.2 Plasticity in the visual cortex

Wiesel and Hubel (1963) have been fundamental to the discovery of neural plasticity. They observed that neurons in the primary visual cortex (V1) of cats tend to favour one eye over the other, and that V1 can be separated into columns (perpendicular to the surface) in which neurons favour the same eye. Yet, when kittens were deprived of visual stimulation by being reared in darkness, these columns were much less segregated. Relatedly, depriving only one eye during the same early life period increased the preference for the non-deprived eye. Importantly, only early-life deprivation had such effects; no effects were seen for deprivation later in life. This research and work based on it (Wiesel & Hubel, 1965a; Shatz & Stryker, 1978; Hensch, 2005) delineated three periods in the development of organised representation: initial development, in which imprecise maps are formed mainly following genetic templates; the critical period, in which experience (in this case: visual input) fine-tunes the initial map; and adulthood. Although the on and offset of the critical period vary greatly between species, brain areas and domains (Hensch, 2004; Berardi et al., 2000), it is generally agreed sensory cortex of the mammalian brain does not stay equally liable to change in adulthood. It is a question of current debate for many brain areas whether adulthood sees no retuning at all or merely less than in the critical period. In this thesis, in order to emphasise the difference between these developmental stages, I will distinguish between two kinds of change: *alternative development* and *reorganisation*. They are respectively change during and after the critical period. For particular observations of representational variation, it may not yet be clear which process has caused it, i.e. whether it is alternative development or reorganisation, in which case more general terms such as *alternative representation* will be used. Furthermore, given our current understanding of genetics, it is often even difficult to tell whether alternative development is driven by a different genetic framework or different early life experience. In its broad sense, experience – ranging from sensory impressions

and motor behaviour to the specific biochemical makeup of the environment in which axonal growth cones, by chance, find themselves – explains only about 50% of phenotypic variation (Mitchell, 2018). For instance, the specific columnar organisation of the early visual cortex - often treated as subject-level variation - contains a genetic component as well, i.e. it is more similar between siblings than expected from chance (Kaschube et al., 2002). For this reason and others, I will not attempt to distinguish in this thesis between different drivers of alternative development, but focus on the dichotomy between alternative development and reorganisation. Finally, the term *plasticity* will be used as a general term, encompassing all forms of representational change, but also neural change that may not fundamentally affect tuning, e.g. gain changes in activity or differences in between-area functional connectivity (Kelly & Castellanos, 2014). As such, the original findings that ocular columns are less segregated following dark rearing, is an example of plasticity and alternative development, but not visual reorganisation per se.

Much research on visual reorganisation in humans focuses on topographic maps of the retina, hereafter: *retinotopy*. The term topography describes an organisation in which two stimuli that are near each other in one domain (e.g. space, frequency, temperature etc.) are represented by neural populations that are spatially similar in the brain. Although retinotopic maps may be a simplified depiction of the true representation of the visual field, they are a fruitful tool to study plasticity in the visual cortex  not in the least because they can be easily assessed in humans using fMRI (Dumoulin & Wandell, 2008). As the first cortical foothold of visual information, the primary visual cortex (area V1) exhibits clear retinotopy, as do many other visual areas. Retinotopy is typically measured by systematically stimulating the entire visual field, i.e. the entire retina, and consequently mapping the responses for each voxel in the region of interest (Dumoulin & Wandell, 2008). Because the receptive fields of neighbouring neurons are similar in retinotopic areas, the responses of each voxel

can be modelled as if it responds to light stimulation within a one single population receptive field: typically, a circular area at some location on the retina and with some width (Dumoulin & Wandell, 2008). Although the typical population receptive field may be too simplistic (Zuiderbaan et al., 2012), the approximation is good enough to map retinotopy in the visual cortex.

In the presence of localised eye damage, later in life, no information from the affected part of the retina is propagated to V1 any more. Retinotopy, however, does not appear to be disturbed. Although earlier reports have argued for cortical reorganisation on the basis of different maps for patients from controls (Baker, Peli, Knouf, & Kanwisher, 2005; Dilks, Serences, Rosenau, Yantis, & McCloskey, 2007; primarily receptive field size increases), the reported differences in the non-deprived territory appeared to be caused by no longer being able to stimulate the deprived territory. Baseler et al. (2011) showed that when they simulated a retinal lesion for controls by not stimulating a certain part of the visual field, the maps for these controls were no different from those with real damage (macular degeneration). Later, this was repeated for other kinds of abrupted input to the visual cortex (Haak et al., 2014). As it stands, there is little evidence for reorganisation of retinotopy, in adulthood. In contrast, reports of altered retinotopic representation in humans following congenital damage (Muckli et al., 2009; Reitsma et al., 2013), with atypical developmental conditions (Albinism; Hoffmann, Tolhurst, Moore, & Morland, 2003), and after hemispherectomy below the age of 4 (Haak et al., 2014; see also Levin, Dumoulin, Winawer, Dougherty, & Wandell, 2010) suggest that the window for plasticity in the early visual cortex is solidly confined to early childhood. This conclusion is supported by work with cats and non-human primates, with plenty of examples of alternative visual development (in the critical period), but no reorganisation (stability in adulthood; Yinon, Shemesh, Arda, Dobin, & Jaros, 1993; Smirnakis et al., 2005; Wandell & Smirnakis, 2009).

## 1.3 Organisation in the somatosensory cortex

### 1.3.1 Somatotopy

The first cortical terminal of the sensorimotor network is the primary somatosensory cortex (S1), located on the postcentral gyrus (see section 1.4 for an overview of the other brain areas in the sensorimotor network). Traditionally, S1 comprises of four Brodmann areas: 1, 2, 3a and 3b, each of which focus on various aspects of proprioceptive and tactile processing. Roughly speaking, areas 3b and 1, located on the posterior bank of the central sulcus, receive most inputs from the cutaneous skin, whereas areas 3a, at the fundus of the central sulcus, and area 2, on the anterior bank of the postcentral sulcus, largely process feedback from the muscle spindles. For touch experiments, one may be most interested in areas 3b and 1 (mainly responsive to cutaneous receptors, Kaas, 1993). Some have argued that areas 3a, 3b and 1 form the true low-level S1 (area 2 responds to more complex stimuli and can be seen as an intermediate relay station, Ruiz, Crespo, & Romo, 1995). Yet, because the areas are highly interconnected, are all recruited during a typical movement task and are difficult to delineate reliably using non-invasive methods, most fMRI studies treat all four areas as a singular area.

Akin to the retinotopic map in V1, each of the areas in S1 contains a somatotopic map, a topographic maps of the body. The map ranges from the feet at the dorsomedial end via the trunk and upper limbs to our face and internal organs on the ventrolateral end (see Figure 1.1A). Unlike the retinotopic map, the somatotopic map contains discontinuities (Recanzone, Merzenich, Jenkins, Grajski, & Dinse, 1992); most notably, the representation of the hand borders that of the upper face. The map is also heavily distorted in favour of areas of the skin that contain more mechanoreceptors (cortical magnification; Sur, Merzenich, & Kaas, 1980). For instance, the lips are represented by about as much cortical real estate as the entire

rest of the face. The hand is also amply represented: our heavily innervated fingertips are the closest the sensorimotor system may come to a fovea.

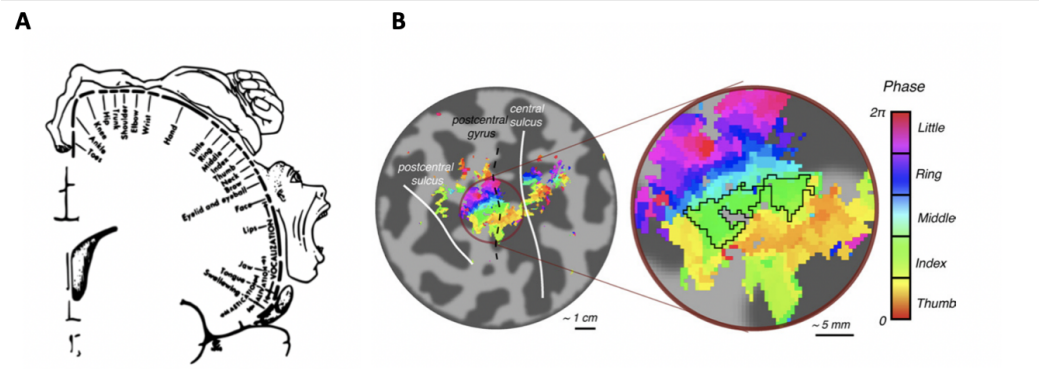



Figure 1.1: Somatotopy in the primary somatosensory cortex. A) The sensory homunculus in S1, coronal view. Adapted from Penfield & Boldrey (1937). B) Digit somatotopy within hand area, measured using fMRI, presented on inflated surface, sagittal view. Colours indicate preferred phase while stimulating each digit passively in a cycle. Adapted from Sanchez-Panchuelo et al. (2012).

The traditional account of the body map in S1 by Penfield and Boldrey (1937); Penfield and Rasmussen (1950) was acquired using invasive electrophysiology in human epilepsy patients. Following stimulation of a cortical site, participants would report where on the contralateral side of their body they felt a sensation. The downsides of this method (e.g. each site can only represent one body part, representations by signals too weak to induce a sensation are not recorded, subjective reports may be biased, and electrical stimulation was mainly limited to area 1) have since been mitigated by using many others methods to map S1. In particular, in the last two decades, the non-invasive methods magnetoencephalography (MEG) and fMRI have been applied extensively (Mogilner et al., 1993; Nakamura et al., 1998; Besle et al., 2013; Schellekens et al., 2018) to characterise body representation in S1.

The area devoted to the hand can be further separated into finger specific territories. As shown in figure 1.1B, the thumb tends to activate the most lateral part of the hand area and the little finger primarily the medial side. In the hand area, the separation between fingers is apparent, unlike that of the subcomponents of other

body part (e.g. toes of the feet or pectorals of the chest). The considerable chunk of cortex dedicated to the human hand makes the hand area a great model to study the questions of this thesis.

### 1.3.2 Beyond somatotopy

Although Penfield's map has formed the basis of our early understanding of the distribution of body parts along all of S1, the depiction may be too simplified, especially when focusing on the section that is selective for the hand. In this section, I will provide a more detailed description of hand representation.

The heterogeneous distribution of mechanoreceptors across the body plays a role in the cortical magnification of some body parts, but another factor may be involved. Body parts that are behaviourally more relevant may be additionally magnified. For instance, the most used module in the nose of the star-nosed mole appears to be over-represented (with respect to its size and receptor density; Catania, Leitch, & Gauthier, 2011). A classic study showed that monkeys who use their tail for object manipulation, have increased representation of the glabrous skin of their tail (Fulton & Dusser de Barenne, 1933). Rat species that use their whiskers to navigate near-space more show increased whisker representation (Campi & Krubitzer, 2010). It is currently an open question whether habitual behaviour plays a role in the cortical magnification of the human hand as well; other aspects of representation do seem to reflect human behavioural statistics (see below).

Although the cartoon in figure 1.1A gives the impression that the functional parcellation in the hand map is discrete, voxels in the hand area can be activated by stimulation of any digit. When discussing representation at a univariate level, we typically refer to clusters of digit selectivity, where activity to one digit is significantly higher than that to the average of the others, rather than significantly greater than that of any other digit individually. These results have been replicated invasively

in primates (Reed et al., 2008; Lipton et al., 2010). There is even evidence for multi-finger receptive fields (R. M. Friedman et al., 2008). This complication is important for the questions in this thesis, because of the types of plasticity it allows. If neighbouring digits under normal circumstances already activate a digit-selective cluster - but less strongly - input removal of the selected digit could in some cases be sufficient to unmask the representation of another digit and give the impression of reorganisation. If digit-selective clusters only represented one digit, reorganisation would be required. With multi-digit receptive fields, differences in gain and thresholding can be enough to produce certain digit maps.

While the traditional body map mainly describes how S1 is activated by the contralateral side of the body, the area also contains information about the ipsilateral side. This is particularly apparent during fMRI studies of movement. At the spatial resolution of fMRI, it appears as if the same neural populations are recruited during ipsilateral and contralateral movement, but during ipsilateral movement also S1 is simultaneously suppressed (Diedrichsen, Wiestler, & Krakauer, 2013; see chapter 3). Nevertheless, it is possible to decode which finger was moving from ipsilateral signals alone (Diedrichsen et al., 2013; Berlot et al., 2018). In other words, both sides of the body share one body map in each hemisphere's S1. This will be exploited in chapter 3.

A notable deviation from somatotopy is the double thumb. In some participants (e.g. see (Kikkert et al., 2016; Sanders et al., 2019)), the thumb also activates voxels medially to those that are responsive to the little finger. Consequently, there appear to be two thumb clusters, a medial and a lateral one. Although these instances could be peculiar examples of variability between individuals, a more succinct explanation is that offered by Ejaz, Hamada, and Diedrichsen (2015). They noticed that the spatial layout of finger-specific activity patterns was highly variable between individuals, but inter-digit relationships were not. Activity patterns for neighbouring digits were

more highly correlated than those of far removed digits in a manner that reflects the correlation structure of everyday finger behaviour. For example, the thumb activates S1's voxels more similarly to the little finger, than to the ring finger. This parallels daily behaviour in which thumb and little finger often coordinate. Participants whose digit map did not show a 'double thumb' showed a similar correlational structure. Apparently, these inter-digit relationships are instantiated in some individuals by the traditional somatotopic mediolateral gradient, but in others by split selectivity clusters for the thumb. Because examining the multivariate representational structure of hand representation has been productive, this thesis will examine exactly that aspect. The following paragraph will reason why this aspect is likely a good approximation of hand representation, even though a lot of information is not included (notably any absolute spatial information about the activity). The technical details about this method will be discussed in chapter 2.

In studying the complexity of biology, it is difficult to assess at which level of precision meaningful representation occurs. A key aim of cognitive neuroscientists is trying to understand how neural activity facilities interacting with and conveying information about the world. As such, 'meaningfulness, here, should be tied to behaviour and the outside world. Descriptions that are too abstracted, i.e. with low precision, do not capture meaningful variation between individuals' sensorimotor control and have little explanatory power. Conversely, descriptions of representations that are too low-level, i.e. with high precision, may include unessential fluctuations 'under the hood' that are unavoidable due to the stochastic nature of biological processes, not to mention measurement noise. Because each individual's brain is slightly different, even when their representations perform the same functions, some component of the brain organisation is best ignored. More specifically related to the hand map, although the multivariate inter-digit relationships, described above, are stable across individuals, there is much variance in the exact location of digit-selective clusters.

Apparently, for S1 to perform its functions adequately, hand representation needs to have some multivariate representational structure - constrained by genetics and/or, as will be argued in this thesis, behaviour - but the neuronal location is not further determined. In this thesis, we are looking at brain representations that afford movement and touch at the level of individual fingers. At the current level of precision, daily statistics of behaviour perform near the noise ceiling, i.e. inter-digit relationships in behaviour explain inter-digit relationship in neural representation virtually as well as one participant's neural representation informs the group average. Conversely, I will introduce other groups whose hand representations come nowhere close the noise ceiling: congenital one-handers, hand representation in the visual cortex of the congenitally blind, or stabilising foot representation around the hand knob of foot painters. Also, this RSA measure will be used to study missing hand representation of acquired amputees, which resulted in a range of values correlated with phantom kinaesthesia. As this measure has spanned the full range of values, from non-existent hand representation to similar to controls, and values in between, we are confident the RSA measure of hand representation, even though it is less detailed than technically feasible, has been sufficiently powerful and flexible to use as a diagnostic feature to study plasticity with.

## 1.4 The sensorimotor system

Body representation is not only present in S1, but, to varying degrees, in all areas of the sensorimotor network. The thalamic ventral posterior lateral nucleus channels the afferent inputs from the body to area 3b (Kaas, Merzenich, & Killackey, 1983; note that inputs from the face are relayed through the ventral posterior medial nucleus). It contains an even crisper body map than S1 (Song & Semework, 2015), but it is difficult to record from there non-invasively. In cortex, there are two principally

somatosensory higher-order areas: the secondary somatosensory area (S2) and the parietal central area (PV; Disbrow, Roberts, & Krubitzer, 2000). Both contain less precise somatotopic maps than S1 (L. Krubitzer et al., 1995; Disbrow et al., 2003) and the direction of the gradient is reversed (feet are represented the most medial). Area 1 and 2 additionally send signals to the posterior parietal areas 5 and 7, which play a role into multisensory coordination/integration, mostly with vision (Disbrow et al., 2003).

The other half of the sensorimotor system, the motor areas, also receives inputs from (and sends to) S1 (London & Miller, 2013). The primary motor area (M1), on the anterior bank of the central sulcus, has many bidirectional connections with S1, but pre-motor cortex, supplementary motor area (SMA), basal ganglia, cerebellum, and various areas in the midbrain all receive (direct or indirect) somatosensory inputs. Varying degrees of somatotopy have been shown in these areas, ranging from somewhat discernible finger maps in M1 (Raffin et al., 2015; Schellekens et al., 2018; L. Huber et al., 2019) and the cerebellum (Wiestler et al., 2011; van der Zwaag et al., 2013) to barely separated foot, hand and face separation in those further removed from S1 (Zeharia et al., 2015, 2019). The conflict between organisational principles (somatotopy versus behavioural similarity; described in section 1.3.2) seems to be won by the representation of movement in the motor areas. First of all, somatotopic maps are not consistently shown, leading some to argue that M1 body representation was not somatotopy is a poor model for the area (Graziano, 2016; Schieber & Hibbard, 1993)). The multivariate hand representation (inter-digit relationships; Ejaz et al., 2015) are stable, however, and in fact, similar to those in S1. The only difference in the multivariate representation of the fingers between S1 and M1 is that in the latter area, the fingers are less starkly separated. This suggest that, despite the debate regarding M1 somatotopy; at the behaviourally relevant level, both areas contain comparable representations. Such multivariate representations have not yet

been demonstrated in higher-order motor areas, but will be discussed in chapter 4.

The separation between somatosensory and motor areas are not as sharp as sometimes suggested. For instance, even low-level S1 has been reported to send output to the spinal cord (Rathelot et al., 2017) and M1 contains many neurons that respond to somatosensory stimulation (Meyer, 1987; Adams et al., 2013). Typical sensorimotor behaviour supposedly requires bidirectional interplay between S1 and M1 (Kleinfeld et al., 2006; Lee et al., 2008). On top of this, movement recruits a combination of peripheral receptors, encoding a range of somatosensory modalities (e.g. surface and deeper mechanoreceptors; proprioceptors), plus, according to some theorists, the predicted somatosensory outcomes from any motor command (corollary discharge; Sirigu et al., 1996; Wolpert & Ghahramani, 2000). Even the higher-order somatosensory areas in the posterior parietal cortex project to supplementary motor areas, presumably to influence object manipulation and navigation of the environment (Andersen et al., 1997). Hence, it is not surprising that representational principles are shared throughout the entire sensorimotor system.

## 1.5 Plasticity in the somatosensory cortex

### 1.5.1 Alternative development

Analogous to the work done in the 1970s in the visual cortex, the primary somatosensory cortex requires input to develop typical representations. Van der Loos and Woolsey (1973) showed this in mice. Typically, mice's S1 contains localised clusters, called barrels, that are selective for individual whiskers and visible in histologic sections. Mice whose whiskers were plucked at birth, did not have any clusters for missing whiskers.

At birth, the somatosensory cortex can adapt to certain body adaptations. For instance, people with fully functional polydactyly, i.e. more than 5 controllable digits

per hand, have dedicated muscles and nerves for their super-numerous digits. Recently, Mehring et al. (2019) demonstrated that the primary sensorimotor cortex, in this case, develops independent representation for a sixth digit as well.

### 1.5.2 Reorganisation

Under normal circumstances, as long as the sensory input patterns remain constant, body representations are stable in adults (Chen et al., 2005; Kolasinski, Makin, Jbabdi, et al., 2016). Initially, the adult somatosensory cortex was assumed to be generally immutable in adulthood. Since the 1980s, however, consensus of the field has shifted and now sensorimotor areas are generally believed to be highly plastic. Here, I will discuss a number of studies on adult hand representation in humans and non-human primates. For plasticity due to motor learning, see Ostry, Darainy, Mattar, Wong, and Gribble (2010). For rodent plasticity, see Glazewski, Chen, Silva, and Fox (1996); Wallace, Glazewski, Liming, and Fox (2001); Feldman and Brecht (2005).

Animals that habitually use a certain body part a lot typically develop enlarged representations for that body part, compared to evolutionary homologues of animals who don't (L. A. Krubitzer & Prescott, 2018). Interestingly, a similar phenomenon has been reported in fully developed adults. After stimulating specific fingers of various primates for a prolonged period (weeks to months), the representation of these fingers expands (W. M. Jenkins et al., 1990; Xerri et al., 1999; Recanzone, Merzenich, & Jenkins, 1992). Along those lines, Gindrat, Chytiris, Balerna, Rouiller, and Ghosh (2015) argued for an expanded representation for those digits that are used more often by mobile phone users.

The representations of multiple fingers can also merge (or become more similar) following synchronous stimulation. This has been demonstrated by simultaneously stimulating multiple fingers (X. Wang et al., 1995) or even by surgically fusing two fingers (Clark et al., 1988; Allard et al., 1991). These results have been taken as

evidence that substantial reorganisation occurs, i.e. receptive fields enlarge to cover multiple digits. Later, however, others have demonstrated that receptive fields in S1 can typically be responsive to multiple digits (Tommerdahl et al., 2010). This leaves open the possibility that these findings have been caused by a rapid adjustment in inhibition rather than stable reorganisation. For example, after the removal of one digit it may appear like reorganisation (other digits invading its space), but it could also be unmasking (the other digits had always been represented there). Whichever mechanism produces such plasticity should probably be rapid: Fingers that have been glued together for only 24 hours already demonstrate more similar representations than before Kolasinski, Makin, Jbabdi, et al. (2016).

The effects of input loss have also been reported on. Lissek et al. (2009) studied individuals who had their limbs immobilized for around six weeks (their arms were in a cast as a consequence of bone fracture). Following removal of the cast the subjects' tactile sensitivity of the fingers was lower than control subjects. The activity in S1 was also reduced. Similar findings had been found for the forepaw of rats (Coq & Xerri, 1999). In both studies, however, little evidence was found for reorganisation of S1 per se, as opposed to reduced recruitment, i.e. different use of the area that is otherwise not changed.

The most extreme form of deprivation is amputation. Following digit amputation in New World monkeys, Merzenich et al. (1984) showed that, within 2 months, the digits neighbouring the amputated digit start activating the deprived cortical region in S1. When the entire hand is missing, the deprived cortex has also been reported to be activated by other body parts, potentially those that are used to compensate for hand loss - both in humans (Makin, Cramer, et al., 2013; Philip & Frey, 2014; Hahamy & Makin, 2019) and non-human primates (Jain et al., 2008).

There have also been studies that have shown that suggest that after input loss due to amputation, sensory cortex does not lose its original function. Despite any

reorganisation that may have occurred, some part of the missing hand representation can be reactivated as if nothing has changed. After hand amputation, stimulation of the injured nerve reportedly induces somatosensory percepts coming from the hand (Tan et al., 2014; Dhillon et al., 2004; Ehrsson et al., 2008). Similarly, direct cortical stimulation of the somatosensory hand area can cause vivid sensations of the hand (Ojemann & Silbergeld, 1995). Some amputees can even instruct their missing limb to move, congruent with the experienced somatosensory percept (phantom sensations). By doing so, three human amputees with highly vivid phantom sensations have been shown to have unaltered representation for their missing hand (Kikkert et al., 2016).

In some cases, the somatosensory cortex can artificially be sent different inputs. After median nerve repair by means of reinnervation, the hand map (in either cortical or sub-cortical areas) typically needs to be readjusted, because axonal regrowth cannot be guided perfectly. Adult patient have less capacity for such plasticity, indicative by the recovery of hand sensibility: patient below 10 years old virtually regain healthy hand function, but this sharply declines with age (Lundborg & Rosén, 2001). After puberty, patients no longer regain typical tactile acuity. This demonstrates that the sensorimotor system is capable of functionally relevant reorganisation (at a young age), but it is still unclear whether S1 is affected or that remapping is confined to the brainstem (Jones & Pons, 1998). Relatedly, it is also not yet known whether people who have regained hand sensibility after nerve reinnervation maintain the original hand representation through any plasticity, or how to test that.

In sum, the current evidence in favour of plasticity in human participants is thinner than typically assumed (see Makin and Bensmaia (2017) for additional review). The issues with certain popular studies on amputees and blind individuals will be further discussed in chapter 3 and 4, respectfully. In another often cited study, Elbert, Pantev, Wienbruch, Rockstroh, and Taub (1995) reported expanded finger representation in S1 for musicians compared to controls, correlating to the age in which they

started playing. Yet, it is often cited incorrectly. The authors did not find significantly increased spatial distance between digit D1 and D5 nor any direct evidence for reorganisation. Instead, they found greater dipole strength (an MEG marker of neuronal activity) and, as the authors explain, consequently a shift of the dipole centre for both digits in medial direction. Even considering more lenient statistical standards at the time, the study may have suffered from MEGs poor localisation, a heterogeneous group of musicians (6 violinists, 2 cellists, and 1 guitarist) and no difference between digit D1 and D5 despite the fact that these digits' behaviour during play is starkly different. Because only two digits were tested, a recent fMRI study testing all 5 fingers of violinists provides a better picture (Ogawa et al., 2019). They found no apparent differences in representational structure, although average dissimilarity between digits was increased in musicians. The simplest explanation of the results of both studies is that the recruitment of S1, rather than its organisation per se, has changed in musicians. As will be shown in chapter 6, area-wide excitability can change in adulthood, but this does not require reorganisation per se. Similar refutations of often cited studies have recently been conducted on dystonia (Ejaz et al., 2016 vs Elbert et al., 1998; Butterworth et al., 2003) and stroke patients (Nijboer et al., 2017; Branscheidt et al., 2019 vs Liu & Rouiller, 1999), both reporting absent reorganisation. Given the relative difficulty of publishing null results, the actual number of findings indicating little sensorimotor reorganisation in adulthood may even be higher.

## 1.6 Aims of this thesis

The primary aim of this thesis is to develop a better understanding of plasticity of the primary somatosensory cortex. What is the role of behaviour at various stages of development in shaping the organisation and driving the reorganisation of the

somatosensory cortex?

First, in chapter 3, I will compare a diverse group of individuals with acquired hand loss, i.e. amputees, with individuals with congenital handlessness and two-handed controls. I will demonstrate that the representation of missing limb is preserved in S1 for amputees, some of whom have not had a hand in several decades. In contrast, I show that congenital one-handers do not have any representation in S1 for the hand they do not have. Using these starkly contrasting groups, I will comment on the role of early life experience in the formation and preservation of typical hand presentation.

In chapter 4, I will examine the hand representation of a set of expert hand users: three congenitally blind individuals with high tactile sensitivity. These individuals allow us look at how acquired tactile experience relates to brain plasticity, or a lack thereof, in two brain areas: a traditional sensory area that is developed in typically skilled individuals and 'novel territory' that is not recruited by the typically skilled. First, I will argue there is limited evidence for differences between the SI of ordinary controls and the highly skilled blind group, suggesting that the extent to which skill continues to shape low-level sensory areas in adulthood is limited. Secondly, I will show that finger movement recruits the occipitotemporal cortex in the blind, which is typically regarded a visual area in the sighted. Although I will present results in favour of cross-modal plasticity, I will argue that this cross-modal recruitment should not be interpreted as the formation of a de novo sensory area.

In chapter 5, I will discuss two individuals with high sensorimotor skill: foot artists. Both participants were born without either arm (congenital amelia) and have learned to use their feet for many tasks that are ordinarily performed with one's hands, including professional painting. Here, I will show that the foot area of the artists' S1 contains distinct representation of the toes, whereas these are lacking in SI of controls. In fact, the organisation of the artists' foot representation strongly resembles the organisation of hand representation as it's typically found in controls.

The results of this chapter suggest that the scope of early sensorimotor plasticity due to divergent behaviour may be greatest when behaviour occurs early in life and is in line with our evolutionary history.

Finally, in chapter 6, I will explore how plasticity may occur in humans after a brief (2 hr) pharmacological block of the afferent input from one digit of the hand. Here, I will demonstrate that even at this time scale, finger representation in S1 is affected by a change away from its typical input. I will show that, unlike what the current literature predicts, finger selectivity is reduced following anaesthesia across the entire hand area. This suggest the presence of a mechanism that can rapidly alter S1 recruitment following an extreme change in input, while inter-digit relationships are preserved.

As a whole, this thesis will stress the importance of early-life behaviour in shaping the primary somatosensory cortex and how later in life, the scope of sensorimotor plasticity is much more limited.

# Chapter 2

# General methodology

## 2.1 Introduction

One of the broader aims of this thesis, and perhaps cognitive neuroscience, is to link behaviour to brain organisation, specifically for the sensorimotor representation of hands. A technique that facilitates doing so is Representational Similarity Analysis (RSA). This is a multivariate analysis technique that can be applied to uncover the underlying structure in both behaviour and brain activity. Most promisingly, it gives the power to infer representational structure from fMRI data, rather than solely average activity levels. During the course of the research included in this thesis, the technique has become one of the state-of-the-art tools in functional MRI (Kriegeskorte et al., 2008).

Because all experimental chapters will discuss results produced using of this technique, this chapter will outline some background and considerations aimed to facilitate the interpretation of such results.

## 2.2 Univariate versus multivariate analysis

In traditional fMRI analysis, inference is done on the level of the individual voxel. After pre-processing to make the signal less noisy, an output statistic is calculated for each voxel. Although it is computationally light to treat each a single timeseries at a time, there are a number of downsides to consider. First, considerable post-hoc corrections are required to keep the false positives inherent to doing many and also non-independent tests under control. This is typically addressed in one of two ways. One could make it harder to find false positives by essentially raising the significance threshold in some manner or another, e.g. cluster correction or false discovery rate correction. These methods, although useful and used in this thesis, also increase false negatives. One could also cut their losses and only do inference on the average within a region of interest (ROI), but this constitutes a big loss in information. Essentially,

multivariate analysis works like an average, but instead of blindly averaging all voxels, another linear combination of voxels is found which is more informative.

More fundamentally, many representations in the brain that can be measured using fMRI are not captured on the level of individual voxels. Small but consistent tendencies in the distribution of activity patterns can be compounded by multivariate analysis, making it a powerful. There is even evidence to suggest that for many representations the location of a voxel is not important, but rather the collective behaviour of all voxels in an area (see chapter 7). Multivariate analysis can pick up on (some of) that.

The biggest downside of multivariate analysis compared to mass univariate tests is still the loss of information that comes with abstraction, although 'average activity' loses even more information. The spatial organisation of a representations substrate is completely ignored. The same representational structure can be brought about by a well sorted brain region where each voxels selectivity profile is similar to its neighbours as by a region in which the voxels (with the same tuning) are distributed randomly. Spatial information is discarded and the each voxel is simply treated as a column in a matrix. Evidently, the exact layout matters: spatial clustering of collaborating neurons saves energy, time and wiring costs; and downstream neurons are likely also better able to read out the output from neurons in close proximity. At the macroscale, the topographic organisation of sensory areas is apparent. However, as discussed in chapter 7, at some spatial scale, variability across people is the consequence of (random) developmental variation. When the representational structure is both stable across individuals and reflects kinematics/experience - as it appears to be for hand representation in the early sensorimotor cortex - the representational structure seems to be the right level of abstraction that is relevant for the models that we currently have of neural function. Also note that doing inference on the average of an ROI constitutes an even greater loss of information.

### 2.2.1 Comparison between modalities

Although these methods are introduced within the framework of fMRI analysis, representational similarity analysis can be done equally well with other types of data. The only requirement is that the conditions (.e.g. stimuli, movements, cognitive states etc.) can be assigned activity patterns that can be compared. It does not matter whether the dissimilarity between conditions is calculated based on fMRI voxels, single-cell electrophysiology, muscle kinematics or even perceptual judgments. As such, the analysis method is powerful when the aim is to compare neural representation and behaviour: both modalities would be difficult to compare directly, but the underlying representational structure (the RDM) that RSA unveils is in the same format and can be compared directly. The technique has also been proven useful to reduce variability in inter-individual and even inter-species comparisons (e.g. L. Wang, Uhrig, Jarraya, & Dehaene, 2015). The comparison between representations in different brain areas within the same person is also made easier by RSA.

## 2.3 Representational similarity analysis

Representational similarity analysis (RSA) measures how different the activity patterns across on entire region of interest are between conditions. Although the dissimilarity between two conditions can be insightful, RSA is especially useful when more than two conditions span a representational geometry.

There are two families of measures to calculate the difference: 1) correlational distances, where two patterns are more similar when they correlate more strongly (positively) and 2) Euclidean distances, where the difference would be the shortest distance between two conditions if they were points in a high-dimensional space in which each voxel is a dimension. The most important difference between these two families of measures is that correlations do not depend on the absolute strength of

the activity, whereas the latter does. Although both types of measures can be used to examine representational structures, in this thesis, only Euclidean distances have been used.

Specifically, we have used the cross-validated Mahalanobis distance (Nili et al., 2014). Whereas the ordinary Euclidean distance treats each voxel (read: dimension) equally - it is the squared root of the sum of squares - the Mahalanobis distance discounts voxel that are noisier. The idea behind this is that voxels that are activated differentially between conditions in a stable manner, it is particularly informative. More precisely, the activity patterns are divided by the covariance matrix of the residuals, such that each voxel is not only affected by its own noise but also by how that noise relates to the other voxels. Furthermore, our measure is cross-validated, which means it is calculated using multiple acquisition runs. Instead of squaring each voxel, we multiply values acquired in different runs:

$$d^2_{i,j,a,b} = (u_{j,a} - u_{i,a})^T \cdot \Sigma^{-1} \cdot (u_{j,b} - u_{i,b}) \tag{2.1}$$

where $d^2_{i,j,a,b}$ is the measure for a pair of conditions $(i, j)$ and a pair of runs $(a, b)$, $\Sigma$ is the estimated covariance matrix and $u_i, a$ the activity pattern for the $i^{\text{th}}$ condition in the $a^{\text{th}}$ run. This measure is averaged over all pairwise combinations of $n$ runs:

$$d^2_{i,j} = \frac{\sum_{a=1}^{n} \sum_{b=a+1}^{n} d^2_{i,j,a,b}}{\frac{1}{2} n(n-1)} \tag{2.2}$$

Finally, a square root that preserved the sign of the squared measure gives an unbiased estimate of the true distane between the activity patterns:

$$d_{i,j} = |d^2_{i,j}|^{\frac{1}{2}} \cdot sign(d^2_{i,j}) \tag{2.3}$$

Although the contribution of noise to a voxel's activity can be either positive or nega-

tive, its square is always positive. Assuming noise over voxels is independent between runs, multiplying noise factors from different runs, however, should still result, on average, in 0 added noise. As a consequence, when there truly is no difference between how two conditions are represented in a brain area, the expected dissimilarity value is 0 for the cross-validated Mahalanobis, but some value above 0 (depending on the noise) for the regular Mahalanobis distance. The former allows inference against 0. A downside of this option is that when the true dissimilarity is 0, some participant will have negative dissimilarity values. Because this is difficult to represent visually, negative values are treated as zero for visualisation (see below). They remain unchanged for any inference and statistics.

## 2.4 Visualisation

In order to visualise the RDMs more intuitively, classical multidimensional scaling (MDS) was used (Borg & Groenen, 2005). Because the dissimilarity between conditions is expressed as the Mahalanobis distance, a generalisation of the Euclidean distance, each condition can be assigned a location 'in space' such that the distances are equal to the Mahalanobis distance. Although theoretically an RDM with N conditions could require N-1 dimensions to be represented faithfully, often this dimensionality can be reduced without too much loss of data. The inter-digit representational structure of the hand is represented well by 2 dimensions (Ejaz et al., 2015). Since these dimensions are relatively arbitrary, they can either be informed by a principle component analysis, or by another pre-defined contrast. Because of this flexibility, one should always be mindful that the visualisation is an imperfection depiction of the data.

One consideration to make when visualising data is whether or not to remove the mean pattern. When interested in differences between conditions, the mean patterns

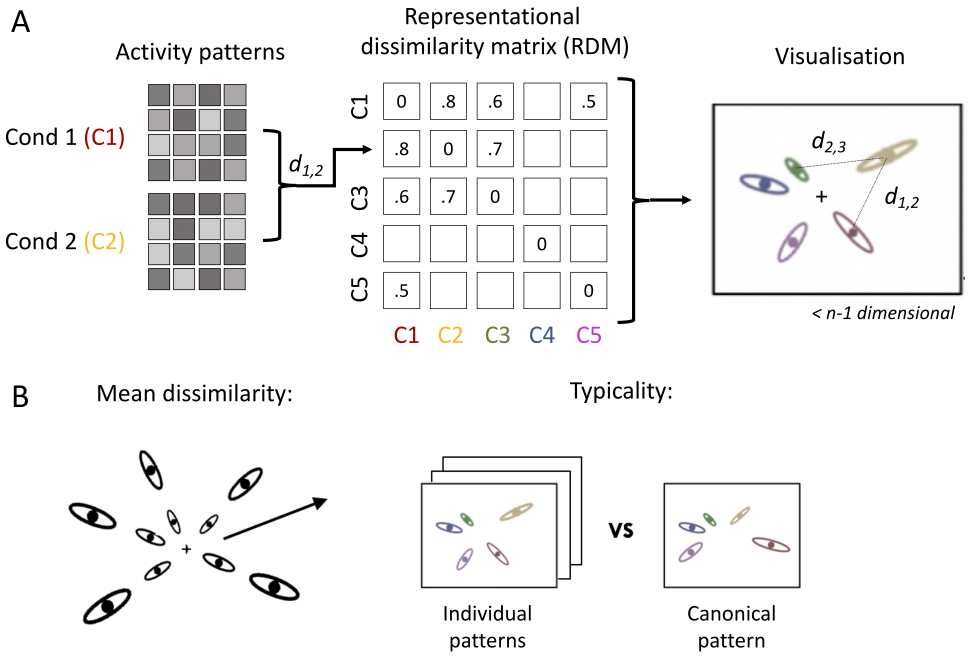



Figure 2.1: Overview of Representation Similarity Analysis. A) For each condition, activity patterns are estimated. By comparing the dissimilarity between each pair of conditions we fill a representational dissimilarity matrix (RDM). Note how the matrix is symmetrical across the diagonal (identical conditions), which is 0. On the basis of the RDM, a visualisation can be made in which each condition is placed such that the distances between conditions reflect the dissimilarity values in the RDM. Theoretically, this visualisation can have a dimensionality of n-1 (where n is the number of conditions), but in practice, this is much lower. For hand representation, 2D representations are relatively faithful (see main text). B) The two main measures that will be used in this thesis. Mean dissimilarity reflects amount of information encoded in the cortical activity, independent of condition. Typicality, an RDM's correlation with a canonical RDM, reflects the structure in which this information is encoded. Both measures are calculated on the RDM, rather than the visualisation.

is typically removed, so the average patterns is at the origin. Alternatively, when the mean pattern is not removed, the origin reflects rest. In certain cases, this can be informative if one is interested how certain conditions relate to rest.

# Chapter 3

# Acquired versus congenital hand-loss

This is adapted from: Wesselink, D.B.*, van den Heiligenberg, F.M.*, Ejaz, N., Dempsey-Jones, H., Cardinali, L., Tarall-Jozwiak, A., Diedrichsen, J. and Makin, T.R. (2019) Obtaining and maintaining cortical hand representation as evidenced from acquired and congenital handlessness. eLife, 8, p.e37227.

* Equal contribution

## Chapter contributions:

All analysis

## 3.1 Abstract

A key question in neuroscience is how cortical organisation relates to experience. Kikkert et al. (2016) previously showed that amputees experiencing highly vivid phantom sensations maintain cortical representation of their missing hand. Here, we examined the role of sensory hand experience on persistent hand representation by studying individuals with acquired and congenital hand loss. We used representational similarity analysis in primary somatosensory and motor cortex during missing and intact hand movements. We found that key aspects of acquired amputees' missing hand representation persisted, despite varying vividness of phantom sensations. In contrast, missing hand representation of congenital one-handers, who do not experience phantom sensations, was significantly reduced. Across acquired amputees, individuals' reported motor control over their phantom hand positively correlated with the extent to which their somatosensory hand representation was normally organised. We conclude that once cortical organisation is formed, it is remarkably persistent, despite long-term attenuation of peripheral signals.

## 3.2 Introduction

A fundamental organising principle in primary somatosensory cortex (SI) is somatotopic mapping, where adjacent body parts are represented more proximally on the cortical sheet than those further apart (Penfield & Rasmussen, 1950). In the cortical hand area, this topographic organising principle results in a detailed digit map (Kaas et al., 1979), where neighbouring digits on the hand are represented closer together on the neocortex than non-neighbouring digits, as can be shown with functional MRI (fMRI) (Kolasinski, Makin, Jbabdi, et al., 2016). More generally, cortical activity patterns for neighbouring fingers overlap more and are therefore more similar than non-neighbouring fingers, independent of the exact spatial arrangement of these pat-

terns (Ejaz et al., 2015). The representational structure (i.e. the relative dissimilarity of activity patterns for different movements) is thought to reflect the natural statistics of hand use over one's life course (Graziano & Aflalo, 2007; Overduin et al., 2012): Concurrent inputs to neighbouring digits will increase representational similarity (X. Wang et al., 1995), while greater individuation of inputs will induce greater representational dissimilarity (Ejaz et al., 2015). Some have even suggested that alterations of these inter-digit representational boundaries after the hand map has been formed, e.g. due to digit overuse, can disrupt (musician's dystonia; Elbert et al., 1998; but see Ejaz et al., 2016) or improve perception and action (tactile discrimination; Recanzone, Merzenich, & Jenkins, 1992; Pleger et al., 2003).

Kikkert et al. (2016) and others (Flesher et al., 2016; Bruurmijn et al., 2017; Serino et al., 2017) recently challenged the view that structured input from the periphery is required for preserving sensorimotor hand representation (Dempsey-Jones et al., 2016; see also Davis et al., 1998; Mercier, Reilly, Vargas, Aballea, & Sirigu, 2006; Garbarini, Bisio, Biggio, Pia, & Bove, 2018 for related brain stimulation and behavioural findings). We took advantage of a well-documented phenomenon whereby some amputees report being able to volitionally move their phantom hand, resulting in kinaesthetic phantom sensations (Henderson & Smyth, 1948). Phantom limb movements have been shown to elicit both central and peripheral motor signals that are different from those found during movement imagery (Reilly et al., 2006; Raffin, Giraux, & Reilly, 2012; Raffin, Mattout, et al., 2012; Makin, Scholz, et al., 2013). Using 7T imaging we explored whether three amputees experiencing exceptionally vivid phantom sensations maintained the canonical hand representation, exemplified by somatotopically organised representation of individual digits. We found that although digit selectivity was reduced, digit order and the extent of the missing hand maps in SI were similar to what is observed in controls.

Our previous findings demonstrate the stability of SI hand organisation despite

decades of amputation. It remains unknown, however, whether hand representation after amputation reflects phantom sensations, and as such only persists in individuals with highly vivid phantom sensations. Here, we asked whether persistent representation of a missing hand reflects an organisational principle in the sensorimotor cortex, and thus will even be observed in amputees with little phantom sensations. To address this question, we measured cortical hand representation in 18 acquired amputees with varying vividness of their phantom sensations (hereafter amputees). To test the idea that the development of a hand representation requires sensory experience, we also tested 13 individuals missing one hand from birth (due to congenital amelia; hereafter congenital one-handers). All participants underwent fMRI while performing a visually cued motor task involving individual digit movements (of both the missing hand and the intact hand). Activity patterns in the missing hand of SI and M1 were analysed using representational similarity analysis (Walther et al., 2016; Diedrichsen et al., 2016). We hypothesised that normal peripheral input is necessary to establish normal sensory hand representation, but not to maintain it.

## 3.3 Methods

### 3.3.1 Participants

We tested 18 acquired amputees with an average of 18 years since amputation (mean age: 50 ± 12; 8 left-handed; 4 female), 13 congenital one-handers (mean age: 46 ± 10; 4 left-handers; 6 female), and 12 two-handed control participants (mean age: 45 ± 15; 5 left-handers; 5 female). All amputees reported experiencing phantom sensations after amputation, but vividness of these sensations varied across participants at the time of the study mean chronic vividness score 58 ± 38 on a 0-100 scale, as assessed using questionnaires (Makin, Scholz, et al., 2013; Makin et al., 2015); see table 3.1 and section Questionnaires below for further details]. 3 participants in

the amputees group tested here also took part in our previous study (Kikkert et al., 2016). The congenital one-handers had never experienced any phantom sensations. In addition, we also recruited and excluded a further congenital one-hander (due to technical difficulties during data pre-processing) and two control participants (due to incomplete data collection and due to abnormal digit selectivity, i.e. more than 3 standard deviations from the mean). Recruitment was carried out in accordance with Oxford University's Medical Sciences inter-divisional research ethics committee (MS-IDREC-C2-2015-012). Informed consent and consent to publish was obtained in accordance with ethical standards set out by the Declaration of Helsinki. Control participants were recruited as to match the other two groups in term of age, gender and handedness (with respect to the intact hand). When possible, control participants were friends and family of the one-handed participants. All participants were compatible with local magnetic resonance imaging (MRI) safety guidelines.

### 3.3.2 Experimental procedures

The experimental procedures described in this manuscript were run as part of a larger study (the full study protocol can be found on https://osf.io/gmvua/). Here we focus on procedures related to the representation of the missing hand in amputees and congenital one-handers.

#### Questionnaires

To measure phantom sensations, as well as other demographic and clinical details of potential relevance to the missing hand representation, amputees and congenital one-handers completed a range of questionnaires (as summarised in table 3.1). Amputees rated intensities of phantom sensations, using a 0 - 100 scale, as experienced during the last week (or in a typical week involving such sensations). Chronic phantom sensation was calculated by dividing intensity by sensations frequency (1- all the

time; 2- daily; 3- weekly; 4- several times per month; and 5- once or less per month), as previously implemented (Makin, Scholz, et al., 2013; Makin et al., 2015). Having used this measure in multiple studies with partly overlapping participant pools (Makin, Scholz, et al., 2013; Kikkert et al., 2016; van den Heiligenberg et al., 2017), we can assess the consistency of this measure within participants and across studies (i.e. measure reliability). We found excellent inter-study consistency (intra-class correlation coefficient: 0.79, 95% CI: .48-.93, $F(13,13)=8.46$, $p<.001$), when considering all amputees that participated in at least one other study (n=14, earlier questionnaire taken 1-4 years before current study). In addition, participants reported the number of phantom digits that afford kinaesthetic sensations during volitional control of movements (kinaesthesia). This report was further validated by a demonstration of afforded phantom movements during the study's main task with the intact hand, as detailed below.

**MRI tasks**

All participants underwent one experimental session with four fMRI runs, using a block-design. The task involved individual digit-movement blocks for each of the five digits (12s blocks) of either hand, as well as no movement (rest) blocks. Each condition was repeated 3 times in a semi-counterbalanced order within each run. Each run comprised a different block order.

To probe somatosensory digit representation, we used a visually cued active (motor) task. In an intact sensorimotor system, movement recruits a combination of peripheral receptors, encoding a range of somatosensory modalities (e.g. surface and deeper mechanoreceptors; proprioceptors), as well as efferent information from the motor system. Using an active task, we have previously shown high consistency of SI digit topography across multiple scanning sessions (Kolasinski, Makin, Jbabdi, et al., 2016; see also Ejaz et al. (2015) for validation using RSA). Participants were

| AMP | Age (years) | Sex | Amputation | | | | Phantom sensations | | | | |
|---|---|---|---|---|---|---|---|---|---|---|---|
| | | | Side | Years since | Age at (years) | Level | Kin (0-5) | Viv (0-100) | Pain (0-100) | AViv (0-100) | APain (0-100) |
| Mean | 50.4 | | | 17.6 | 32.9 | | 3 | 58 | 46 | 65 | 21 |
| St. dev. | 12.1 | | | 10.4 | 11.8 | | 2 | 38 | 37 | 30 | 23 |
| A01 | 44 | M | R | 15 | 29 | 2 | 5 | 100 | 100 | 100 | 50 |
| A02 | 53 | M | L | 32 | 21 | 2 | 5 | 50 | 100 | 60 | 70 |
| A03 | 40 | M | L | 11 | 29 | 2 | 4 | 100 | 50 | 100 | 20 |
| A04 | 51 | M | L | 32 | 19 | 2 | 5 | 100 | 0 | 100 | 0 |
| A05 | 27 | F | R | 7 | 20 | 4 | 2 | 50 | 40 | 60 | 0 |
| A06 | 71 | M | R | 16 | 55 | 2 | 1 | 20 | 85 | 60 | 20 |
| A07 | 46 | M | R | 18 | 28 | 2 | 3 | 70 | 90 | 70 | 50 |
| A08 | 56 | M | L | 26 | 30 | 4 | 5 | 6 | 40 | 10 | 0 |
| A09 | 64 | M | L | 31 | 33 | 2 | 4 | 100 | 40 | 100 | 10 |
| A10 | 58 | M | L | 2 | 56 | 2 | 3 | 90 | 0 | 80 | 0 |
| A11 | 28 | M | L | 8 | 20 | 5 | 4 | 40 | 40 | 20 | 0 |
| A12 | 57 | M | R | 29 | 28 | 2 | 1 | 80 | 90 | 80 | 40 |
| A13 | 50 | F | L | 1 | 49 | 4 | 0 | 0 | 0 | 0 | 0 |
| A14 | 52 | M | R | 27 | 25 | 2 | 5 | 100 | 80 | 80 | 50 |
| A15 | 68 | M | R | 26 | 42 | 4 | 1 | 16 | 0 | 80 | 0 |
| A16 | 39 | F | R | 9 | 30 | 3 | 4 | 35 | 40 | 50 | 30 |
| A17 | 58 | M | L | 12 | 46 | 4 | 5 | 2 | 0 | 65 | 0 |
| A18 | 46 | F | L | 14 | 32 | 4 | 3 | 80 | 30 | 50 | 30 |

| CTR | Age (years) | Sex | ND hand |
|---|---|---|---|
| | | | Side |
| Mean | 45.3 | | |
| St. dev. | 14.9 | | |
| C01 | 29 | M | R |
| C02 | 24 | F | L |
| C03 | 47 | F | L |
| C04 | 39 | M | L |
| C05 | 32 | M | R |
| C06 | 53 | F | R |
| C07 | 38 | F | R |
| C08 | 67 | M | R |
| C09 | 42 | M | R |
| C10 | 41 | M | R |
| C11 | 69 | M | L |
| C12 | 63 | F | L |

| 1H | Age (years) | Sex | Missing hand | |
|---|---|---|---|---|
| | | | Side | Level |
| Mean | 45.7 | | | |
| St. dev. | 10.4 | | | |
| H01 | 41 | M | L | 4 |
| H02 | 37 | M | R | 4 |
| H03 | 31 | F | L | 4 |
| H04 | 60 | M | L | 4 |
| H05 | 39 | F | L | 4 |
| H06 | 54 | F | L | 4 |
| H07 | 34 | M | L | 4 |
| H08 | 63 | M | L | 4 |
| H09 | 44 | F | R | 4 |
| H10 | 55 | F | L | 4 |
| H11 | 46 | M | R | 4 |
| H12 | 37 | M | R | 4 |
| H13 | 53 | F | L | 4 |

Table 3.1: Summary demographic details and phantom sensations. Data is shown for amputees (AMP), controls (CTR) and congenital one-handers (1H). Congenital one-handers did not feel any phantom limb sensations. All controls have full kinaesthetic sensations. F: female, M: male. Side: side of missing hand; L: left, R: right. Amputation Level: 1: shoulder, 2: above elbow; 3: at elbow; 4: below elbow; 5: at wrist. Kin: Phantom limb kinaesthesia (number of independent controllable parts of the hand), Viv: Chronic phantom limb vividness (0: no sensation, 100: intact hand's vividness), Pain: Chronic phantom limb pain (0: no pain, 100: worst pain imaginable), AViv/APain: Acute Viv/Pain (on the scanning day), Std: standard deviation, ND: nondominant.

presented with five vertical bars, corresponding to the five digits, shown on a visual display projected into the scanner bore. To cue the participant which digit should be moved, the bar corresponding to this digit changed (i.e. by flashing in a different colour).

On 'missing hand blocks', participants were instructed to perform individual digit movements (1 Hz) with their nondominant (controls), phantom (amputees), or missing hand (congenital one-handers). Handless individuals were instructed to attempt performing actual movements with the digits of their missing hand, even when not being able to feel their digits, rather than using motor imagery. Controls moved their nondominant hand digits in mid-air. To ensure good understanding of these instructions, outside the scanner, the amputees were asked to demonstrate to the experimenter the extent of volitional movement they felt they were able to carry out in each of their phantom digits, by mirroring each movement onto their intact hand.

On 'intact hand blocks', all participants performed a comparable task with their intact/dominant hand by exerting force on a button box. Participants received real-time visual feedback of how much force each digit exerted by means of moving vertical bars on 'intact hand blocks', but not on 'missing hand blocks'. The dominant hand of controls was paired up with the intact hand because, through intensive use, amputees' and congenital one-handers' intact hand becomes their de facto dominant hand (Philip and Frey, 2014). All groups were able to carry this task equally well, as verified in post-hoc analysis: each trial was assigned to the digit whose force output correlated most strongly with the instructed time course and the percentage of correctly performed trials, i.e. trials that were assigned to the instructed digit, was not different between, congenital one-handers and amputees (74.2%, $t(29)=1.13$, $p=.266$), or between congenital one-handers (81.1%) and controls (75.3%; $t(23)=.93$, $p=.362$). This behaviour brought forth high representational typicality in intact SI for all three groups (controls: $rho=.85$; amputees: $rho=.81$; and congenital one-handers: $rho=.89$;

group comparisons all p's > .11).

### 3.3.3 MRI acquisition

MRI images were acquired using a 3T MAGNETON Prisma MRI scanner (Siemens, Erlangen, Germany) with a 32-channel head coil. Functional images were collected using a multiband T2*-weighted pulse sequence with a between-slice acceleration factor of 4 and no in-slice acceleration. This provided the opportunity to acquire data with high spatial (2mm isotropic) and temporal (TR: 1500ms) resolution, covering the entire brain. The following acquisition parameters were used: TE: 32.40ms; flip angle: 75, 72 transversal slices. Field maps were acquired for field unwarping. A T1-weighted sequence was used to acquire an anatomical image (TR: 1900 ms, TE: 3.97 ms, flip angle: 8, spatial resolution: 1 mm isotropic).

### 3.3.4 MRI analysis

MRI analysis was implemented using tools from FSL, SPM and Connectome Workbench software (Smith et al., 2004; Jenkinson, Beckmann, Behrens, Woolrich, & Smith, 2012, fsl.fmrib.ox.ac.uk/fsl, fil.ion.ucl.ac.uk/spm, and humanconnectome.org) in combination with other Matlab scripts (version R2016a), both developed in-house (D. Wesselink et al., 2018) and as part of the RSA Toolbox (Nili et al., 2014). Cortical surface reconstructions were produced using FreeSurfer ((Dale et al., 1999; Fischl et al., 2008), freesurfer.net).

#### fMRI pre-processing

Functional data was first pre-processed in FSL 5.0. The following steps were included: Motion correction using MCFLIRT (Jenkinson et al., 2002), brain extraction using BET (Smith, 2002), and high pass temporal filtering with a cut-off of 100s. Co-registration to each individual anatomical T1 scan was accomplished using

FLIRT and, where needed, manual adjustments were performed to ensure precise co-registration around the hand knob of the central sulcus.

Anatomical T1 images were used to reconstruct the pial and white-grey matter surfaces using Freesurfer. Surface co-registration across hemispheres and participants was done using spherical alignment. Individual surfaces were nonlinearly fitted to a template surface, first in terms of the sulcal depth map, and then in terms of the local curvature, resulting in a nearly perfect overlap of the fundus of the central sulcus across participants (Fischl et al., 2008).

### Regions of Interest (ROI) definition

Since the focus of the study was on persistent sensory representation, our main analysis was restricted to the individualised hand-selective ROIs in SI. Further analysis was focused on the M1 hand areas. The ROIs were always in the hemisphere contralateral to the missing/nondominant hand. The anatomical ROIs were defined on the group surface using probabilistic cytotectonic maps aligned to the average surface (see Wiestler & Diedrichsen, 2013). These regions were then projected into the individual brains via the reconstructed individual anatomical surfaces. For the hand area of SI, we selected all surface nodes with the highest probability for any of BA 3a, 3b, 1, and 2 surrounding the anatomical hand knob (Yousry et al., 1997). The hand area of M1 was selected similarly using BA 4. We note that given the probabilistic nature of these masks, the dissociation between SI and M1 is only an estimate. For one acquired amputee, surface alignment failed; for this subject, the ROIs were drawn manually within the surface ribbon using the above anatomical definitions. The ROIs were not significantly different in size across groups (one-way ANOVA on area volume: SI: $F=1.27$, $p=.29$; M1: $F=1.37$, $p=.27$). In addition, for control purposes, we also used an ROI of visual area V5 which we defined anatomically, based on the parameters previously published by Wiestler and Diedrichsen (2013). The ROI was constructed

bilaterally and RSA outcome measures were averaged across both hemispheres.

### fMRI analysis

Voxel-wise General Linear Model (GLM) analysis was carried out, as implemented in SPM12. In brief, each of the experimental conditions was modelled for each run separately against rest. Regressors were created by convolving stimulus presentation (as a boxcar function) with a double-gamma hemodynamic response function (HRF). In the GLM estimation, the functional data was weighted using the robust Weighted Least Squares approach (Diedrichsen & Shadmehr, 2005), which estimates the heteroscedasticity of the time series and then soft-excludes noisy image volumes (e.g. due to movement). Task-related activity was quantified by averaging the BOLD response, averaged across all digits, versus baseline within each ROI. The voxel-wise parameter estimates (hereafter: activity patterns) and residuals from this analysis were also used to calculate the dissimilarity, as detailed below.

The dissimilarity between activity patterns within each ROI was measured for each digit pair using the cross-validated squared Mahalanobis distance, or crossnobis distance (Nili et al., 2014). We calculated the distances using each possible pair of imaging runs and then averaged the resulting distances. Before estimating the dissimilarity for each digit pair, the activity patterns were pre-whitened using the residuals from the GLM. Due to cross-validation, the expected value of the distance is zero (but can go below 0) if two patterns are not statistically different from each other, and larger than zero if there is differentiation between the digits of the hand.

We extracted two measures from the resulting inter-digit representational dissimilarly matrix (RDM). As a measure of strength of the representation, we used the mean dissimilarity, the average dissimilarity between the ten unique digit pairs (excluding the diagonal). The typicality of the representational structure was assessed by calculating the Spearman's rho correlation between the measured RDM and the

average RDM of the dominant hand of two-handed controls (independently acquired; see below). Because the representational structure can be related to behavioural aspects of hand use and is highly invariant in controls (average correlation r = 0.9, Ejaz et al., 2015), this measure serves as a proxy for how normal the hand representation is. Being able to study this measure was a main reason for using RSA in this study.

As an aid to visualise the RDMs, we also used classical multidimensional scaling (MDS). MDS projects the higher-dimensional RDM into a lower-dimensional space, while preserving the inter-digit dissimilarity values as well as possible (Borg & Groenen, 2005). MDS was performed on data from individual participants and averaged after Procrustes alignment to remove arbitrary rotation induced by MDS. Note that MDS is presented for intuitive visualisation purposes only, and was not used for statistical analysis.

As mentioned above, to determine typicality we correlated RDM from the current study with the average representational structure of the dominant hand of two-handed controls, in an independently acquired cohort of participants. The full details of the acquisition parameters are described at osf.io/d9g3t. In short, 8 two-handed participants performed an active digit tapping task using a button box (4 repetitions per digit of 8s blocks of 1 Hz single-digit presses), without online visual feedback. The data was acquired at 7T (TR: 2000 ms, TE: 25 ms, voxel size: 1x1x1 mm). The ROI was defined similarly to the SI ROI used in the current study.

### 3.3.5 Statistical analysis

Statistics were calculated using Matlab R2016a. Subsequent to normality validation (using the Shapiro-Wilk test), we used paired/independent-sample two-tailed Student's t-tests to compare activity levels and distance measures within/between groups, and one-sample t-tests to compare group measures to zero. Correlations were calculated as Spearman's rho. Partial correlation effects were calculated using linear

regression. For the main analysis concerning RSA, within each ROI group t-tests were adjusted to 3 comparisons, using the Bonferroni correction (=.05/3), to account for the 3 inter-group comparisons. Post-hoc correlations between SI typicality and key clinical measurements (phantom sensations, phantom kinaesthesia and time since amputation) were also corrected for 3 comparisons (=.05/3). One post-hoc comparison involving a small subset of amputees was done using a Mann-Whitney U test (see p. 8). For the control analysis, involving visual and somatosensory ROIs, we also used a mixed-design analysis of variance (ANOVA) to identify interactions across groups and ROIs.

In order to assess whether any aspect of the representational structure in the amputees was not different from that in controls, we used Bayesian statistics as implemented in Javascript (Dienes, 2014). Our alternative hypothesis is that amputees have no preserved hand representation. To construct our prior (i.e. to quantify the effect of having hand representation) we calculated the effect size of controls' nondominant hand representation vs. congenital one-handers missing hand representation. We then compared the effect size of amputees' missing hand representation (compared to controls) against that prior. More specifically, our alternative hypothesis assumes an effect size following a one-tailed t-distribution centred at 0 and a width of the difference between congenital one-handers and controls. The measured difference between amputees and controls (also modelled as a t-distribution) are tested against this hypothesis. Support for the null hypothesis was interpreted as supporting preserved hand representation. While it is generally agreed that it is difficult to establish a cut-off for what consists sufficient evidence, we used the threshold of BF$<$1/3 as positive evidence in support of the null, consistent with others in the field regarding this threshold as providing substantial evidence (Wetzels et al., 2011; Dienes, 2014). Note, however, that this threshold is not considered as providing strong evidence by all accounts (Kass & Raftery, 1995).

In order to gauge which aspects of phantom sensation and key demographics may relate to the amputees' representational structure's typicality, we performed an exploratory forward stepwise regression. The dependent variable was S1 typicality in amputees. The following factors were used as independent variables (see also table 3.1): typicality of the intact hand (rho; calculated from the intact hand SI area; time since amputation (in years); age at amputation (in years); vividness of non-painful phantom sensations, as experienced during the study (on a 0-100 scale) and chronically (accounting for both intensity and frequency; Makin, Scholz, et al., 2013); intensity of phantom limb pain, as experienced acutely during the study, and chronically (as detailed for nonpainful sensations). Only linear factors were considered, i.e. no interaction terms, and the criterion for inclusion was an increase in $R^2 > 0.1$. As a large number of predictor variables were included in the model and stepwise regression is generally only recommended for exploratory analysis, we aimed to establish internal replicability using bootstrap resampling (e.g. Thompson, 1995). In particular, we randomly sampled (with replacement) the full data matrix and repeated the stepwise regression 1000 times. We subsequently computed the proportion of bootstrap samples in which each factor was included in the final model, as well as confidence bounds on the model's adjusted $R^2$. We interpreted high proportion of inclusion ($p>.75$) as evidence for internal replicability (e.g. Thompson, 1995).

## 3.4 Results

### 3.4.1 Acquired amputees

We first focused our analysis on the representation of the missing hand, as revealed by instructing individuals to move individual digits of their missing hand (or non-dominant hand in controls). We interrogated fMRI activity in the SI hand area contralateral to the missing/nondominant hand (see Materials and methods for re-

gions of interest (ROI) definition). We examined univariate task-related activity, as quantified by averaging the BOLD response across all the digit conditions within the missing hand ROIs (Figure 3.1A, see Figure 3.2 for M1 ROI results). Overall, all participants, including congenital one-handers, were able to engage the missing/nondominant hand area to some degree. Although activity was reduced in SI for the congenital one-handers' missing hand compared to controls ($t(23)=3.5$, $p=.002$), activity was significantly greater than baseline ($t(12)=2.6$, $p=.02$).

To investigate digit discriminability in the hand area, we next estimated the dissimilarity between activity patterns for individual digit movements, measured using the cross-validated Mahalanobis distance (Nili et al., 2014). By comparing all possible pairs of digit-specific activity patterns, we obtained the representational structure (Figure 3.1D-E). The resulting inter-digit dissimilarity values were averaged across digit pairs and participants within each group (Figure 3.1B). Small inter-digit dissimilarity indicates that voxels in the hand area are similarly activated across individual digits; larger dissimilarity implies individuated digit representation. In amputees, mean dissimilarity was slightly, though inconclusively, reduced compared to controls ($t(28)=1.13$, $p=.27$, $BF=.772$), but significantly greater than in congenital one-handers ($t(29)=3.54$, $p=.001$). Congenital one-handers showed no differentiation between digits of their missing hand (mean dissimilarity not different from 0; $t(12)=.73$, $p=.48$) and dissimilarity was significantly reduced compared to controls ($t(23)=4.86$, $p<.001$).

While the extent of discriminability is greater in amputees than congenital one-handers, it is possible that the pattern of individuated digit activity is atypical in amputees. To determine whether the inter-digit organisation of a missing hand is normal, we next studied the representational structure's typicality, i.e. the correlation of the representational dissimilarly matrix (RDM) with a dataset of hand RDMs in 2-handed controls drawn from a different study (Chapter 4; see Figure 3.1C and Ma-

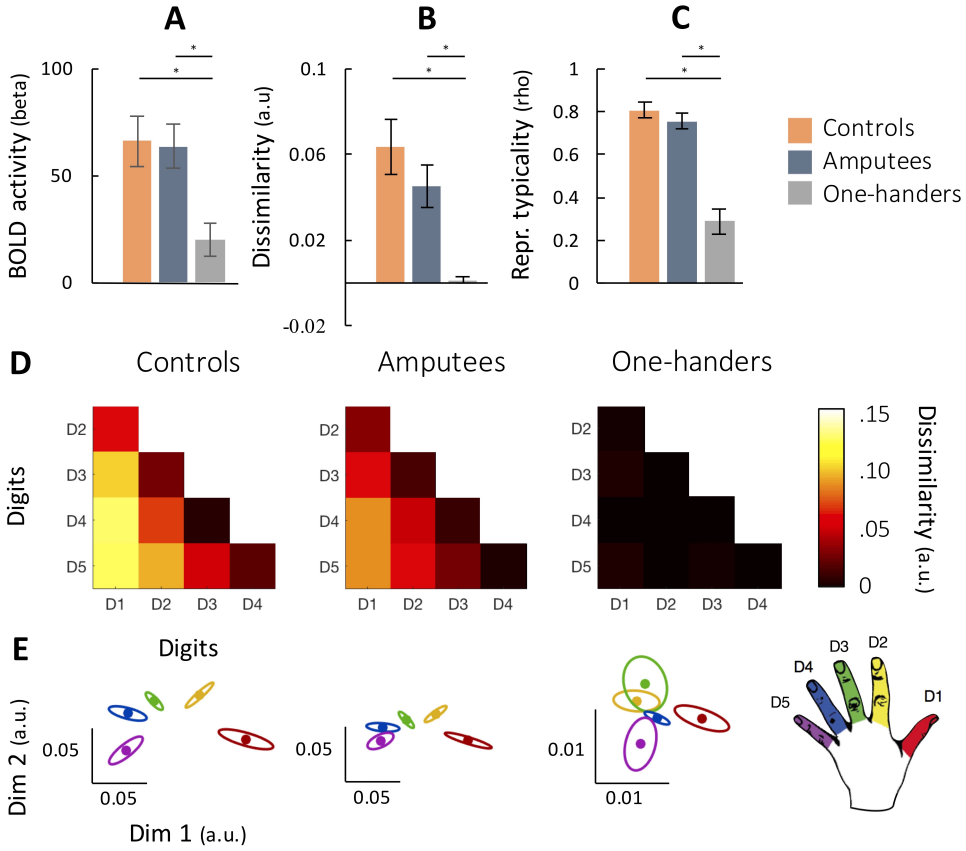



Figure 3.1: Similar representation in primary somatosensory cortex (SI) for amputees' missing hand and controls' nondominant hand, but not for congenital one-handers' missing hand. A Activity (averaged digit movement versus rest) in SI for amputees (n=18), two-handed controls (n=12), and congenital one-handers (n=13). B-C Mean dissimilarity and typicality of the representational structure of contralateral SI activity for the three groups. D Representational dissimilarity matrix for the three groups. D1-D5 correspond to the five digits (thumb-little finger). E Two-dimensional projection of the representational structure (D) (using multi-dimensional scaling; note that this is included for visualisation purposes only and was not used for statistical analysis). Dissimilarity is reflected by distance in the two dimensions; individual digits are reflected by different colours (see colour key, bottom right); and ellipses reflect the between-subject standard error after Procrustes alignment. Please note the different scale for one-handers compared to amputees and controls. Abbreviations: a.u.: arbitrary unit; *: significant difference, after accounting for multiple comparisons.

terials and methods). In amputees, on average, typicality was high (rho=.75) and was not significantly different from controls (t(28)=.991, p=.33, BF=.128). Hence, the organisation of digit representation after hand-loss remained statistically unchanged, after an average of 18 years of handlessness. As expected, congenital one-handers' missing hand representation did not correlate with a normal hand pattern, reflected in diminished representational typicality (mean rho=.29) compared to both controls (t(23)=5.86, p<.001) and amputees (t(29)=6.09, p<.001).

The results in M1 were generally in line with our findings in SI, but, as expected (Ejaz et al., 2015; Bruurmijn et al., 2017), digit individuation was weaker (see Figure 3.2). Univariate activity in congenital one-handers' M1 was not significantly reduced compared to controls (t(23)=2.00, p=.058) and greater than baseline (t(12)=4.60, p=.001). Congenital one-handers showed significantly lower dissimilarly compared to controls (t(23)=.4.23, p<.001). In amputees, mean dissimilarity was slightly reduced compared to controls, but these differences were not significant (t(28)=.53, p=.60, BF=.325). Typicality was also significantly lower in congenital one-handers than in either controls (t(23)=3.42, p=.002) or amputees (t(29)=3.50, p=.002), while the latter groups were not different from each other (t(28)=.11, p=.91, BF=.253).

Although the inter-digit representational structure of congenital one-handers is atypical with respect to canonical hand representation, it is possible that it is still consistent within participants. To explore this idea, we split individual participants' data to odd and even scans. For each participant, we calculated an RDM in the missing/nondominant hand area using the odd and even runs, and correlated the two RDMs. The correlation between odd and even RDMs was significantly lower in congenital one-handers (rho=-.02) compared to both amputees (rho=.41; $p_{1H\text{-}AMP}$=.001) and controls (rho=.52; $p_{1H\text{-}CTR}$=.001). We note that by splitting the data we are reducing the effectiveness of our analysis. Nevertheless, the relative reduction in split-half consistency indicates that there is no strongly consistent digit information

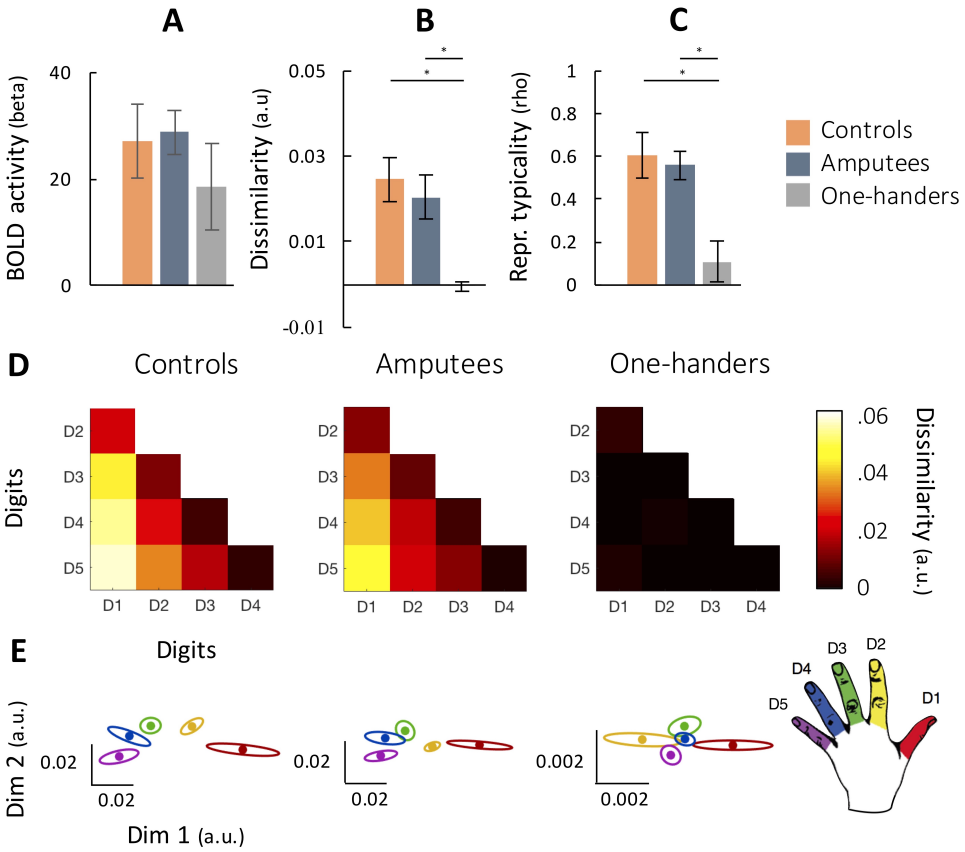



Figure 3.2: Similar representation in primary motor cortex (M1) for amputees' missing hand and controls' nondominant hand, but not for the congenital one-handers' missing hand. All annotations are detailed in Figure 3.1.

in the missing hand area of congenital one-handers during this task.

### 3.4.2 Phantom sensations

Next, we evaluated whether the consistency of hand representation in SI during missing hand movements correlates with amputees' subjective reports of phantom sensations. We first carried out an exploratory forward stepwise regression with typicality as the dependent variable. The following factors were tested as independent variables: kinaesthesia of phantom sensations - the number of phantom digits perceived as independently moving during the phantom movement task; vividness of non-painful phantom sensations as experienced both during the study and chronically; intensity of phantom limb pain, as experienced both acutely during the study and chronically; time since amputation; age at amputation and typicality of the intact hand (calculated from the intact hand SI area). The final model ($F=19.9$, $p<.001$, adjusted $R^2=.645$ included only kinaesthesia of phantom sensations ($\beta=.07$, $t=4.46$, $p<.001$) and the intercept ($\beta=.52$, $t=8.89$, $p<.001$). This regression was submitted to a bootstrapping analysis, allowing us to estimate the consistency of the final model (see Materials and Methods). This bootstrapping analysis returned kinaesthesia as the final variable in .963% of the iterations (final model fit: median adjusted $R^2=.645$; 95% CI: .30-.99). The proportion of the other included factors in the final model was: typicality of the intact hand (7.0%); time since amputation (9.5%); age at amputation (9.6%); vividness of nonpainful phantom sensations (acute: 12.2%; chronic: 20.8%); phantom limb pain, acute: 22.7%; chronic: 10.1%).

Post-hoc analysis confirmed a significant correlation between typicality and kinaesthesia in amputees (Figure 3.3A; rho=.72, df=16, p=.001). No significant correlation was found with non-painful phantom vividness (the chronicity of experiencing the missing hand as existing; Figure 3.3B; rho=.13, df=16, p=.61), or years since amputation (rho=.17, df=16, p=.49). The correlation between kinaesthesia and dis-

similarity in S1 approached significance (rho=.447, p=.063).

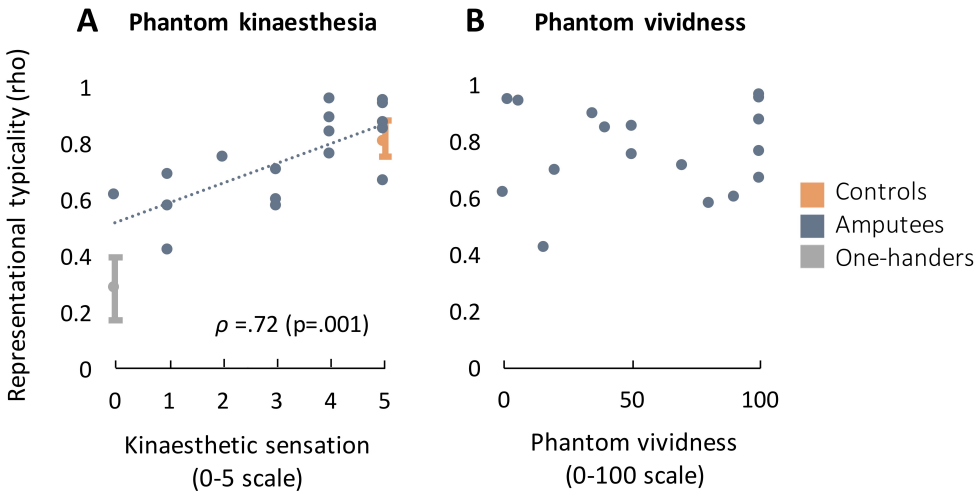



Figure 3.3: Kinaesthetic sensations during individuated phantom hand movements in amputees correlate with typicality in the missing hand's primary somatosensory cortex (SI). Typicality is the correlation coefficient of the representational dissimilarity matrix (RDM) with an independent hand RDM in controls. Phantom kinaesthesia (A) shows the number of digits that produced a sensation of movement during volitional phantom digit movements, based on amputees' self-reports. Grey and orange ranges show the mean and confidence intervals for typicality in one-handers and controls, respectively. The regression line is only presented for visualisation. Nonpainful phantom vividness (B) conveys the chronicity of the experience of the existence of a missing hand, where 0 indicates no sensations and 100 sensations identical to the intact hand.

Further analysis confirmed that the correlation between kinaesthesia and typicality remained significant in SI after accounting for typicality in M1 (mean rho=.44) as a covariate (F=17.73, p<.001, Adjusted $R^2$ =.51; $\beta_{\text{Kinaesthesia}}$ = .74, p<.001). This analysis suggests that although better recruitment of M1 is expected in individuals with clearer kinaesthetic sensations, the strong correlation between kinaesthesia and typicality in SI does not merely reflect information in M1.

Regardless of the positive relationship between kinaesthesia and typicality, amputees with little to no kinaesthetic sensations still showed missing hand representation. As stated above, the regression line between kinaesthesia and typicality

had an intercept of $\beta_{\text{intercept}}$=.52. This was also the case when phantom vividness was the (non-significant) dependent variable (F=.021, p=.89, Adjusted $R^2$ =-.061; $\beta_{\text{intercept}}$=.75, p<.001). These results predict that even amputees who do not experience any phantom sensations will retain some typical missing hand representation. To test this prediction directly, we examined the 3 amputees in our dataset showing weak to no chronic phantom vividness (below 10/100). Despite not being able to experience clearly their phantom hand when performing the phantom movements task, these individuals showed high typicality (average typicality (rho) = .83). Moreover, when comparing their typicality to that found in the congenital one-handers (who were arguably better matched to this sub-group in terms of task demands), the amputees with diminished phantom sensations showed significantly stronger correlations with the canonical hand structure (Mann-Whitney U = 38, p=.007). Typicality was not different between these 3 amputees and controls (Mann-Whitney U = 29, p=.52, BF=.089). Together, these additional analyses confirm that the representational structures' typicality in SI of amputees is still present in those with little to no phantom or kinaesthetic sensations.

### 3.4.3 Congenital one-handers

While the task involving phantom hand movements was suitable to test the persistence of missing hand representation in individuals with phantom sensations, it was not designed to rule out the existence of missing hand representation in congenital one-handers. Indeed, it is possible that congenital one-handers have typical sensorimotor representation of their missing hand, but they did not access it due to unnatural task demands (see Striem-Amit et al. (2015) for analogous results in visual cortex organisation in congenitally blind individuals).

To probe digit structure in the missing hand cortex using an alternative task, we examined whether we could observe a representation of the ipsilateral (intact) hand

in the missing hand cortex. In two-handed controls, finger movements lead to activity in specific cortical patches in ipsilateral M1 and SI, which tightly correspond to the activity patches engaged in the movement of the mirror-symmetric contralateral finger (Diedrichsen et al., 2013). Indeed, this ipsilateral representation fully overlaps with the representation of the contralateral hand (Diedrichsen et al., 2018). Furthermore, ipsilateral representation disappears completely during asymmetric bimanual finger movements, during which activity in M1 and SI is fully determined by the contralateral hand (Diedrichsen et al., 2013). As such, the ipsilateral representation of one hand is likely elicited due to recruitment of the representation of the contralateral hand (Diedrichsen et al., 2018; Berlot et al., 2018). Ipsilateral representation of the intact hand can therefore provide an indirect assay into the representation of the missing hand, while controlling for task demands across groups. Importantly, all three groups were able to perform the individuated digit movement task equally well (see Materials and Methods). We compared the intact/dominant inter-digit representational structure in the missing/nondominant hand area of one-handers/controls (respectively). We predicted that persistent missing hand representation in amputees should result in similar ipsilateral representation in their missing hand cortex as controls. If missing hand representation is diminished in congenital one-handers, then ipsilateral representation of their intact hand (in the missing hand area) should show reduced representational features as those found in amputees (see Discussion for an alternative mechanism, where the deprived cortex develops separate representations for both the contralateral (missing) and ipsilateral (intact) hands).

Mean (intact-hand) ipsilateral digit dissimilarity and typicality were not significantly different between amputees and controls (Figure 3.4; dissimilarity: $t(28)=1.42$, $p=.166$, $BF=.209$; typicality: $t(28)=.69$, $p=.498$, $BF=.244$). In contrast, ipsilateral representation in congenital one-handers was significantly lower than in amputees (dissimilarly: $t(29)=3.81$, $p<.001$; typicality: $t(29)=3.05$, $p=.005$) and showed simi-

lar trends versus controls (dissimilarity: t(23)=2.20, p=.038; typicality: t(23)=2.19, p=.039). Together, these findings provide additional support for the reduced existence of inter-digit representational difference in the missing hand cortex of congenital one-handers versus amputees, independent of missing hand motor skill.

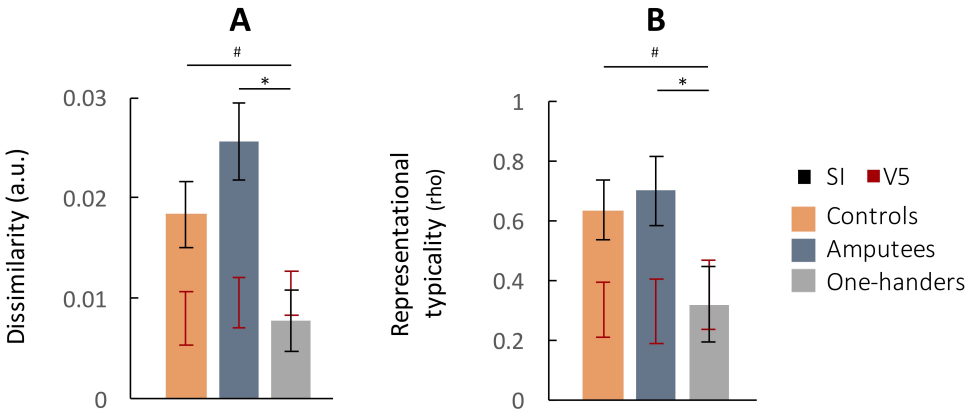



Figure 3.4: Similar ipsilateral hand representation in primary somatosensory cortex (SI) for amputees' and controls' intact hand. A-B Mean dissimilarity and typicality of the representational structure of ipsilateral SI activity for the three groups. Both dissimilarity and typicality of ipsilateral hand representation indicate a difference between missing hand representation in congenital one-handers and amputees, independent of missing hand motor skill. The red error bars indicate the dissimilarity and typicality values (standard error of the mean) in a visual control area V5 for the same groups, designed to capture visuomotor representation that is not strictly somatosensory. While amputees and controls showed significantly greater digit representation in SI than V5 (both in terms of dissimilarity and typicality), congenital one-handers did not, further indicating reduced SI digit representation. Abbreviations: a.u.: arbitrary unit; *: significant difference; #: trending difference (.02<p<.05).

It is important to consider that we found some potential support for the existence of an ipsilateral digit representation in the missing hand cortex of congenital one-handers. The cross-validated dissimilarity measurement in this group was significantly larger than zero (t(12)=2.51, p=.027), indicating that there were significant differences between the activity patterns associated with each finger. We therefore wished to determine whether the dissimilarity measures reflect meaningful (though reduced) sensorimotor digit information, or rather the increased sensitivity of RSA to

other (not sensorimotor) inter-digit differences (e.g. visual task differences). For example, a recent study demonstrated that visual information about touch on the hand is sufficient to induce some residual digit-selective activity patterns in SI (Kuehn et al., 2018). We therefore compared representational measurements between SI and visual area V5, previously shown not to contain individual sensorimotor digit representation (Beauchamp et al., 2009). Although it is difficult to set a benchmark at a particular dissimilarity value, we suggest that representation crucial to somatosensation in SI should at least outperform V5. Congenital one-handers showed no significant differences in representation between SI and V5 (dissimilarity: $t(12)=-1.03$, $p=.322$; typicality: $t(12)=.78$, $p=.448$), whereas both amputees and controls showed significant differences (all p's$<.02$), resulting in a significant group x area interaction (dissimilarity: $F(2,85)=4.25$, $p=.018$; typicality: $F(2,85)=4.42$, $p=.015$; Figure 3.4). These findings corroborate that the digit dissimilarity values in congenital one-handers are likely not specifically indicative of sensorimotor representation, but may rather reflect other task demands.

## 3.5 Discussion

Here, we demonstrated long-term stability of SI hand representation in a group of acquired amputees with diverse phantom sensations, including those experiencing limited phantom sensations. Using RSA, we find that amputees show individuated digit representation for their missing hand, as exemplified by significantly greater inter-digit dissimilarity values in amputees versus congenital one-handers. The inter-digit pattern comprising the missing hand representation was typical to SI hand representation in amputees and was not significantly different from controls (as supported by a Bayesian analysis). Importantly, by studying individuals with a varying range of phantom sensations, we were able to confirm stable hand representation even after

phantom sensations have diminished. This result confirms the persistence of hand representation as a general principle in amputees. Using the same task, we were unable to identify similar digit representation for the missing hand of congenital one-handers, demonstrated by significantly reduced pattern typicality compared to both amputees (and even in comparison to those few amputees with little phantom sensations), as well as controls. This result confirms that the persistent hand representation observed in amputees does not reflect mere cognitive task demands (e.g. visual feedback, Kuehn et al., 2018; attention, Puckett, Bollmann, Barth, & Cunnington, 2017). We also explored whether we could activate the representation of the missing hand indirectly by movements of the fingers of the intact hand. Previous studies in two-handers have demonstrated that contralateral and ipsilateral hand movements produce identical representational patterns (Diedrichsen et al., 2018). Since this ipsilateral representation is completely overwritten by the contralateral hand if the two hands are engaged in dissociated movements (Diedrichsen et al., 2013, Exp. 2), it has been proposed that the ipsilateral hand reactivates the cortical resources associated with the contralateral hand. Based on this evidence, the ipsilateral digit representation can serve as an indirect measure of the contralateral hand representation. This discovery provides us with a unique and novel opportunity to interrogate the information content underlying the deprived hand cortex despite the physical absence of the hand. This approach provided converging evidence, but using different task demands, for similar (missing) hand representation for amputees and controls, but not for congenital one-handers. It might be worth considering whether congenital one-hander's deprived cortex could have developed separate representations for both the contralateral (missing) and ipsilateral (intact) hand, which are uncorrelated due to anatomical or behavioural differences from two-handers. If this were possible, we would predict maintained, or even stronger, ipsilateral representation of the intact hand. Yet, our data does not reflect this hypothesis. Moreover, poor ipsilateral representation in the

deprived cortex does not seem to stem from reduced inter-hemispheric connectivity, which appears to be functionally and structurally preserved in congenital one-handers, depending on lateralisation strategies in daily behaviour (Hahamy et al., 2015, 2017; Makin, Cramer, et al., 2013). Finally, it is still possible that rudimentary missing hand representation, e.g. determined by genetic factors (Miyashita-Lin et al., 1999; Rubenstein et al., 1999), has originally formed in congenital one-handers but later diminished due to lack of consistent sensorimotor input. Bearing this caveat in mind, our findings suggest that early-life experience is potentially necessary to create typical functional sensory organisation, but not to maintain it.

It has previously been shown that restored peripheral input, e.g. via hand transplantation (Frey et al., 2008) or targeted reinnervation (Serino et al., 2017) can reinstate sensorimotor hand representation, indicating that the canonical hand representation is, to an extent, immutable to change. Moreover, we reported that the SI hand map can persist independently of the original peripheral input, as observed in a patient sustaining a brachial plexus avulsion injury, abolishing communication between the periphery and the central nervous system (Kikkert et al., 2016). Similarly, in the current study amputees showed, on average, persistent SI representation despite suffering diverse nerve injuries spanned varying degrees of amputation (table 3.1). It is therefore necessary to consider alternative inputs that might contribute to the stability of the missing hand map in amputees. Considering that our task required active phantom movements, it is likely that the SI representation pattern is driven by motor efferent inputs. Indeed, while motor signals can no longer reach their final output muscle terminal, the motor cortex in amputees remains functional (Raffin, Giraux, & Reilly, 2012; see Kokotilo, Eng, and Curt (2009) for similar results in spinal cord injury patients). When a motor command is sent out (e.g. in the form of an attempted hand movement), efference signals are thought to reach SI and generate corollary discharge, suggested to resemble the expected sensory feedback

activity pattern, resulting from the movement (London & Miller, 2013; Adams et al., 2013). Since congenital one-handers have never operated a hand, it is likely that this sensorimotor predictive coding architecture never formed in the first place, explaining the lack of inter-digit dissimilarity found in the present study. It is important to consider how the finding of robust persistence of hand representation, despite the physical absence of a hand, conceptually aligns with other reports of brain reorganisation. Since the pioneering work of Hubel and Wiesel, demonstrating that input loss to visual cortex in early development leads to profound physiological changes (Wiesel & Hubel, 1965b, 1965a), it has long been established that sensory deprivation causes cortical reorganisation. Later seminal electrophysiological studies in monkeys further demonstrated that deprivation-driven reorganisation following peripheral input-loss also occurs in adults (Kaas et al., 1983). For example, following peripheral deafferentation of the hand and arm, the missing hand SI area becomes responsive to touch applied to the monkey's lower face (Pons et al., 1991), likely due to subcortical re-routing of inputs (Kambi et al., 2014; Liao et al., 2016). Recent research in humans indicates extensive reorganisation of multiple body-part representations onto the deprived hand area of congenital one-handers (Hahamy et al., 2017; Striem-Amit et al., 2018a; Stoeckel et al., 2009). In amputees sustaining input loss in adulthood, original reports emphasised facial remapping in SI, akin to the reorganisation observed in monkeys (Flor et al., 1995), as a driving mechanism for phantom limb pain (maladaptive plasticity; Flor, Nikolajsen, & Staehelin Jensen, 2006). Later research challenged the notion that the deprived hand area gets taken over by facial inputs (Makin, Scholz, et al., 2013; Makin et al., 2015; Raffin et al., 2016) and instead emphasised increased representation of the intact hand in the missing hand cortex as a potential neural correlate of adaptive plasticity (Philip & Frey, 2014; Makin, Cramer, et al., 2013; see further discussion below). More recently, we have suggested that functional reorganisation is more limited than originally considered (Makin &

Bensmaia, 2017). Regardless of the ongoing debate over the functional role of SI reorganisation in the adult (Andoh et al., 2017; Kuner & Flor, 2017) and developing brain (Hahamy et al., 2017; Striem-Amit et al., 2018a), common to all these previous studies of reorganisation is that to activate the deprived cortex researchers studied representations of the spared body parts (e.g. the face or the intact hand). While this approach is suitable for documenting cortical remapping, it leaves unexplored the possibility that the original functional organisation of the now-deprived area may be preserved, though latent. We propose that reorganisation in the missing hand cortex does not necessarily abolish the original functional layout in sensory cortex. For example, persistent representation, in the form of efferent cortico-cortical input would engage a separate cortical layer (Felleman & Van Essen, 1991; Adams et al., 2013) than brainstem and thalamic facial inputs to the deprived cortex (Kambi et al., 2014). It still remains to be determined whether these two forms of persistent representation and reorganisation are functionally orthogonal, or interactive (Andoh et al., 2017).

As mentioned above, the missing hand cortex in amputees, but not in congenital one-handers, has been previously shown to receive inputs from the intact hand (Bogdanov et al., 2012; Makin, Cramer, et al., 2013; Hahamy et al., 2017; Philip & Frey, 2014), presumably through functional reorganisation. Here, we used RSA to dissect the information content underlying ipsilateral activity of the intact hand. We find that amputees, but not congenital one-handers, showed similar measures of dissimilarity and typicality as controls. However, the fact that ipsilateral dissimilarity was not significantly greater in amputees than in controls is inconsistent with the interpretation of increased intact hand activity as a neural correlate of adaptive reorganisation (Makin, Cramer, et al., 2013). Regardless, the existence of ipsilateral digit-specific organisation in the missing hand cortex of amputees might provide an alternative mechanism for the preservation of the missing hand digit maps. While

we previously showed that the phantom hand map is activated by phantom hand movements independently of the intact hand (Kikkert et al., 2016; Philip & Frey, 2014), it is still possible that structured inputs from the intact hand (via ipsilateral pathways) sustains the missing hand map, despite the loss of the original peripheral inputs. To conclude, here we show that once sensorimotor hand-representation is formed, it is generally immutable to change: We identified stable hand representation in amputees' sensorimotor cortex using representational similarity analysis, despite years (and even decades) of amputation and irrespective of their phantom sensations vividness. In contrast, individuals born with a missing hand (congenital one-handers) did not show normal representation of their non-existing hand. We therefore suggest that consistent sensory representation despite input loss may be a common organising principle (Striem-Amit et al., 2015; Collignon et al., 2013; Baseler et al., 2011). How can our findings of persistent representation, despite massive and long-lasting input change, be resolved with multiple observations of updated hand representation due to altered experience [e.g. due to nerve/digit deafferentation (Merzenich et al., 1983, 1984), increased usage (W. M. Jenkins et al., 1990), syndactyly (Allard et al., 1991; X. Wang et al., 1995), or mobile phone usage (Gindrat et al., 2015)]? Here we show that amputees with greater phantom kinaesthetic sensations better retained their missing hand representation. In light of this, we suggest that daily life experience could shape the fine-grained aspects of hand representation, but the large-scale functional organisation of the hand area is fundamentally stable.

# Chapter 4

# Congenital blindness

This is adapted from: Wesselink, D.B., Kikkert, S., Bridge, H. and Makin, T.R. (Submitted) Finger representation in the cortex of the congenitally blind.

## 4.1 Abstract

Hand representation in the primary somatosensory cortex (S1) is thought to be shaped by experience. Individuals with congenital blindness rely on their sense of touch for completing daily tasks that in sighted people would be informed by vision, and possess superior tactile acuity. It has therefore been proposed that their S1 hand representation should differ to sighted individuals. Alternatively, it has been proposed that the improved tactile acuity in blind individuals is due to cross-modal plasticity, when regions in the occipital and temporal cortex are typically used for processing vision become activated by touch. We probed finger representation using psychophysics and 7T fMRI in three individuals with bilateral anophthalmia, a rare condition in which both eyes fail to develop, as well as sighted controls. Despite anophthalmic individuals increased reliance on touch and superior tactile acuity, we found no evidence that they had more pronounced hand representation in SI. This is in line with recent research highlighting the stability of early sensory cortex, despite altered sensorimotor experience in adulthood. Unlike sighted controls, anophthalmic individuals activated the left hMT+ during finger movement. This area did not express any hallmark of typical sensorimotor organisation, suggesting this and previously reported activity does not indicate low-level sensorimotor hand representation. However, left hMT+ contained some single finger information, beyond than found in sighted controls. This latter finding suggests that when the developmentally flexible area hMT+ is unaffected by retinal inputs, it can acquire novel cross-modal processes, which are potentially unrelated to the areas function in sighted people. As such, our findings highlight the opportunity for other organising principles, beyond domain specific plasticity, in shaping cross-modal reorganisation.

## 4.2 Introduction

To successfully interact with their environment, individuals with congenital blindness are forced to rely on other senses, such as touch. Congruently, both congenitally and early blind people show superior performance on a variety of tactile tasks (Goldreich & Kanics, 2003; Van Boven, Hamilton, Kauffman, Keenan, & Pascual-Leone, 2000; Norman & Bartholomew, 2011; though see Alary et al., 2009). Given previous evidence for a relationship between tactile ability and recruitment of the somatosensory system, particularly the primary somatosensory cortex (S1; e.g. Recanzone, Merzenich, & Jenkins, 1992), it is not surprising that researchers have hypothesised that S1 hand representation of blind individuals should be altered from that of the sighted. Blind individuals fingers, in particular the reading finger(s) of Braille readers, have been shown to be represented in a more pronounced manner in S1, in terms of activity level and spatial spread (Pascual-Leone & Torres, 1993; Burton, Sinclair, & McLaren, 2004; but see Gizewski, Gasser, de Greiff, Boehm, & Forsting, 2003; Burton et al., 2002; see Discussion for full details). This is consistent with the suggestion that following increased sensory demands on the fingers, such as by learning to play an instrument (Elbert et al., 1995), or mere repeated exposure to tactile stimuli (Recanzone, Merzenich, & Jenkins, 1992; W. M. Jenkins et al., 1990; Gindrat et al., 2015), cortical magnification becomes more pronounced. Following these findings, it has been proposed that the increased tactile perceptual abilities documented in blind individuals could be caused by different finger representation in S1 (e.g. Van Boven et al., 2000; Lissek et al., 2009).

Other studies have suggested that some support to the increased tactile acuity found in blind individuals may arise from the (repurposed) visual cortex. Cross-modal cortical reorganisation is commonly observed in traditionally visual areas, as over-excitability during non-visual tasks (Merabet & Pascual-Leone, 2010; Bavelier & Neville, 2002). For example, previous research has shown that early blind individuals

activate both the primary visual cortex (V1; Sadato et al., 1996) and occipitotemporal cortex (Burton et al., 2002; Sadato et al., 2004) during Braille reading. Yet, the exact function of emergent processes in the visual cortex may not be comparable with that of S1. For example, V1 appears to provide linguistic, rather than strictly sensory support during Braille reading (Hamilton et al., 2000; Bedny et al., 2011). Regardless, the initial findings led to suggestions that cross-modal reorganisation could support the heightened behavioural needs for touch processing in blind individuals by enabling new functions. Since then, this interpretation has been challenged. Instead, it has been suggested that the specific computations performed by a repurposed area remain similar following cross-modal reorganisation (domain specificity). As such, the only difference between occipital processes of blind and sighted individuals is their input modality (Pascual-Leone & Hamilton, 2001; see also B. Z. Mahon, Anzellotti, Schwarzbach, Zampini, & Caramazza, 2009). For example, in the visual cortex of the sighted, the extrastriate body area has been implicated with visual processing of body parts (Downing et al., 2001; Kontaris et al., 2009). Accordingly, in blind individuals, this body-selective region is specifically activated during recognition of body parts and body postures through touch (Kitada et al., 2014) or auditory cues (Striem-Amit & Amedi, 2014). This and other related findings suggest that cross-modal reorganisation is more restricted than initially thought, with only limited capacity for reassignment of function.

The framework of domain specificity has been highly productive (Ricciardi et al., 2014; Maidenbaum et al., 2014; Kupers & Ptito, 2014) and many findings have accumulated supporting the principle for medium to high-level functions (e.g. Striem-Amit, Cohen, Dehaene, & Amedi, 2012; Dormal, Rezk, Yakobov, Lepore, & Collignon, 2016; Peelen et al., 2013; Amedi et al., 2007; Amedi, Raz, Azulay, Malach, & Zohary, 2010; Wolbers, Klatzky, Loomis, Wutte, & Giudice, 2011; Kitada et al., 2014). Yet, restricting the scope for functional reassignment of resources is seemingly at odds

with some evidence for emergent low-level sensory processing in the occipitotemporal cortex. Watkins et al. (2013) studied individuals with bilateral Anophthalmia, a rare condition in which both eyes completely fail to develop. Unlike other forms of early blindness, Anophthalmia guarantees the visual cortex has never been influenced by retinal input, not even prenatally. The authors observed structured activations by pure tones (tonotopy) in the occipitotemporal cortex, corresponding to motion-sensitive area hMT+ (see E. Huber, Jiang, and Fine (2019) for a replication in early blind participants). in other words, hMT+ appeared to perform an early (low-level) sensory function that has emerged independently from known visual processes in the sighted, or at least to have extended its original function beyond a cross-modal input shift (see Shiell, 2014). This finding may contradict the framework of domain specificity, but it does not demand developmental anarchy. A moderate account would be that rigid functional domains (i.e. domain specificity) develop when the brains coarse proto-organisation (Arcaro & Livingstone, 2017; L. A. Krubitzer & Prescott, 2018) is supplied with typical inputs, irrespective of which modality they are in. Completely different inputs, however, may result in domains that are unrecognizably different, in both function and organisational structure (Bedny, 2017)).

In the current study, we interrogated the low-level somatosensory processing in the same anophthalmic population mentioned above. We focused on the representation of the fingers, which, especially in the human hand area of S1, shows strong selectivity (Kurth et al., 1998; Sanchez-Panchuelo et al., 2010), as well as an idiosyncratic pattern of inter-finger overlap. These properties are shared by a range of low-to-medium-level sensorimotor areas (van der Zwaag et al., 2013; Zeharia et al., 2015; Berlot et al., 2018). Using 7T fMRI, it is possible to identify these characteristic finger maps in humans, with high inter- and intra-subject reliability (Kolasinski, Makin, Jbabdi, et al., 2016; Ejaz et al., 2015), providing opportunities for studying specialised case studies (Kikkert et al., 2016; Dempsey-Jones, Wesselink, et al., 2019).

We wished to determine whether the anophthalmic individuals S1 shows stronger finger representation, in terms of inter-finger selectivity and overlap. We also examined their visual cortex (and area hMT+ in particular) to determine whether it supports low-level finger processing.

We focused on hMT+ because it has previously been shown to have undergone low-level functional reorganisation in congenitally blind individuals (Watkins et al., 2013). Indeed, some have suggested that due to its connectome and in particular its direct connections with sub-cortical structures (Gaglianese et al., 2015), hMT+ resembles a primary area (see Ajina, Kennard, Rees, and Bridge (2015) for a comparable argument based on people with blindsight). By effectively being able to bypass V1 inputs, hMT+ can develop an independent functional organisation. As such, this area may be awarded more developmental flexibility than higher-order visual areas further downstream. According to this account, functional plasticity can occur here more-or-less unconstrained by the occipital cortex organisational template, potentially even allowing hMT+ to develop novel finger representation, organised in a different manner than those found in S1.

We found that despite superior tactile perceptual abilities and a lifetime of increased reliance on touch for typically visual tasks, S1 finger representation was not more pronounced in anophthalmic individuals, relative to controls. Additionally, finger-specific information was detectable in the left hMT+ area of anophthalmic individuals, although the organisational representational structure in occipitotemporal cortex differed from hand somatotopy. Our findings show that, in exceptional circumstances, the visual cortex retains some ability to acquire functional organisation which might not be native to the region, suggesting the prevalent principle of domain specificity does not bridle the development of all sensory areas to the same extent.

## 4.3 Methods

### 4.3.1 Participants

Four individuals with bilateral Anophthalmia, a rare congenital condition in which both eyes fail to develop, participated in this experiment (hereafter, anophthalmic individuals; mean age: 33 ± 3; 3 male; 1 left-handed; see Table 4.1 for demographic details). One anophthalmic individual was excluded from all data analysis due to inability to perform the fMRI task (see fMRI task section below for details; this data is not reported in the current manuscript). The full experimental protocol involved a battery of behavioural tasks and fMRI measurements over the course of 1-2 sessions, as elaborated in the full protocol available online: https://osf.io/d9g3t/. Here, we focus on the procedures relevant to the key analyses described below. Eight sighted healthy control participants (mean age: 25 ± 3; three male) with normal (or corrected) vision underwent the same neuroimaging procedures. To compare fMRI S1 representation with a larger control group, further data was retrieved from a study using similar scanning parameters (n=15, 26 ± 4; 9 male; 1 left-handed; Sanders et al., 2019). One key difference with our current study protocol is that participants received visual feedback and were not blindfolded. All participants used their right hand for the various tasks.

In addition, to compare the tactile acuity of the anophthalmic individuals to a larger group of sighted control participants we used data collected as part of two larger studies: 1) For tactile acuity comparisons, data was retrieved from Dempsey-Jones et al. (2016, n=21, age=26.4±7.1, 1 left-handed) and (Dempsey-Jones, Themistocleous, et al., 2019, n=36, age=27.7±6.7, 5 left-handed). The anophthalmic tended to be older than the control group used for tactile acuity comparisons (U=143, p=.083). Had the control group been younger, any age imbalance in tactile perception should have advantaged them, which is contrary to our findings (for the effect of age on

tactile acuity, see e.g. Legge, Madison, Vaughn, Cheong, & Miller, 2008).

Experimental procedures were approved by the Medical Sciences Interdivisional Research Ethics Committee of the University of Oxford (C2- 2013-05 and C1- 2011-101). All participants gave their informed consent prior to the study.

### 4.3.2 Behavioural task & analysis

Tactile acuity was measured for the index (D2), middle (D3) and ring finger (D4) of the right hand, using standard orientation grating testing. A detailed description of the task can be found in Dempsey-Jones et al. (2016). In short, participants were asked to make a tactile judgement on the perceived orientation (horizontal or vertical) of plastic dome gratings varying in groove width and isometric groove spacing (between .25 - 3.5 mm). Each grating was presented either parallel or orthogonally to the distal finger pad for 1-2 blocks of 10 trials on each finger. Blocks were randomly interspersed. At the end of each trial, participants reported the perceived orientation using a right or left button press on a mouse held in their left hand. No time limitations were posed, and participants were encouraged to perform the task as accurately as possible. A psychometric function was fit to the data using least squares fitting and the tactile threshold for each finger was interpolated at 82% accuracy (see Dempsey-Jones et al., 2016). Finally, the tactile thresholds were averaged across the three fingers for each participant.

### 4.3.3 fMRI task

Finger representations were probed using an active finger-tapping task, adapted from Diedrichsen et al. (2013). This task has been previously shown to yield strong inter- and intra- subject reproducibility of SI finger representation (Kolasinski, Makin, Jbabdi, et al., 2016; Ejaz et al., 2015; see further validation against passive paradigms in Berlot et al. (2018); Sanders et al. (2019)). Specifically, our task involved individ-

| ID Code | Age | Gender | Handedness | Braille hand(s) |
|---|---|---|---|---|
| A1 | 36 | M | R | - |
| A2 | 31 | M | R | R & L |
| A3 | 30 | M | R | R & L |
| C1 | 24 | F | R | - |
| C2 | 22 | F | R | - |
| C3 | 27 | M | R | - |
| C4 | 26 | M | L | - |
| C5 | 22 | F | R | - |
| C6 | 30 | M | R | - |
| C7 | 25 | F | R | - |
| C8 | 25 | F | R | - |

Table 4.1: Demographic details. Demographic details of participants. A: Anophthalmic individuals; C: Sighted controls.

ual finger movement blocks (8s each) for each of the five fingers, and a no movement (i.e. rest) condition (8-16s each). Each run was made up of four repetitions of each finger movement condition, presented in counter-balanced order, and five repeats of the rest condition at regular intervals. Each participant underwent 8 runs and run order was also counterbalanced across participants. Participants used a button box with four buttons to perform the task; they pressed the side of the box with their thumb. Participants were instructed to perform these button presses at a constant rate of approx. 1Hz, while keeping non-instructed fingers still.

Sighted participants were blindfolded and all participants were cued tactilely. To cue the participant which finger should be moved, an experimenter lightly patted the participants leg at a specific location at the start of each movement block. The cues followed a spatial pattern that the participants were trained on prior to scanning: thumb movement was instructed by a touch at the ball of the left foot, index  outer left ankle, middle  inner left ankle, ring  inner right ankle, and little  outer right an-

kle. Rest blocks were cued by a double-tap on the balls of both feet simultaneously. The experimenter received auditory instructions specifying the block order through MR-compatible headphones. In order to ensure a steady movement pace of 1 Hz, participants were instructed to follow the sound of the vibrating magnetic coils of the MRI at every gradient switch. In our case, a gradient switch occurred every two seconds; participants were instructed to make two button presses between two gradient switches. To ensure good understanding of these instructions, the experimenter trained the participants on both the motor and the cueing component of the task. The auditory cueing to the experimenter and the recording of the button responses were implemented using Presentation software (version 0.70, www.neurobs.com). Correct task performance was further verified off-line using button box responses that were recorded during the experiment. Note that one anophthalmic individual was unable to maintain a steady 1Hz pace and was subsequently discarded from all analysis.

### 4.3.4 MRI acquisition, pre-processing, and low level analysis

High-resolution BOLD fMRI data was obtained using a Siemens (Erlangen, Germany) whole-body 7 tesla Magnetom scanner with a 32-channel head coil. Task fMRI data was acquired using Multi-Band Echo Planer Imaging (EPI) with an acceleration factor of 2 (Moeller et al., 2010) and a limited field of view (FOV), designed to capture both the hand knob of the central sulcus and the lateral occipitotemporal cortex bilaterally. The following parameters were used: spatial resolution: 56 slices with a 192 x 192 in-plane FOV, 1mm isotropic spatial resolution, TR: 2000ms, TE: 25ms, PE acceleration factor: 3, flip angle: 85 , and phase partial Fourier: 6/8. Please note that due to the increased spatial resolution and the consequential limited FOV, we were unable to acquire other potential areas of interest (e.g. secondary somatosensory cortex, cerebellum, primary visual cortex) consistently across participants. Fat suppression was done by CHESS. Because data acquisition expended a large part of

the scanners CPU and memory capacity, image reconstruction was performed offline. For some participants this caused data acquisition delays or partially corrupted data. As a result, only 7, 6 and 4 usable runs were obtained for sighted control C2 and anophthalmic participants A1 and A3, respectively.

Anatomical T1-weighted (MPRAGE) whole-brain images with a 1 mm isotropic resolution was also acquired. When available, images were collected at using 3T MRI machine, as they suffer less from intensity biases due to field inhomogeneity (Vaughan et al., 2001). For all anophthalmic individuals and sighted participant P2, the anatomical T1-weighted image was acquired at 3T using standard parameters (TE: 6.0ms, TR: 15ms). For the remaining participants an anatomical T1-weighted image was acquired using the 7T MRI scanner in the same session as the fMRI measurements, using the following parameters: FA: 7, TI: 1050ms; TE: 2.82ms; TR: 2200ms. Fat suppression was done by means of water excitation.

Data pre-processing, GLM analysis and cortical surface reconstruction were implemented using software from FSL (Smith et al., 2004; Jenkinson et al., 2012; fsl.fmrib.ox.ac.uk/fsl) and Freesurfer (Dale et al., 1999; www.freesurfer.net). Connectome Workbench software (www.humanconnectome.org) was used for visualisation on the cortical surface. These tools were complemented by scripts written in UNIX or Matlab (version 8.5, R2015a) which were developed in-house (https://github.com/ronimaimon).

Each individual imaging run was pre-processed using FEAT (version 6.0). This included the following steps: motion correction using MCFLIRT (Jenkinson et al., 2002), brain extraction using BET (Smith, 2002), high-pass temporal filtering (100s), and spatial smoothing using a 2mm FWHM (full width at half maximum) Gaussian kernel. In addition, the motion estimates were inspected for excessive participant motion: no run contained more than 1mm (i.e. our voxel size) of relative displacement.

Images were registered to each other using FLIRT (Jenkinson et al., 2002). First, all fMRI runs were realigned to their average space (midspace), by iteratively aver-

aging and coregistering. This procedure ensured the final coregistration was minimally biased towards a single run and all runs were minimally reoriented. Then, all functional images were registered to the anatomical volume. All coregistration was visually checked and manually adjusted if needed. Anatomical T1 images were further used to reconstruct the pial and grey matter inflated surfaces using Freesurfer (http://surfer.nmr.mgh.harvard.edu).

First-level parameter estimates were computed for each run using a voxel-wise general linear model (GLM), as implemented in FEAT, based on the double-gamma hemodynamic response function (HRF) and its temporal derivative. 11 contrasts were defined: each individual finger movement versus rest, movement of all fingers versus rest, and each individual finger movement versus movement of all other fingers. The voxel-wise parameter estimates were averaged across runs for each participant using a fixed effects model. The resulting Z-statistic images were thresholded using clusters determined by $Z > 3.1$ and p ¡ 0.05 family-wise-error-corrected cluster significance thresholding was applied. For visualisation purposes, the resulting Z-statistic images were projected to two-dimensional surface space using a cortical ribbon mapping method.

Regions of interest (ROIs) were defined on the cortical surface. To initially identify the anatomical hand regions in S1, a rectangle was drawn on the Freesurfer standard surface stretching 2 cm medially and 2 cm laterally to the anatomical location of the hand knob (Yousry et al., 1997) within areas BA3a, BA3b and BA1, defined by Freesurfer based on ex-vivo cytoarchitectural data. This is where finger maps are typically reported. This anatomical hand ROI was then projected to each individual surface. Next, all voxels within said rectangle that showed selectivity for at least one finger (i.e. contrast any one finger versus the others, Z>3.1) were grouped together for each participant to create the final individualised hand ROI.

To delineate the regions of interest within the visual cortex, each individual

anatomical surface was aligned to the cortical atlas of the Human Connectome Project (Glasser et al., 2016). ROIs for the functional region hMT+ was created by combining regions FST, V4t, MT and MST. Various definitions exist for hMT+ and our liberal anatomical definition should overlap with previously functionally defined ROIs for hMT+ (Dumoulin et al., 2000). since our main methods (representational similarity analysis and classification) can cope with unnecessary non-informative voxels, this was preferable to failing to capture any emergent representation that is just outside MT/MST proper. This methodological choice has likely influenced the relatively low average activity reported in Figure 4.4B. ROIs were defined separately for the left and right hemisphere.

### 4.3.5 fMRI analysis

#### Univariate analysis

In order to visualise finger maps in S1, for each participant the Z-statistic images for each contrast 1 finger > mean of other fingers were averaged across runs and projected onto the participants inflated surface. Univariate inference was done on two measures: 1) average activity (mean all fingers versus rest) inside the ROI, and; 2) number of active voxels (mean of all fingers > rest; Z > 3.1) inside the ROI, corrected for whole-brain false discovery rate (q(FDR) = .01).

#### Representational similarity analysis

In order to assess whether hand-related activity contained a representational structure within an ROI, the dissimilarity in activity patterns (for each finger versus rest) were calculated for each finger pair for each participant and ROI. Our dissimilarity measure was the Mahalanobis distance (Nili et al., 2014; Ejaz et al., 2015), cross-validated over each possible pair of runs and then averaged. This ensures that the expected distance is zero if two patterns are not statistically different from each

other, whereas larger distance values indicate greater dissimilarity/separation. The resultant inter-finger distances were arranged into one dissimilarity matrix (RDM) per participant per ROI. Next, we extracted the mean dissimilarity between all possible finger pairs as an indication of finger separability. If there is no representational structure, one would expect the average dissimilarity (or separability) to be 0. We further calculated the Spearman correlation between the participant specific RDMs and the sighted controls average RDM of the S1 hand area (using a leave-one-out approach for the controls). In order to assess whether RDMs were reliable at the level of the individual participant, this process was repeated separately for odd and even runs. Decent cross-half correlation (rho>.6; a liberal threshold: Kline, 2000) between odd and even RDMs was a prerequisite to interpret the RDM calculated using all runs.

### Classification

Classification was implemented using the Princeton MVPA toolbox for Matlab available at https://code.google.com/p/princeton-mvpa-toolbox/ (see Wolbers et al. (2011) for an implemented example). The classifier algorithm used consisted of a backpropagation neural network with one hidden layer consisting of 10 nodes (Duda et al., 2012). In short, the network was trained to classify activity patterns for each finger and subsequently had to classify unseen patterns as belonging to 1 of the 5 tested fingers. The classification was cross-validated in a leave-1-run-out fashion. For example, training was performed on 7 runs x 5 finger patterns and testing on the remaining 5 finger patterns from 1 imaging run, which was then repeated such that each run functioned as a test once. For each ROI, this classification was repeated 20 times with random initial weights and averaged, in order to minimise the effect of the networks initial state. Final classification accuracy was calculated by averaging across the 5 individual fingers. Given the 5 fingers on a hand, chance level was 20%. In addi-

tion, we wanted to determine whether the classification performance was significant in individual participants. For this purpose, classification performance was compared against a chance distribution simulated for each ROI and participant. This distribution was created by running the above classification on the same data but with finger identify scrambled within each run. This was repeated 200 times and significance was determined by a one-sided ranked-order test.

### 4.3.6 Statistical analysis

All group comparisons were done using Mann-Whitney U tests ($\alpha = 0.05$), suitable for small groups, as implemented in Matlab. In order to assess our confidence in supporting any null results, we used Bayesian t-tests, as implemented in JASP (https://jasp-stats.org/). The specific alternative hypothesis that was tested (greater than, smaller than, or different from the null), is specified in the main text for each test. A Bayes Factor (BF) above 3 was interpreted as substantial evidence for the alternative hypothesis; a BF below 0.33 as substantial evidence towards the null (Wetzels et al., 2011).

## 4.4 Results

### 4.4.1 Increased tactile acuity in anophthalmic individuals

First, we measured tactile acuity using a psychophysical task: participants were asked to judge whether gratings of varying fineness were placed horizontally or vertically on their fingertips. This allowed us to construct a psychometric (Weibull) function per finger and participant to determine the tactile threshold (defined at 82% correct performance; see Methods). The average tactile threshold (across the three fingers tested) was significantly lower in the anophthalmic individuals compared with sighted participants (U=15, p=0.01; see Figure 4.1), indicating greater tactile acuity. This is

in accordance with previous reports showing superior tactile acuity in the congenitally blind (Van Boven et al., 2000; Norman & Bartholomew, 2011).

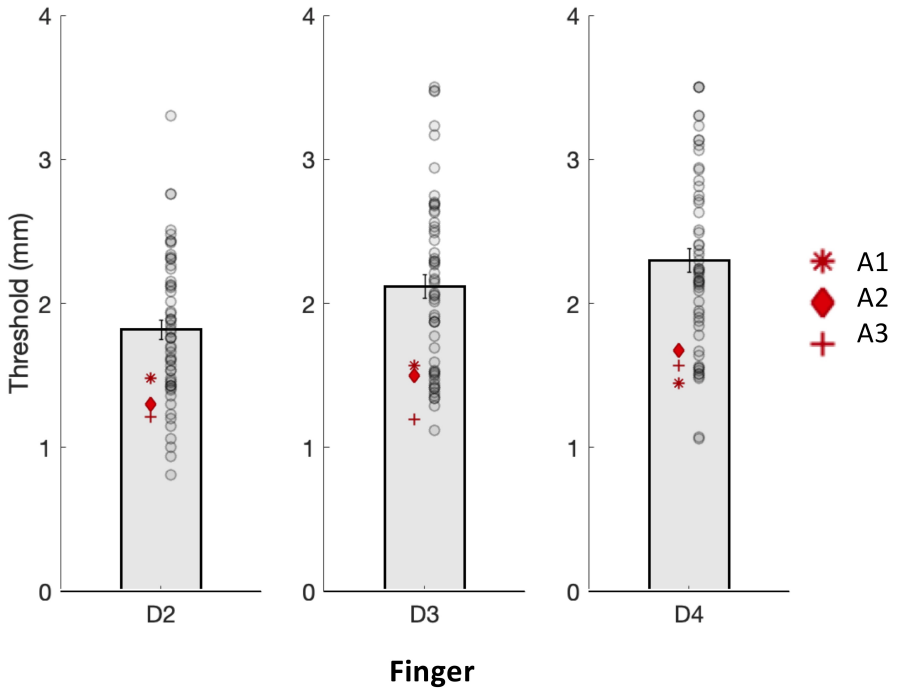



Figure 4.1: Tactile thresholds in anophthalmic individuals (n=3; red symbols) and sighted controls (n=57; grey circles) for index (D2), middle (D3), and ring finger (D4). On average, the anophthalmic individuals showed greater tactile acuity (lower thresholds) then the sighted controls. Bars shows control mean; error bars indicate the standard errors.

### 4.4.2 Hand representations in S1 is similar in anophthalmic individuals and sighted controls

To explore whether S1 would reflect these improved tactile abilities, we first interrogated finger representations using fMRI. All participants performed single-finger movements in a blocked design. As expected, for all participants, there was clear finger selectivity in S1, defined by contrasting each fingers movement activity against the mean activity for all other fingers. Selectivity maps were qualitatively similar be-

tween the anophthalmic individuals and controls (see Figures 4.2A and 4.3). Classical univariate analysis did not indicate hand representation was more pronounced in the anophthalmic individuals: Neither average activity during finger movement (U=23, p=.376) nor the spatial spread of the hand map, i.e. the number of voxels that showed finger selectivity (U=23, p=.376), were different between groups. To further quantify hand representation, we calculated multivariate measures, previously suggested to reflect habitual behaviour in typical populations (Ejaz et al., 2015). Specifically, we performed representational similarity analysis (RSA; see Methods) on the activity patterns in S1 for each finger to calculate a value (i.e. dissimilarity value) for each finger pair indicating how distinctly the fingers activated S1. Mean dissimilarity indicates finger separability. All finger pairs dissimilarity values together define a representational structure that is a low-dimensional summary of hand representation. Neither measure was greater for the anophthalmic individuals than for the sighted controls (separability: U=12.5, p=.303; representational structure: U=17, p=.921).

Thus. in all measures, the anophthalmic individuals did not significantly differ from controls (Figure 4.2B-C). We followed up on our original group comparisons using a Bayesian one-tailed t-test, designed to produce conclusive evidence in favour of the null (i.e. the blind group not showing greater finger representation relative to controls). Both the average activity (BF=.659) and the spatial spread of the hand map (BF=1.08) produced inconclusive results, but there was substantial evidence that the anophthalmic individuals did not show greater separability than sighted controls (BF=.314). The Bayesian t-test on the representational structure was inconclusive (BF=.454). Together, these results suggest that the enhanced tactile abilities commonly observed in blind people may not result from more pronounced finger representation in S1. Yet, the inconclusive results for some of our Bayesian t-tests may have resulted from our small sample size. A key advantage of our multivariate measure for representational structure is its high consistency both within and across participants

(Ejaz et al., 2015; Walther et al., 2016), particularly when compared to traditional finger selectivity analyses using univariate measures. To further ameliorate the concern of small sample size, we compared the typicality of the hand representational structure from the anophthalmic individuals to a relatively large distribution of sighted controls, by combining data from this study with that of another study with similar methodology (15 additional control participants, (see chapter 6, see Methods). When repeating the statistical comparison with the larger control group, we again found that the representational structure was not different between the anophthalmic individuals and sighted controls; U=24, p=.199). A Bayesian t-test confirmed that there was substantial evidence (BF=.285) to support that the anophthalmic individuals do not show greater (or less noisy) hand representation than the sighted controls.

Finally, as an additional measure of finger selectivity, we trained a basic artificial neural network on the unthresholded multivariate patterns in S1 to classify individual finger movements (leave-one-out classification; see Methods). Although the classifier tells us little about the structure of S1 hand representation, it is a sensitive indicator of finger-specific information in the area. As expected, the classifier was able to correctly classify the five fingers (chance level 20%; created using finger label permutation) with high accuracy for both anophthalmic individuals (mean=79.1%) and sighted controls (mean=82.6%; Figure 4.2D). When comparing the average classification accuracy between the two groups, the anophthalmic individuals did not show greater classification values (U=16, p=.776), confirmed by a one-tailed Bayesian t-test (BF=.321). Visual inspection of the classification patterns, e.g. which finger is mistaken for which, hinted at reduced performance specifically for the index finger (D2). This was confirmed by a group comparison (U=6, p=.012) and strong support for the alternative hypothesis that D2 classification is lower in the anophthalmic individuals (BF=15.1). Together, these results make clear that finger selectivity in S1, as well as other measures of hand representation, are not increased in the anophthalmic

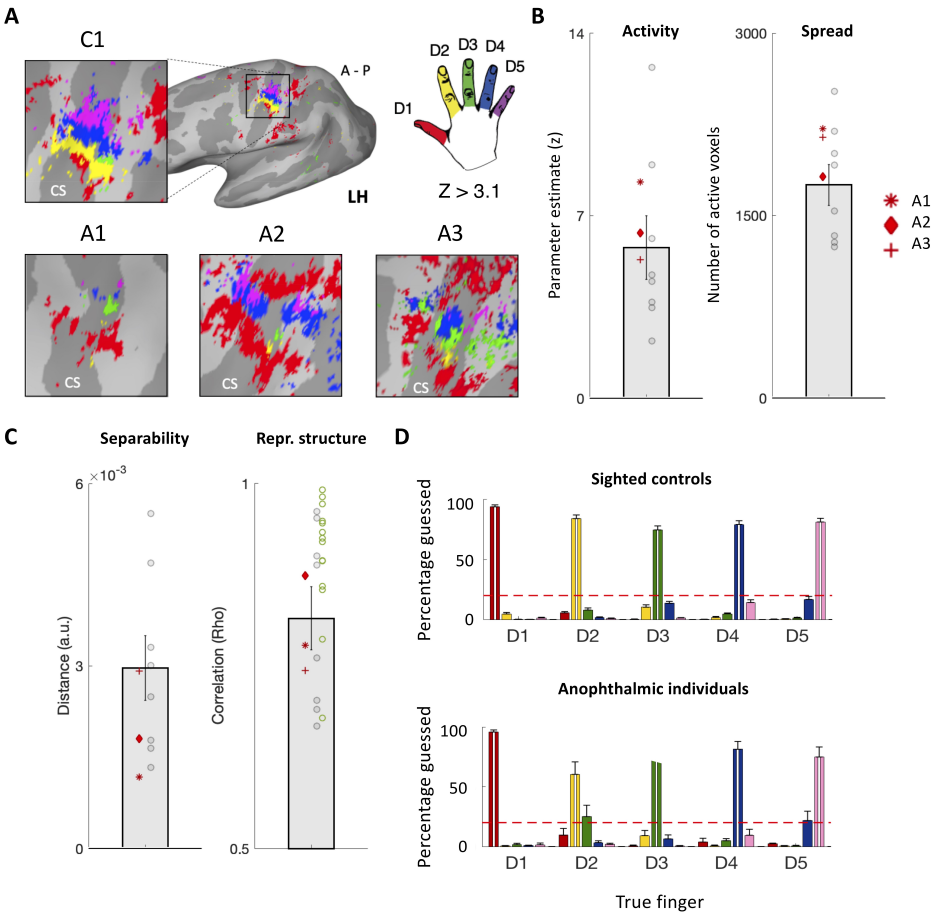



Figure 4.2: Hand representation in primary somatosensory cortex (S1). A) Finger maps for three anophthalmic individuals and a representative sighted control in S1. The sighted control had median (4th/8) average classification performance on fingers (88.1%; see D). Colours indicate selectivity (Z>3.1) for each finger relative to the average of all other fingers (see hand legend for colour code). Each of the anophthalmic participants presented distinct clusters showing selectivity to each of the five fingers, in a typical lateral to medial order. Note that the double D1 representation is commonly observed in sighted controls (e.g. Figure S1 in Sanders et al., 2019; for finger maps of all controls, see Figure 4.3). B) Univariate proxy measures of hand representation are not higher in anophthalmic individuals than sighted controls. Activity relates to the average parameter estimate (z) for all fingers versus rest; Spread relates to the number of voxels surviving correction for multiple comparisons within the S1 area. C) Multivariate proxy measures are not higher in anophthalmic individuals than sighted controls. Separability and representational structure are two outcome measures of representational similarity analysis. Separability indicates average dissimilarity (representational individuality of each finger pair). Representational structure indicates correlation between the inter-finger representation for each individual subject and to the mean group representation in controls. Supplementary pattern structure data obtained from a separate dataset are indicated in green (n=15). (Continued on next page)

(See previous page.) D) Average classification performance across participants for sighted controls (top) and anophthalmic individuals (bottom). Chance classifier performance is at 20% and perfect performance is at 100%. For each true finger (highlighted with a white vertical line), few trials were misclassified (neighbouring bars; colours as in A). Misclassifications tended to be more prominent for the neighbouring digits (e.g. D3 was most commonly confused with D2 and D4) in both sighted and anophthalmic groups. Other symbols as in Figure 4.1.

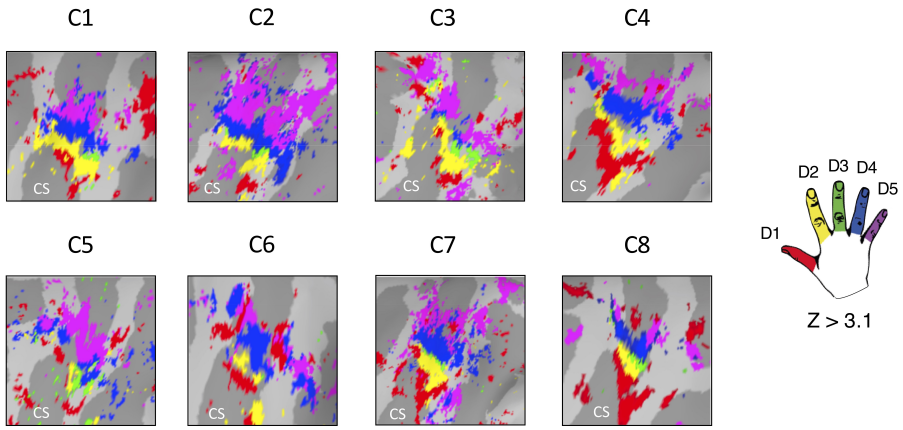



Figure 4.3: Finger maps for all sighted controls. Related to Figure 4.2. Colours indicate selectivity (Z>3.1) for each finger relative to the average of all other fingers (see hand legend for colour code). Each participant presented distinct clusters showing selectivity to each of the five fingers, in a typical lateral to medial order. CS: Central sulcus.

individuals compared to sighted controls.

### 4.4.3 Finger-specific information in the occipitotemporal cortex of anophthalmic individuals

Next, we examined finger representation in the occipitotemporal cortex, more specifically area hMT+. Finger movements (when contrasted against baseline) results in bilateral activity in area hMT+ in the anophthalmic individuals (see Figure 4.4A-C). In order to quantify the gross recruitment and any fine-scale organisation within hMT+, we calculated the measures introduced for S1 above in a pre-defined ROI (see

Methods). Because we had no a priori predictions concerning laterality cross-modal activity has previously been observed in either or both hemispheres we analysed hMT+ for each hemisphere separately.

In the left hemisphere, average activity was significantly greater for the blind group than for the sighted group (U=30, p=.012, BF=3.71). In the right hemisphere, this difference was not significant (U=27, p=0.085, BF=1.89). Spread of the activity showed similar lateralisation to the left (left hemisphere: U=30, p=.012, BF=959; right hemisphere: U=26, p=0.133, BF=1.85). All Bayesian t-tests had as their alternative hypothesis that anophthalmic individuals activate hMT+ differently than sighted controls (2-sided).

In order to determine whether the fine-scale finger organisation in hMT+ resembled that of S1, we initially correlated the representational structure (using RSA) to that that of S1. Yet, left hMT+ did not produce a reliable structure (indicated by poor split-half reliability; mean rho=.04). In fact, the split-half correlation was not even different from 0 (Wilcoxon signed rank test: rank=34; p=.966). Therefore, if any information content is facilitated by the increased activity, this is not reflected by a consistent representational structure measurable at the voxel level. Our hypothesis predicting that due to cross-modal plasticity, hMT+ would manifest an organisational structure similar to that of low-level somatosensory areas (greater overlap in representation across neighbouring fingers) was therefore not confirmed.

To examine digit information in hMT+ more directly, we repeated the classification analysis of individual fingers, as described for S1. In left hMT+, all anophthalmic individuals performed significantly above chance level (20%), whereas only 1 control performed better than chance. As a group, classification was significantly higher for the anophthalmic individuals (32%) than for the controls (23%; U=28.5, p=.036; BF=4.49; see Figure 4.4B). In right hMT+, classification performance was significant in 2/3 anophthalmic individual and 1 control. Because not all anophthalmic

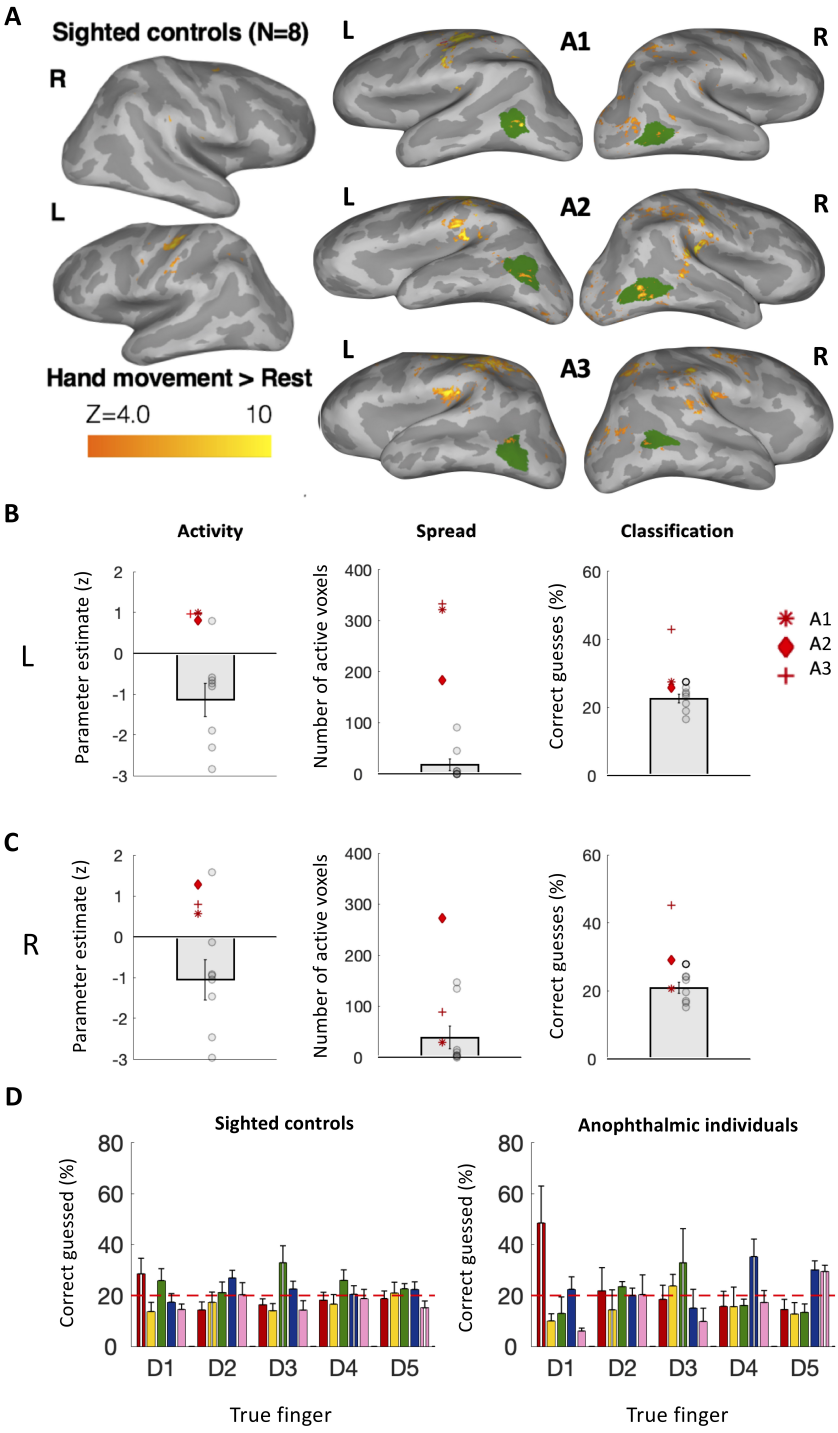



Figure 4.4: (See next page)

(See previous page.) Hand representation in area hMT+. A) Whole-brain activity for finger movement (contrasted against rest) in hMT+ for sighted controls (group average) and three anophthalmic individuals. Sighted controls do not show activity in hMT+, whereas the anophthalmic individuals do. hMT+ in the anophthalmic is indicated in green. B) Proxy measures of hand representation in left hMT+. Activity and spread tended to be higher in anophthalmic individuals than sighted controls. Classification showed significant finger-specific information in all anophthalmic individuals and 1 control (indicated by bold circle). C) Proxy measures of hand representation in right hMT+. Activity and Spread group differences are trending, and classification showed significant finger-specific information in 2/3 anophthalmic individuals and 1 sighted control (indicated by bold circle). D) Average classification performance in left hMT+ across participants for sighted controls (left) and anophthalmic individuals (right). Note that the classifier performed best for finger D1 in the anophthalmic individuals. Other symbols as in Figure 4.2.

individuals showed increased finger information, no follow-up group comparison was performed. To determine whether the increased information content in the left hemisphere was driven by specific fingers, misclassifications were examined separately per finger, for both groups (Figure 4.4C). If there were hidden topographic regularities in the finger representations, then the classifier should show more confusion between neighbouring fingers (as illustrated by the classification errors in the S1 topography, Figure 4.2D). Misclassifications did not seem to be structured in a certain way, except for the little finger (D5) often being mistaken for the ring finger (D4). Instead, the thumb (D1) was the most distinct of all classified fingers, in line with other literature (Ejaz et al., 2015). On the whole, improved (albeit slight) classification performance in the anophthalmic individuals suggest there is more information about fingers, and the thumb in particular, in left hMT+ of anophthalmic individuals than of sighted controls.

## 4.5 Discussion

Here, we examined cortical representation of the hand in S1 and found that anophthalmic individuals did not show a more pronounced finger map than sighted controls,

in any measure that was tested. Compared to sighted controls, there was, however, significantly more information about individual fingers in left hMT+ of the anophthalmic individuals.

### S1 hand organisation is stable in anophthalmic individuals

Previous studies reported that S1 hand representation of congenitally blind individuals is different from that of the sighted, in terms of spatial spread of activity (Burton et al., 2004; Pascual-Leone et al., 1993; Pascual-Leone & Torres, 1993), strength of activity (Giriyappa et al., 2009), or a shifted inter-finger balance (Sterr et al., 1998). This has been interpreted as a positive adaptation towards more effective tactile processing for people who rely more on touch in their daily lives. Conversely, Burton et al. (2002) who also examined S1 activity following tactile stimulation to the Braille reading finger in congenitally blind participants, reported that, qualitatively, they cannot infer differences between congenitally blind and sighted individuals.

The study of sensorimotor behaviour in blind individuals is dominated by the study of Braille users. Similar to the debatable benefits of blindness for tactile performance (Norman & Bartholomew, 2011; Alary et al., 2009; Wong et al., 2011), it is unclear how much impact Braille reading has. For example, grating orientation thresholds have been reported to be reduced on Braille reading fingers (Van Boven et al., 2000), but also to be not different between blind participants who do and do not read Braille (Norman & Bartholomew, 2011). The role of Braille in everyday life of blind people has progressively been taken over by various forms of (non-tactile) technology (Institute, 2009), exemplified by one of the anophthalmic individuals tested here who does not read Braille at all. The only difference with sighted controls we observed regarding S1 hand representation was poorer classification performance for the index finger (D2) of the anophthalmic individuals. Therefore, our results seem to go against greater individuation of finger representation in blind individuals, which

one would conjecture on the basis of more individuated finger usage during Braille reading (Mogilner et al., 1993; Vidyasagar et al., 2014).

Non-human evidence in favour of S1 changes following blindness, i.e. altered somatosensory receptive fields in the barrel cortex of blind rodents and cats (Rauschecker et al., 1992; Toldi et al., 1994), is also accompanied by altered behaviour (whisker use) from early life onwards. Yet, beyond Braille reading, blind individuals may actually not use their hands differently from sighted individuals, simply more. This may explain why the anophthalmic individuals S1 hand representation is not different from that of sighted controls. As a measure strongly correlated to everyday hand use (Ejaz et al., 2015), the canonical structure of hand representation has been found to be remarkably stable, despite hand loss (Chapter 3, Kikkert et al., 2016), extensive behavioural training (Beukema et al., 2019), or expert musicianship (Ogawa et al., 2019). While average dissimilarity between fingers may vary, indicating altered signal strength, the representational structure is stable. Our anophthalmic individuals complement these findings by demonstrating both stable representational structure and dissimilarity. Although evidence exists that sensory cortex is capable of considerable reorganisation (congenital one-handers: chapter 3, expert foot users: chapter 5), it appears that a large deviation from typical input early in life, rather than later, is paramount. Given a recent report of typical hand representation in two macaques who were near-blind in the first year of their life (Arcaro et al., 2019), it is not evident early life behaviour of blind individuals deviates far enough from normalcy to trigger representational change.

An alternative account is that the behaviour of blind individuals is sufficiently different to induce plasticity in the (adult) sensorimotor system, but that the plasticity only manifests transiently and depends heavily on the immediately preceding experience. Kolasinski, Makin, Logan, et al. (2016) showed altered hand representation after two fingers had been glued together for 24 hours, but it was not irreversibly

altered. Similarly, only after a full day of Braille reading did Braille readers reading fingers M1 representation demonstrate signs of expansion (Pascual-Leone et al., 1995); not after rest days without reading. Perhaps, previous support for sensorimotor plasticity following blindness was due to transient effects of immediate (Braille) experience, rather than blindness per se. This would be coherent with the S1 stability found in our anophthalmic participants. If so, some previous findings of sensorimotor plasticity (in blind individuals) may have been facilitated by short-term modulation of input gain (as e.g. seen during stimulation; Pleger et al., 2003) instead of substantial reorganisation due to an increased dependence on touch.

### Sensorimotor information of individual fingers is increased in hMT+ of anophthalmic individuals

In our anophthalmic participants, we found increased activity in hMT+ compared to sighted controls, consistent with other studies showing this for a range of conditions causing blindness (see Burton (2003); Sathian and Stilla (2010) for review). Yet, increased activity does not necessarily underlie functionally meaningful processing, but may also be observed because of increased noise (e.g. due to reduced inhibition) or task irrelevant processing. As an indication of emergent functional processes, we interrogated, using multivariate analyses, whether finger-specific information is conveyed in this activity. Finger-specific information, measured by classification, was increased in the anophthalmic individuals, suggesting some emergent sensorimotor hand-related process in the occipitotemporal cortex (see Beauchamp et al. (2009) for further support of a lack of finger information in the visual cortex of the sighted). Because the activity was not structured similarly to that in low-level somatosensory areas (greater overlap in representation across neighbouring fingers), we suggest any emergent process(es) is/are not a low-level addition to the sensorimotor network.

What non-primary sensorimotor function could be supported by the increased

activity in the anophthalmic individuals? Like its sighted counterpart, blind participants hMT+ is activated during motion processing, in multiple modalities (auditory, Poirier et al., 2005; tactile, Matteau, Kupers, Ricciardi, Pietrini, & Ptito, 2010). Our task, however, did not require any motion discrimination, either explicitly or implicitly. Alternatively, the finger-specific information could relate a more general role of the occipitotemporal cortex in body representation. Previous research has suggested that the lateral occipitotemporal cortex may be involved in visual (Downing et al., 2001), sensorimotor (Astafiev et al., 2004; Orlov et al., 2010) and action related (Peelen & Downing, 2005; Gallivan, 2014) body-part representation. Although we and others (Beauchamp et al., 2009) did not find any indication of single-finger information in the sighted, despite using a sensitive classification method, other studies have reported some increased activity in sighted hMT+ during hand movement (Astafiev et al., 2004; Orlov et al., 2010; Amedi et al., 2002; Beauchamp et al., 2007). As such, finger information could potentially occur latently in sighted individuals and become unmasked in the absence of vision (Kupers & Ptito, 2014). In fact, cross-modal influences (as opposed to repurposing) may be very common, even in the primary cortices. For instance, Kuehn et al. (2018) showed that viewing fingers can induce activity patterns in healthy participants S1 that are precise, selective and somatotopic; Zangaladze, Epstein, Grafton, and Sathian (1999) demonstrated a role for the visual cortex in tactile judgements; and related findings exist for other modalities (Zangenehpour & Zatorre, 2010). Together, these studies paint a complex picture of sensory specificity in sighted individuals, and opportunities for cross-modal reorganisation. A key consideration to help us disentangle this inconsistent evidence is that increased activity in itself is not strong evidence for reorganisation. Future studies should use well-defined criteria, e.g. organisational hallmarks, to support an interpretation of (low-level) cross-modal plasticity.

In light of the stable finger representation in S1, are the changes in LOTC suffi-

cient to explain the improved tactile performance of the blind? We were unable to correlate measures of brain organisation to behaviour directly given our low sample size. Yet, regardless of how finely tuned low-level representations are, performance on a psychophysical task also depends on the readout of such representations by higher-order areas. For tactile discrimination, readout is likely done in higher-order areas outside of S1 (Romo & Salinas, 2001; Stilla et al., 2007; Sathian et al., 2013) and can, like other decision-making tasks, be improved through training or experience. Notably, after minimal training, sighted controls may demonstrate similar tactile acuity to blind participants (Grant, Thiagarajah, & Sathian, 2000; see also Wong et al., 2011). If sighted controls can show expert tactile acuity, a reorganised occipital cortex is unlikely to be a necessary contributor in anophthalmic individuals. Still, future research should study the higher-order somatosensory and frontal areas involved in readout. If hMT+ plays a role in tactile decision-making in blind individuals, these areas would be expected to receive inputs from hMT+.

In this study, we used a specialised patient group to ensure the occipitotemporal cortex has never received any visual input. In other forms of (congenital) blindness, some input, e.g. retinal waves, may still access and influence the visual cortex during development (Watkins et al., 2013). Most studies on cross-modal activity in diverse congenitally blind populations still show effects indicating cross-modal plasticity (Kupers & Ptito, 2014), even in individuals who got blinded postnatally (typically within the first years; Bedny, 2017). If anophthalmic individuals are not representative of the greater blind population, their idiosyncratic development likely restricts the scope for cross-modal plasticity less than other blind individuals; not more.

To conclude, we have studied three congenitally blind individuals with a rare condition that makes them particularly susceptible to cross-modal plasticity. Although they showed superior tactile acuity compared to sighted controls, the anophthalmic individuals showed no signs of stronger finger representation in S1, suggesting this

area is organised similarly to that of sighted controls. In left hMT+, finger movements induced greater activity for the anophthalmic individuals than for controls. This activity did not express typical markers of low-level sensorimotor areas, but it contained finger-specific information. This suggest that area hMT+ can acquire some novel somatosensory processing that may not be typically present.

# Chapter 5

# Extreme foot behaviour

This is adapted from: Dempsey-Jones, H.*, Wesselink, D.B.*, Friedman, J. and Makin, T.R., 2019. Organised toe maps in extreme foot users. Cell Reports. 28, 2748-2756.e4.

* Equal contribution

## 5.1 Abstract

While the fine-grained features of topographic maps in somatosensory cortex can be shaped by everyday experience, it is unknown whether behaviour can support the expression of somatotopic maps where they do not typically occur. Unlike the fingers, represented in all primates, individuated toe maps have only been found in non-human primates. Using 1mm resolution fMRI we identify organised toe maps in two individuals born without either upper limb who use their feet to substitute missing hand function, and even support their profession as foot artists. We demonstrate the ordering and structure of the artists' toe representation mimics typical hand representation. We further reveal 'hand-like' features of activity patterns, not only in the foot area, but similarly in the missing hand area. We suggest humans may have an innate capacity for forming additional topographic maps that can be expressed with appropriate experience.

## 5.2 Introduction

The hand area of the primary somatosensory cortex (SI), and Brodmann Area (BA) 3b in particular, contains detailed digit maps, with physically adjacent digits showing greater representational overlap than non-adjacent fingers (Besle et al., 2014; Kaas et al., 1979; Sanchez-Panchuelo et al., 2012a; Thakur et al., 2012) (see Figures 5.3A and 5.6C). While the gross features of the canonical hand representation are highly consistent in humans (Ejaz et al., 2015; Kikkert et al., 2016; Kolasinski, Makin, Jbabdi, et al., 2016), the inter-finger selectivity may be shaped by experience: e.g., digits used more frequently together in daily life show more representational overlap (Ejaz et al., 2015), and vice versa (Gindrat et al., 2015).

We investigated whether extreme habitual foot behaviour might associate with organised toe maps in SI, where they have not been found in typically developed

humans (Akselrod et al., 2017), though identified in monkeys (Liao et al., 2016; Nelson et al., 1980). Using 7-tesla neuroimaging during passive toe touch, we studied foot representation of two individuals with developmental upper-limb amelia. Displaying exquisite compensatory adaptation, these individuals perform typically manual daily living tasks (e.g., dressing, feeding, typing) with their feet (see Figure 5.2A-C). Both use one foot for dextrous object manipulation, and the other for stabilising. Both are sufficiently skilled with their dextrous foot to allow writing, drawing and painting to a level that supports their profession as artists (two of only three such foot artists in the UK).

We studied toe activity patterns in the artists' SI foot area and sensorimotor (missing) hand area. Previous studies indicate that uni/bilateral congenital hand absence leads to remapping of inputs from the mouth and feet into the deprived hand/s territory (Hahamy et al., 2017; Hahamy & Makin, 2019; Stoeckel et al., 2009; Striem-Amit et al., 2018a; X. Yu et al., 2014, 2006). However, it is unclear whether such remapping truly represents recruitment of this zone to support toe function, or aberrant activity e.g., due to deprivation-driven inhibition reduction (Hahamy et al., 2017). To step beyond this highly common traditional approach of remapping in deprived cortex, we asked whether the missing hand cortex contained functional representational features of hand representation. Specifically, we focused on two critical representational hallmarks of hand representation in the primary sensorimotor cortices (BA 1-4), i.e., inter-digit selectivity and overlap patterns (Ejaz et al., 2015; Kikkert et al., 2016).

We anticipated that daily foot use to replace hand functions to drive rich and complex sensorimotor input patterns (Dempsey-Jones et al., 2016), which will further interplay with cognitive (Kuehn et al., 2018) and attentional (Puckett et al., 2017) factors to shape and/or consolidate cortical functional architecture. We therefore predicted that artists' toe representation (in both the foot and hand areas) would

resemble the canonical hand representation, i.e., more 'hand-like' in its pattern, compared to controls. This should occur primarily for the artists' dexterous foot due to its striking skill, but perhaps also for the stabilising foot that benefits from increased and specialised usage.

Each foot artist was separately compared to a group of typically developed and age-matched controls (using stringent tests developed specifically for case-study comparison, Crawford t-tests (Crawford & Howell, 1998)), allowing for test-retest verification of the results. Results for the stabilising foot are presented as Supplementary figure S2.

## 5.3 Methods

### 5.3.1 Participants

Foot artists (age 55 and 56, both male) completed all components of the testing procedures. The control group (n=21) were typically developed and age-matched (see Table S4 for full details of all participants). Fifteen controls completed tactile and motor testing (age, M=56.86, 8 males), of which 9 were also tested in the fMRI protocol (age, M=54.67, 4 males). A further 6 controls underwent tactile testing only (age, M=50.67, 3 males). Ethical approval was granted by the NHS National Research Ethics service (Ref: 10/H0707/29) and written informed consent was obtained from all participants prior to the study.

### 5.3.2 Experimental procedures

For participants who completed all three components of the study (sensory, motor, fMRI), data was collected over three separate sessions, completed on different days. Half the participants completed the sensory tasks then imaging, and the other half performed these tasks in reverse. The motor task was collected on a separate session.

All fMRI analysis was restricted to the primary sensorimotor cortex (except for the whole-brain contrasts shown in Figure 5.5).

All participants underwent a passive toe stimulation experiment (main experimental task), an active body-part movement task (localiser task) and a structural scan. A passive rather than active paradigm was chosen since individuated toe movements are impossible to produce consistently in controls (as demonstrated in our kinematics task, see Figure 5.8A); though both active and passive paradigms have been effective in demonstrating digit topography in the hand (Kolasinski, Makin, Jbabdi, et al., 2016; Sanchez-Panchuelo et al., 2012a) and body-part remapping (Hahamy et al., 2017; Stoeckel et al., 2009; Striem-Amit et al., 2018a; X. Yu et al., 2014, 2006).

The main experimental task involved repeated passive tactile stimulation of the foot digits at approximately 1 Hz rate. The design structure was adapted from (Diedrichsen et al., 2013). All participants underwent 4 runs per foot. Each run consisted of 3 repetitions of 12 s blocks of stimulation per digit interspersed with 4 rest blocks. Tactile stimulation was administered by an experimenter receiving auditory cues regarding the stimulation order and timing using Presentation software (version 0.70, www.neurobs.com). Each individual digit pad was touched with force sufficient to minimally deflect the digit. The tactile stimulus covered most of the pad of D2-D5; for D1, the entire pad could not be stimulated at once, and stimulation location was varied to achieve maximum tactile coverage across trials. In order to help the participants focus on the stimulation and maintain attention, they received minimal visual feedback during the block regarding which toe was stimulated (one of five circles on screen would flash when its corresponding digit was stimulated).

Furthermore, the participants were instructed to notice (but not respond physically) the incidence of 'catch trials', in which 1 tap was replaced by a rapid double tap (not reflected in the visual feedback; the remaining trials in the block did not change). There were five catch trials per run (1 per digit). Each run contained 5 catch trials (1

per digit). Prior to analysis we confirmed general activity to passive toe stimulation (average of all digits vs. rest) was equivalent between artists and controls, in both the foot and hand areas (see ROI definition below). This supports consistent brain responses to stimulation, justifying direct comparison. Critically, our primary measure of interest, inter-digit relationships reflected in multivariate patterns (see below) is largely invariant to general activity differences (Arbuckle et al., 2019; Berlot et al., 2018).

The active localiser task involved movement of the left or right foot (all toes flexion/extension), mouth (lip pursing) and rest blocks. Each condition was repeated five times (12s blocks) at roughly 1Hz frequency. Participants were visually instructed to move using text.

As part of an extended protocol, scanned participants also underwent two additional scans that were not included in the manuscript, and subsequently, will not be discussed here. These tasks involved a resting state scan and passive stimulation task using an alternative, phase-encoding protocol.

### 5.3.3 MRI acquisition

MRI measurements were obtained using a Siemens 7 Tesla Magnetom scanner with a 32-channel head coil. fMRI data was acquired using Multi-Band EPI (acceleration factor 2) with a limited (horizontal) field of view, capturing to superior portion of the cortex: 56 slices with a 192 x 192 in-plane field of view. The following parameters were used: spatial resolution: 1mm isotropic; TR: 2000ms; TE: 25ms; FA: 85 deg; phase partial Fourier: 6/8; and PE acceleration factor: 3. Fat suppression was done by CHESS.

Anatomical T1-weighted (MPRAGE) images consisted of a whole-brain single image with a 1 mm isotropic resolution. The following parameters were used: FA: 7 deg; TI: 1050 ms; TE: 2.82 ms; TR: 2200 ms. Fat suppression was done by means of

water excitation.

### 5.3.4 MRI analysis

#### fMRI pre-processing and low-level analysis

Data pre-processing, general linear model (GLM) analysis and cortical surface reconstruction were implemented using Freesurfer (www.freesurfer.net) and FSL (fsl.fmrib.ox.ac.uk/fsl). Connectome Workbench (www.humanconnectome.org) was used for visualization on the cortical surface. Additional scripts were written in UNIX or MATLAB.

Each run was pre-processed using FEAT 6.0, and included: motion correction, brain extraction, high-pass temporal filtering (100sec) and minimal spatial smoothing using a 1mm FWHM (full width at half maximum) Gaussian kernel (see (Hendriks et al., 2017) for the effect of smoothing on MVPA). The results from the motion estimates were inspected for excessive subject motion: no run contained more than 1 mm of relative displacement. Co-registration was carried out using FLIRT), and manually adjusted for accuracy. Anatomical T1 images were used to reconstruct the pial and grey matter surfaces using Freesurfer.

A voxel-wise GLM was applied to each of the task runs, as implemented in FEAT. The design was convolved with a double-gamma function and its temporal derivative. From the main task, 11 contrasts were defined per run: each individual digit versus rest (for multivariate analysis), each individual digits versus all other digits (for univariate analysis) and all digits versus rest. The voxel-wise estimates were averaged across the four runs for each participant using a fixed effects model. For the active (localiser) task, contrasts were defined for each body part versus rest, each foot versus mouth, and mouth versus the average of both feet.

### Regions of interest

ROIs for each of the foot and hand areas, as well as the mouth, were defined on the cortical surface. The anterior-posterior boundaries were constrained to BA 1, 2, 3a, 3b, 4a, 4p using non-thresholded single-subject parcellations from Freesurfer (www.freesurfer.net). For the foot region, ROIs were defined for each participant separately and within each hemisphere by applying the contrast 'contralateral foot versus mouth' (from the functional localiser described above) using threshold $Z>5$ and choosing the largest contiguous cluster. For the hand region, we used a mask from a previous study (Hahamy et al., 2017) based on group hand movement versus rest. This mask was then converted to individual's native anatomical space.

### Univariate analysis

To identify dexterous digit maps within the primary sensorimotor cortices, contrasts for each individual digit versus all other digits were first corrected for multiple comparisons using family-wise error ($Z>2.3$, cluster determinant $p<.05$; whole brain). Note that this minimal threshold was used in order to minimise Type II errors in controls i.e., missing subtle but present maps. For artists (Figure 5.3), maps were additionally thresholded based on a false discovery rate (FDR) criterion $q(FDR)<0.05$ (accounting for voxel-wise error within the sensorimotor strip) for each contrast separately. This additional step was taken to minimise Type I errors for the reported maps. The Z-values corresponding to the thresholds for the results corrected for FDR are reported in Table S3. Note that the latter step was wavered in Figure 5.4. Resulting maps were projected onto the participant's native inflated surface for visualisation.

To quantify the degree to which the digit maps followed a somatotopic organisation, co-selectivity was assessed. First, within each foot area (described above), for each digit, a sub-region was created from all voxels selective to that digit (according to the contrast above). Within each sub-region, we calculated the difference in

activity between the digit(s) directly adjacent to the most strongly active digit (i.e. the one used to define the sub-region) and the digits further away. These values were averaged across digits, ignoring any digit no voxels were selective for, resulting in a somatotopy score ($D_{soma}$), where a high score indicates somatotopic co-activation. The scores for controls were averaged across hemispheres.

### Representational similarity analysis

To assess the structure of digit-related activity, the similarities between single-digit activity patterns (derived from the pre-processing pipeline as elaborated above) were calculated for each foot in the contralateral hemisphere over the foot and hand ROIs. For each digit pair, the distance metric was the Mahalanobis distance (Ejaz et al., 2015; Nili et al., 2014), cross-validated over each possible pair of the 4 runs and then averaged. Because of cross-validation, the expected distance between identical conditions is 0 (and will therefore be negative half the time) (Nili et al., 2014). The resulting inter-digit distances were arranged in a dissimilarity matrix (RDM), and two measures were taken: individuation, i.e., the average inter-digit distances comprising the RDM; and the shape of the representational structure, i.e. the Spearman correlation between the individual RDM and a group inter-digit RDM for finger representation in the hand area (see Chapter 4). In brief, this hand matrix contained the group average representational dissimilarity values in S1 between the 5 digits of the dominant right hand of two-handed controls (N=9). The values were acquired at 7T using an active single-digit tapping task. The analysis pipeline was similar to above. This hand matrix was taken to represent the canonical activity pattern for the hand. Additionally, the RDM was (Spearman) correlated with the individual's dissimilarity values from the toe individuation kinematics matrices (see below). We used Spearman (rank) correlations, because parametric statistics may be problematic for RDMs containing only 10 unique cells (Bishara & Hittner, 2012).

As an aid to visualise the representational structures, we also used classical multidimensional scaling (MDS). MDS projects the higher-dimensional structure into a lower-dimensional space, while preserving the inter-digit dissimilarity values as well as possible (Borg & Groenen, 2005). MDS was performed on data from individual participants and (if applicable) averaged after Procrustes alignment (without rescaling) to remove arbitrary rotation induced by MDS. The between-subject standard error (in two dimensions, parallel and orthogonal to the direction of greatest error) is depicted by ellipses.

### 5.3.5 Behavioural analysis

#### Experimental procedures and instructions

We assessed the artists' compensatory motor skill through quantitative and qualitative measures. Full details of the quantitative measures (questionnaires) is available in Table S1. The Motor Activity Log is a clinical questionnaire previously validated to assess use of residual limbs and prostheses (e.g., Makin et al., 2013) here adapted for lower limbs. We used an adaptation of the Edinburgh Handedness Questionnaire (Oldfield, 1971) to assess preferred foot for performing 10 daily tasks. The tool use questionnaire assessed how often 42 different tools were used for their typical function with the upper/ lower limbs and mouth.

For quantitative assessment we used a kinematic motor task assessing motor individuation of the toes. Magnetic motion sensors (Ascension trakSTAR) were attached to the nail of each of the toes. An additional reference sensor was taped on the top of the foot. Participants were instructed to move one toe up and down at 1Hz rate (using auditory cures) while keeping all other toes still (Figure 5.1). There were two blocks per toe (10 blocks in total, order randomised). Please see https://osf.io/4q8cs/ for the full experimental protocol.

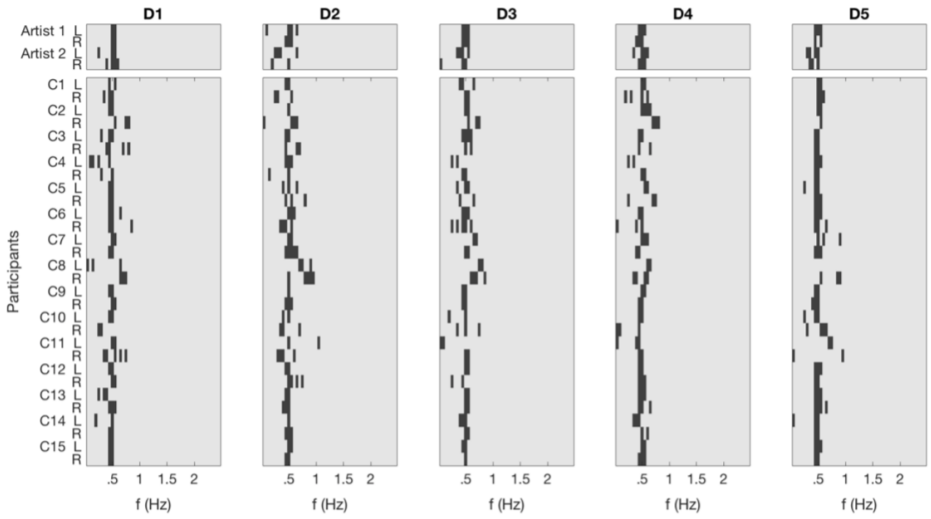



Figure 5.1: Validation of kinematic task performance for the instructed toe, related to STAR Methods. For each participant, a Fourier transform was performed on the kinematic velocity data to isolate the frequency of movements of the toe participants were supposed to move for that block. We determined whether this frequency matched the desired frequency of 0.5Hz, i.e., one up-down cycle every 2 seconds. We found that all participants were moving at the desired frequency (showing a peak within a small frequency range around .5Hz, see above), aside from two participants who had movement frequency outside the acceptable range for one-two instructed toes removing these participants from the analysis did not change our results. In sum, participants were performing the task as required with the instructed toe, indicating meaningful enslaving data could be gathered using this task.

### Calculation of digit individuation

As our measure of individuation, we calculated the Spearman correlation of movement velocity of the instructed and non-instructed toes. Negative correlations were recoded as their absolute values because these also indicate enslaving (though negative correlations were minimal, and when present were of low value  so there was no difference in the pattern of results when using raw correlational values). The resulting correlations were arranged into a 5 x 5 matrix with each cell representing the correlation of one possible pairing of toes (rows represented instructed toe conditions one to five, and columns the non-instructed toes; Figure 5.8A).

### Sensory Tasks

The foot stimulated was the dextrous foot for artists, or one selected (dominant) foot of the controls (typically right; see Table S4 for full details).

### Two-point orientation discrimination

This task involved presentation of a two-pronged instrument (spacing 2,3,4 and 5mm) to the big toe (D1) pad. These prongs were oriented either across or down (trial-by-trial), with respect to the proximal-distal toe axis, using descending spacing order (see (Craig and Johnson, 2000) for advantages of this task over the traditional two-point discrimination). Participants verbally indicated the orientation at each trial. Proportion of correct trials were averaged as a measure of inter-digit tactile spatial acuity.

### Temporal order judgements

Custom made vibrotactile stimulators (Dancer Designs) delivered two single, consecutive pulses (20ms) to either D1-D2 or D2-D3, one pulse per toe. The temporal distance between the two toes varied (inter-stimulus intervals (ISI) 30, 70, 100, 150,

200 and 300ms; 10 repetitions per ISI). Participants indicated which toe was stimulated first, by verbally reporting 'left' or 'right'. The proportion of correct trials was used as the measure of inter-toe tactile spatial acuity.

**Frequency discrimination**

Vibrotactile stimulators delivered two consecutive 500ms pulses of vibrational stimuli (ISI 1sec) to D2 (as described above). The frequency of the first stimulus was fixed at 16 Hz. The frequency of the second stimulus was either the same across the two pulses or different. The original difference between the two frequencies was set to 1.5Hz, and an adaptive descending staircase was used to determine the frequency discrimination threshold over 45 trials. Participants reported whether the two frequencies were the same or different. Three correct responses in a row led to a drop in frequency difference of 5% and one incorrect response to a 5% increase. Average staircase value (indicating frequency difference in arbitrary units) was used for comparisons between participants.

### 5.3.6 Statistical analysis

Statistical analyses were done using MATLAB R2016a. For all tests requiring comparison of the artists to controls, we used two separate Crawford-Howell t-tests to demonstrate test (artist 1), retest (artist 2) consistency. Crawford-Howell t-tests were developed and validated specifically for case-study comparisons: (Crawford and Howell, 1998). To defend our results from type I errors, we only accepted results that were independently observed as significant in both case tests. Therefore, further correction for multiple testing was not required. All statistical comparisons between artists and controls were carried using 2-tailed tests. Since control participants have no dexterous foot, when the same measures were available from both feet these measures were averaged and submitted for group comparisons after verifying no signifi-

cant differences across feet using paired t-tests (though note the difference between sides for behavioural kinematic distances, i.e., raw individuation was trending at p = .092). For the sensory task, we selected the right foot for testing in the majority of participants. Two individuals were tested on the left foot for comparison, but scores were highly consistent and were, therefore, collapsed across feet. Matrices were compared using Spearman correlations. We used Spearman (rank) correlations, because parametric statistics may be problematic for RDMs containing only 10 unique cells (Bishara and Hittner, 2012).

In figures, bar plots indicate the group mean of the controls and the error bars indicate the standard deviation within the control group. Multi-dimensional scaling plots indicate the (2-dimensional) standard error using ellipses. In group comparisons, individual data points represent individual participants (rather than trials).

## 5.4 Results

### 5.4.1 Hand-like foot use in artists' daily life

Assessment of the artists' daily motor repertoire using qualitative questionnaires revealed highly frequent and exceptional toe dexterity (Figure 5.2 and Video 1; for full results see Table S1). These measures indicated that artists performed the vast majority of daily life tasks with their feet (Motor Activity Log (MAL), see Makin et al, 2013; artist 1: 80%; artist 2: 76%) and with ease (MAL difficulty rating  rating 'not difficult'; artist 1: 80%; artist 2: 66%). They both showed clear laterality preference [artist 1: -100; artist 2: +83; as assessed using an adaptation of the classical handedness questionnaire (Oldfield et al., 1971)] and they have used almost all typical tools with their lower limbs (Tool Use Questionnaire, see Striem-Amit et al., 2018a; artist 1: 88%; artist 2: 90%).

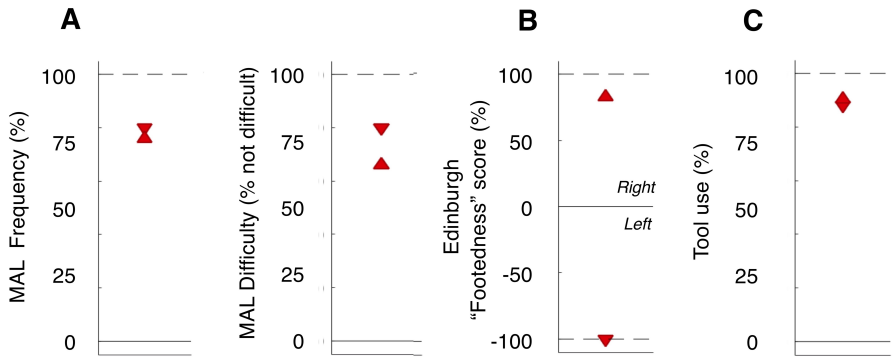



Figure 5.2: Assessment of hand-like foot use in the artist. A. Clinical (motor activity log), B. standard (handedness) and C. expert (tool use) questionnaire scores show close-to-ceiling appropriation of the feet for daily life functions normally involving hands. See also Table S1 and Video 1.

### 5.4.2 Somatotopic toe selectivity in artists but not controls

To describe somatotopic inter-toe selectivity, we used univariate selectivity contrasts between each digit and the average of the other four. As illustrated in Figure 5.3A, a typical hand map consists of digit-selective clusters, progressing from thumb (red, laterally) to little finger (pink, medially) (Sanchez-Panchuelo et al., 2012a). Similarly, both artists showed clear digit-selective clusters for 4 out of 5 digits of their dexterous foot, located in the medial wall of the contralateral postcentral gyrus (Figure 5.3C). Visually, the toe maps mimicked those identified in non-human primates in terms of gross macroscopic organisation and location on medial aspect of the postcentral gyrus (oriented medio-laterally) (Liao et al., 2016).

Using the same thresholds (q(FDR)<0.05), we were unable to observe clear topographic arrangement elsewhere in the sensorimotor strip. Using a more lenient threshold (Z>2.3), similar maps were also found for the artists' stabilising foot, similarly following medial-lateral D5-D1 somatotopic ordering (Figure 5.4). When examining each of the control participants' maps separately (n=18), even using a minimal threshold we only identified one potential rudimentary map (C05; left hemisphere), with selectivity for 3 toes. No other consistent toe selectivity was identified in con-

trols (Figure 5.3B and 5.4). These findings provide a preliminary demonstration of somatotopic toe maps, primarily for the artists' dexterous foot.

### 5.4.3 Somatotopic toe overlap in artists but not controls

We next examined somatotopic overlap by investigating the activity profile within a given digit-selective cluster (e.g. D1 cluster) to the non-preferred digits (e.g. D2-D5). Somatotopic overlap is defined as greater activity for directly adjacent digits vs. non-adjacent digits (Kolasinski, Makin, Jbabdi, et al., 2016). Both artists showed somatotopic gradients of activity levels (Figure 5.3D; see Figure S1 for individual control plots). To quantify somatotopy in the univariate analysis, we calculated activity difference between directly adjacent digit(s) and non-adjacent digits (Figure 5.3E). The score for the artists' dexterous foot was high (artist 1: 1.69 artist 2: 1.36) indicating somatotopic activity gradient, whereas, in controls, the ratio was not-significantly different from zero, though trending ($M = 0.24$, $SD = 0.36$, $SEM = 0.12$; one sample t-test, $t(8) = 1.99$, $p = .082$). Direct comparison revealed somatotopy was greater for artists compared to controls (artist 1: $t(8)=3.87$), $p=.005$; artist 2: $t(8)=2.98$, $p=.018$ (see Figure S2 for similar results for the artists' stabilising foot). This analysis indicates enhanced somatotopy of the artists' toe-map activity patterns.

### 5.4.4 'Hand-like' inter-toe activity patterns in the foot area of artists

The results described above are threshold- and cluster-size dependent. To examine fine-grained, threshold-free toe representation we studied the organisation of multivoxel activity patterns. We assessed inter-digit (dis)similarity, producing a 5 x 5 representational dissimilarity matrix ('RDM'; 1 cell per digit pair contrast; Figure 5.6A), previously extensively studied for hand representation (see Chapter 2).

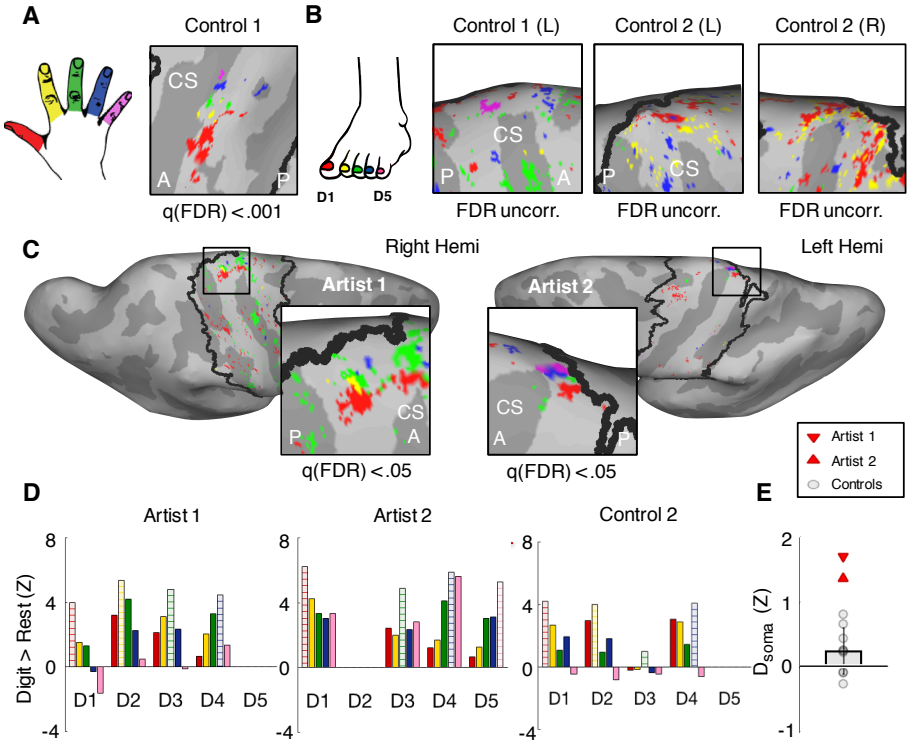



Figure 5.3: Toe maps in the foot area. Univariate selectivity maps (each digit vs. all others contrasts) are presented for A. The hand of one control participant (as a visual reference for 'hand-like' maps; lateral view). B. for the foot of the same control (dorsal view), and the feet of the median control (according to somatotopy scores, see D). Controls did not show topographic toe maps (even without FDR correction; see full results in Figure 5.4). C. Selectivity maps of the artists' dextrous foot (dorsal view) at the medial aspect of the postcentral gyrus contralateral to the dextrous foot, following the medio-lateral somatotopic organisation characteristic of hand maps. Values are FDR corrected (see Table S3). D. Mean activity for each digit (versus rest) in digit-specific clusters (D1-D5, correspond to big-to-little toe) shows topographic organisation for the artists' dextrous foot, but not for controls. Digits used to define each cluster are coloured using horizontal stripes. When no significant cluster was found for a digit, the corresponding space has been left empty (e.g. Artist 1, D5). Controls' result were averaged across hemispheres (See full results in Figure S1). E. Somatotopy score [$D_{soma}$; mean activity differences between neighbouring digits (of each cluster's strongest digit) and other digits] is higher for both artists, than for controls (n=9, averaged across hemispheres). Standard deviation for controls' scores is indicated by a vertical line. See also Figures 5.4, S1 and Table S3.

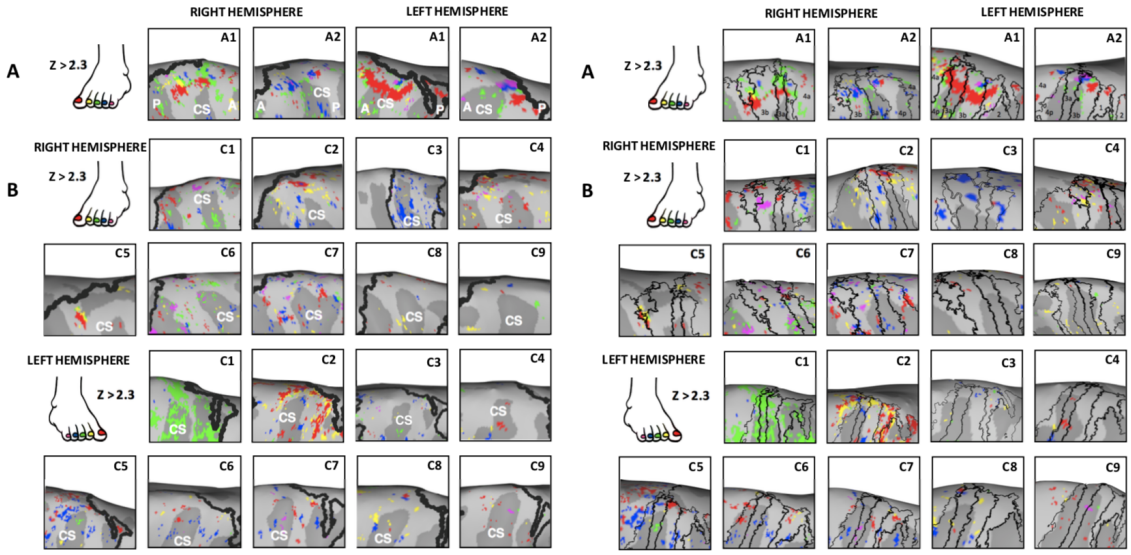



Figure 5.4: Individual toe maps in the foot area. Univariate contrast maps (activity for one digit vs. all others) illustrating selective activity to individual toes in the medial aspect of the central sulcus. Selectivity maps are presented for both hemispheres of artists and individual controls (showing activity for the contralateral foot). Left: Both artists displayed distinct clusters for 4-5 of their toes contralateral to both the dextrous foot (RH for artist 1 and LH for artist 2) and in Artist 1's stabilising foot, following the mediolateral topographic organisation characteristic of hand maps, and of toe maps in monkeys. Overall, controls did not show consistent topographic foot maps in either hemisphere; though see C5 who shows selectivity for digits 2-4 in a generally topographic order on the anterior-posterior plane. All maps are shown on inflated brains; individual digits are presented in different colours (see colour keys in the side panels). Right: The area demarcations for Brodmann areas 2, 1, 3b, 3a, 4p and 4a are shown. Images may be reoriented for clarity.

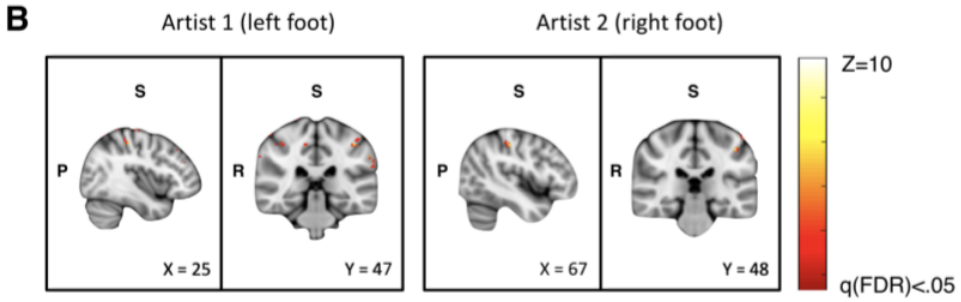



Figure 5.5: Whole brain contrasts for toe activity in artists vs controls. For each participant, an average activity map (across all toes) was generated for the whole brain (slab). Activity maps where then compared between each artist and the group of controls, using the Crawford- Howell t-tests, developed and validated specifically for case-study comparisons. The resulting group contrasts were corrected for multiple comparisons, using a false discovery rate q(FDR)<.05. Red clusters show areas of increased activity in the artists, compared to controls, relating to activity of the dexterous foot. Both artists showed increased activity in the postcentral sulcus, posterior to the central sulcus hand knob. This activity was bilateral for Artist 1 and contralateral for artist 2. No increased activity was observed in the proper S1/M1 hand area.

In the dexterous foot's region of interest (ROI; see Methods), we found no differences in overall activity levels between each of the artists and the controls (averaged across all toes; artist 1: $t(8)=0.36$, $p=.363$; artist 2: $t(8)=0.88$, $p=.404$). To investigate the representational structure of activity in this ROI we first examined the inter-digit RDMs (Figure 5.6A-B). Average inter-digit dissimilarity values (calculated per participant) tended to be higher for artists compared to controls (artist 1: $t(8)=2.01$, $p=.079$; artist 2: $t(8)=2.18$, $p=.06$; Figure 5.6D), suggesting digit representations were more individuated in artists, but this did not reach significance. Critically, however, we wished to examine the organisation of information within this area to determine whether the activity patterns reflected the predicted hand organisational structure, i.e., was toe representation more 'hand-like' for the artists than for controls?

We quantified hand-like representation by correlating the foot area's representational structure (RDM) with a canonical hand RDM, obtained from an independent

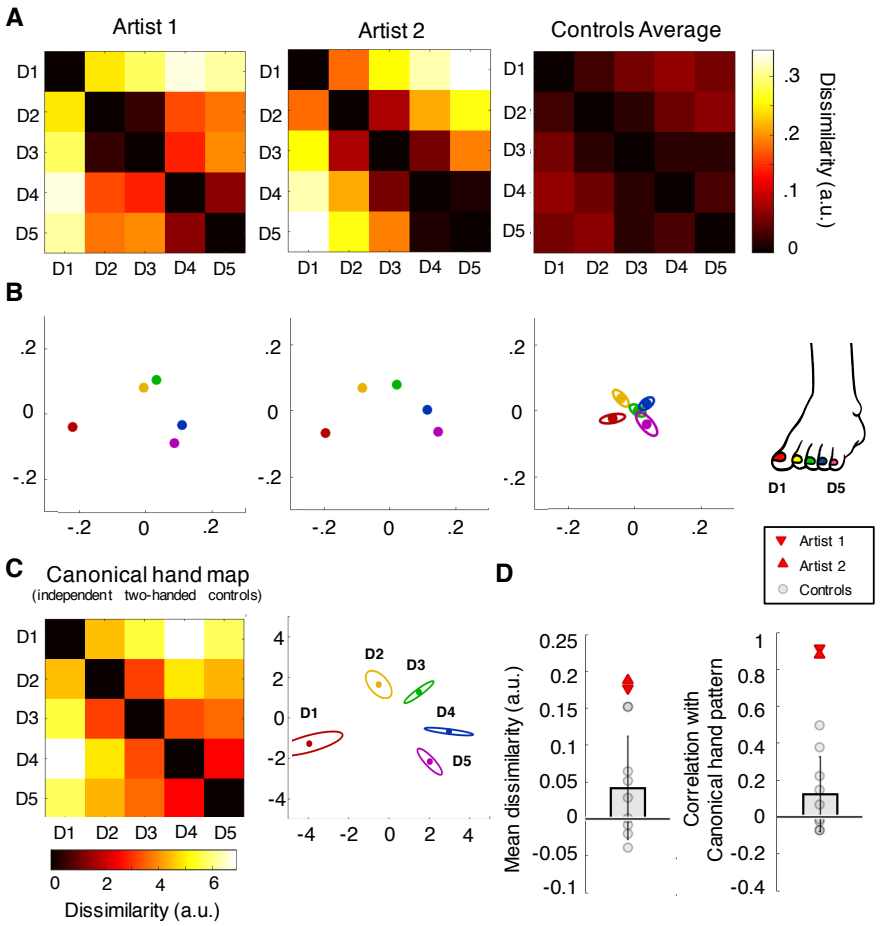



Figure 5.6: Toe activity patterns in the foot area, using representational similarity analysis. A. Representational dissimilarity matrices (RDMs) for the artists' dextrous foot and controls (average, n=9) showing dissimilarity (lighter colours) vs. similarity (darker colours) of inter-digit multivariate representation patterns (Mahalanobis distances). B. Dissimilarity between digit activity patterns represented by spatial distance, i.e., two-dimensional projections of the RDM, using multi-dimensional scaling. Individual digits are presented in different colours (see colour key in C); ellipses reflect controls' standard error after Procrustes alignment. C. As a visual reference, the matrix and projection for a canonical hand in the hand area of typically developed participants (average). D. Mean RDM dissimilarity values and correlations between toe RDM in the foot area and the canonical hand RDM for individual controls (grey) and the artists (red). Both artists showed a stronger correlation between canonical hand RDM and their toe RDM compared with controls, indicating more 'hand-like' patterns. Error bars show standard deviation across controls; a.u.: arbitrary unit. All other abbreviations are as described in Figure 5.3 legend. See also Figure S2 and Table S2.

group of typically developed individuals using similar imaging parameters [(D. B. Wesselink et al., 2019), see Figure 5.6C]. Both artists showed a high correlation (artist 1: rho=0.915, artist 2: rho= .879), resulting in a significantly more hand-like pattern compared to controls (Controls, mean rho (M)=0.125, SD=0.20; t(8)=3.67, p=.006 and t(8)=3.50, p=.008 for artists 1 and 2 versus controls, respectively; Figure 5.6D). This result supports the above observation of a hand-like toe map in the dexterous foot region of artists but not controls (see Table S2 for supplementary results in control ROIs). The stabilising foot of both artists was also more 'hand-like' than controls (see Figure S2).

### 5.4.5 Hand-like inter-toe activity patterns in the hand area of artists

We next examined toe representation in the artists' (missing) hand area, contralateral to the dexterous foot. Contrary to previous reports (Stoeckel et al., 2009; Striem-Amit et al., 2018a; X. Yu et al., 2014, 2006), we found no difference in toe activity levels in artists versus controls (artist 1: t(8)=0.78, p=.456; artist 2: t(8)=1.03, p=.333; see Figure 5.5 for whole-brain contrasts and Discussion). Inter-toe dissimilarity (average RDM) also did not differ significantly (both artists versus controls $p > .553$; Figure 5.7D). Importantly, when examining the hand area representational structure, we found that the dexterous foot's toe representation was significantly more hand-like in both artists compared to controls (artist 1: rho=0.576; artist 2; rho=0.515; Controls M=-.092, SD=0.22). This was demonstrated by a significantly greater correlation between the foot and the canonical hand RDMs in both artists versus controls (artist 1: t(8)=2.85, p=.022; artist 2: t(8)=2.88, p=.020; Figure 5.7D). This result demonstrates that toe-related activity in the missing hand area is at least loosely organised, and that this organisation mirrors native hand organisation features.

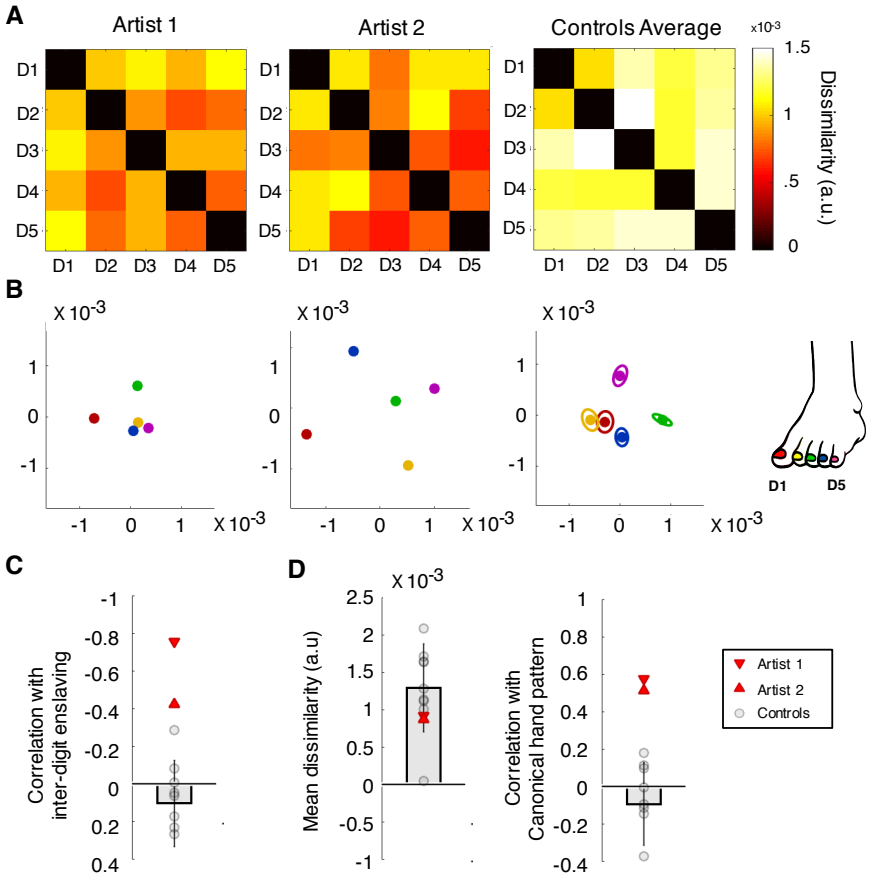



Figure 5.7: Toe activity patterns in the hand area, using representational similarity analysis. A. Representational dissimilarity matrices (RDMs). B. Spatial two-dimensional representation of dissimilarity. C. Correlations between toe RDM in the hand area and toe individuation matrix during free movement (kinematics; Figure 5.8A) were stronger for both artists than controls. D. Mean RDM dissimilarity values, and the correlation between toe RDM in the hand area and the canonical hand RDM. Both artists showed greater hand-like correlation compared with controls (n=9). All other details are as in Figure 5.6 legend. See also Figure S2.

### 5.4.6 Greater correlation between toe representation and toe kinematics in artists

We next studied correspondence between brain activity and individuals' ability to individuate their toes during free movement. For this purpose, we recorded inter-toe kinematics, asking participants to move one ('instructed') digit while keeping the other ('non-instructed') digits still, producing a 5x5 inter-toe motor independence/enslaving matrix (Figure 5.7D). This kinematic matrix was correlated with the toe (RDM) matrices identified in the foot and hand areas.

Despite the artists' exceptional foot dexterity, their net ability to individuate toes in free movement, measured using the mean kinematics matrix, did not differ from controls (n=14; artist 1: $t(14)=0.24$, $p=.816$; artist 2: $t(14)=0.72$, $p=.485$; full details of the task design, analysis and unpublished results can be found in https://osf.io/4q8cs/). Importantly, the organisation of the artists' kinematics matrices with respect to brain organisation was distinct from controls. Specifically, the artists' respective inter-digit enslavement patterns (as captured using kinematics) correlated more strongly with their brain activity pattern (toe RDM pattern), compared to controls (perhaps driven by D1 individuation in both brain and behaviour, see Figure 5.8A). This resulted in significant differences between either artist vs. controls in the hand area contralateral to the dexterous foot (Controls, M=0.103, SD=0.23; artist 1: rho=-.758, $t(8)=-3.96$, $p=.004$; artist 2: rho=-.424, $t(8)=-2.42$, $p=.042$; see Figure 5.7C). A similar pattern (albeit not consistently significant, as artist 2 was only showing a trending effect) was found when comparing kinematics with the toe RDMs of the foot-area (Controls M=-.168, SD=0.28; artist 1: rho=-.867, $t(8)=-2.66$, $p=.029$; artist 2: rho=-.709, $t(8)=-2.06$, $p=.073$). This analysis demonstrates that the patterns of foot movement are more strongly reflected in brain activity patterns of the artists, supporting a role for usage in shaping some aspects of the organised toe representation (alongside other sensory and higher-order usage-related factors,

see Discussion).

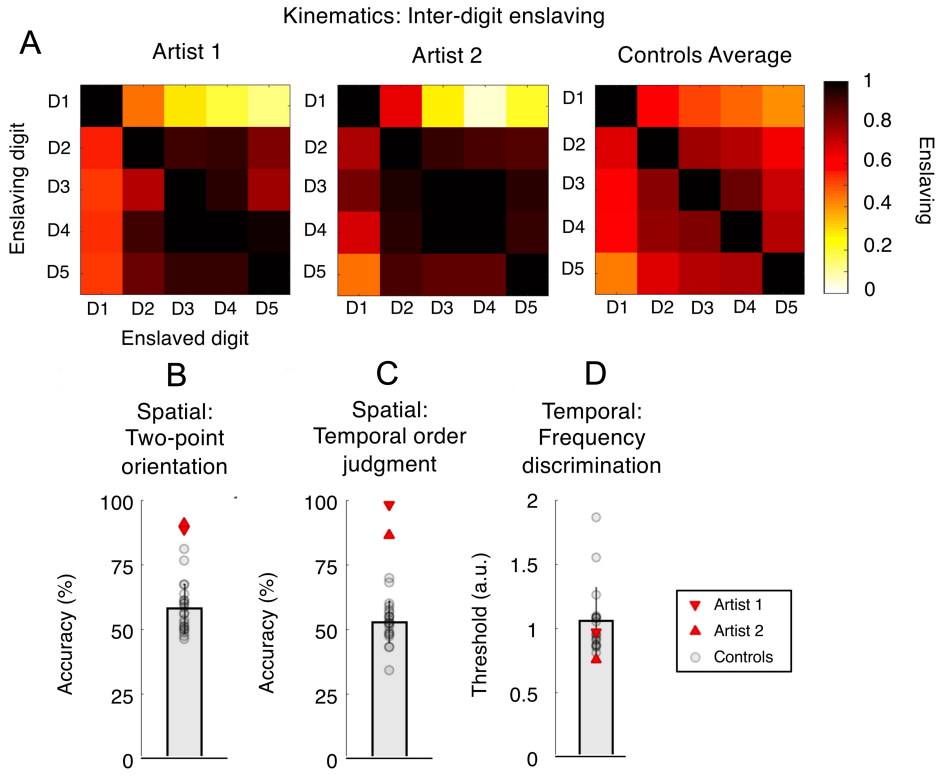



Figure 5.8: Assessment of hand-like foot use in the artist. A. Kinematic toe individuation in free-movement across digit pairs. Artists' mean kinematics were not different from controls (n=9). B Temporal order judgement (on D1). C. Two-point orientation discrimination (on D1-D3). D Temporal frequency discrimination (on D1). Both artists displayed superior inter- and intra-digit tactile spatial acuity compared to controls, but not temporal tactile acuity.

### 5.4.7 Enhanced tactile perception for the toes of artists

Finally, we tested spatial and temporal measures of tactile perception, previously shown to benefit from increased cortical magnification (W. M. Jenkins et al., 1990; W. Jenkins et al., 1990; Recanzone, Merzenich, & Jenkins, 1992). Both artists showed superior tactile spatial acuity with their dextrous foot compared with controls (n=21), as demonstrated in greater intra-toe orientation discrimination ($t(20)=2.27$, $p=.033$ for each of the two artists) and inter-toe temporal order judgements (artist

1: t(20)=3.37, p=.003; artist 2: t(20)=2.50, p=.021), but no differences in tactile temporal frequency discrimination (artist 1: t(19)=-.08, p=.938; artist 2: t(19)=-.28, p=.783; Figure 5.8D). This suggests improved spatial (but not temporal) tactile perception, perhaps due to incidental sensory 'training' through usage (Dempsey-Jones et al., 2016; Harrar et al., 2014), or from changed brain organisation resulting from a combination of deprivation and training (Dempsey-Jones, Themistocleous, et al., 2019; Grant et al., 2000; Heller, 1989); though see Stoeckel, Pollok, Schnitzler, Witte, & Seitz, 2004 for worsening of light touch in bilateral amelics).

## 5.5 Discussion

Here we asked whether we could identify representational features of functional brain organisation that do not exist in controls, in foot artists demonstrating an extreme form of habitual behavioural adaptation. First, we identified somatotopic toe maps in artists, but not typically developed two-handers. We also found multivariate toe activity patterns showed a greater correspondence with the canonical hand organisation (i.e., were more 'hand like') in artists than controls. This was seen for both feet in the foot region, and in the (missing) hand area for the dextrous foot only. Finally, artists had a stronger association between brain and kinematic toe individuation patterns for their dexterous foot, as well as heightened spatiotactile toe perception compared to controls.

### 5.5.1 Complexity in bodily experience

As stated in the introduction, the dramatically divergent profile of the artists' toe behaviour likely supports their detailed toe organisation in the brain. This habitual behaviour extends well beyond extreme motor skill (e.g., striking compensatory behaviours and tool use with the feet and toes, including feeding with cutlery, writ-

ing/ drawing and computer use; see Figure 5.2 and Table S1). For example, the artists' lives spent largely without enclosed footwear will have dramatically altered inter-toe cutaneous stimulation, previously shown to modulate finger selectivity in BA3b (W. M. Jenkins et al., 1990; X. Wang et al., 1995). Visual experience of touch (Kuehn et al., 2018) and spatial attention to tactile stimulation (Puckett et al., 2017) both induce digit-selective activity in SI, and likely also play a role in the generation and maintenance of the artists' somatotopic toe maps. This range of motor, sensory, attentional and cognitive factors accords with the presence of the artists' toe maps in their foot area for both feet (see below for further discussion of foot laterality).

Despite a clear superiority in their toe behavioural repertoire (e.g., in writing and drawing and other tasks detailed in the qualitative analysis), we did not find enhanced individuation of single-toe movement in artists compared to controls using our kinematic task. As such, active toe individuation may not be a critical feature that defines the artists' brain and behaviour (see Ejaz et al., 2016 for similar results in musicians). Indeed, the natural statistics of action (Ingram et al., 2008) which have been identified as the critical link between motor behaviour and sensorimotor brain organisation (Ejaz et al., 2015), encompass complex inter-digit synergic coordination and the resultant sensory and cognitive inputs. Thus, while our task captured rudimentary aspects of motor control that were relevant to functional brain organisation in the artists (as indicated by greater brain-behaviour correlation, versus controls), brain activity may be more completely explained by habitual daily behaviour.

### 5.5.2 Latent genetic template

Medial-to-lateral D5-D1 toe somatotopy has previously been documented in macaques (Liao et al., 2016; Nelson et al., 1980), although toe selectivity may be weaker than that for fingers (Hashimoto et al., 2013). Given the qualitative similarities in terms of gross macroscopic organisation and brain location/ position between the toe map of

non-human primates and our artists, it may be that humans are born with a genetic predisposition for developing toe maps, given sufficiently complex sensorimotor input (L. A. Krubitzer & Prescott, 2018). In non-foot-users, due to the lack of relevant experience, individualised toe representation would fail to develop from its genetic template. Alternatively, toe somatotopy may be realised at birth, but deteriorates due to habitual cooperative toe movement and imprecise tactile input (as seen in rodents' barrel cortex following whisker trimming (Feldman & Brecht, 2005). The latter theory raises the interesting prediction that somatotopic toe mapping may exist in human infants.

### 5.5.3 Bodily experience in the critical period

Our previous work has emphasised that timing of sensorimotor experience is critical for somatotopic organisation. For instance, hand representation persists in arm amputees despite decades of non-use of their missing hand (see Chapter 3). Conversely, people with congenital unilateral limb loss show no organised finger representation for their missing hand. Thus, it appears that early life bodily experience is necessary for the development, but not maintenance of somatotopic maps. Also supporting the timing of experience, some individuals who lose their upper limbs in early childhood were reported to develop extreme toe motor skills akin to those seen in congenital limb loss (X. Yu et al., 2014, 2006). In contrast, it has not been possible thus far to train typically developed adults to improve toe individuation (J. Friedman & Goodman, 2016). Non-lateralised foot-use in early life may also explain the artists' toe maps in the foot area for both feet. Dexterity develops over an extended period over childhood (Michel et al., 2016), meaning semi-skilled behaviour of both the left and right feet in early childhood may have shaped toe somatotopy before the artists developed a dextrous foot preference. Accordingly, finger representation in the typically developed hand area shows no clear differences for the dominant/dexterous versus

stabilising hand (Barnsley & Rabinovitch, 1970; Boakye et al., 2000; Steenhuis, 1999; White et al., 1997).

### 5.5.4 Foot representation in the hand area

Previous studies reported lateral activity clusters in the cortical hand area, in addition to the medial foot area, in response to toe movement in individuals with bilateral congenital amelia (Stoeckel et al., 2009; Striem-Amit et al., 2018a); see also (Hahamy et al., 2017; Hahamy & Makin, 2019)) and passive toe stimulation in individuals with early childhood arm amputation (X. Yu et al., 2014, 2006). Common to all such studies is the usage of univariate fMRI activity, where net changes in signal amplitude are averaged over a region of interest. This method solely informs on whether foot-related brain activity is statistically increased in the missing hand area, e.g., relative to baseline, other body parts or a control group. As such, these previous studies are unable to determine whether such activity represents functional reorganisation supporting sensorimotor foot processing [such as demonstrated using TMS (Stoeckel et al., 2009)], or simply non-functional activity changes subsequent to absence of hand-inputs [e.g., due to upstream reorganisation: (Kambi et al., 2014), aberrant signalling (Vaso et al., 2014), changed local metabolism (Cirstea et al., 2017), or decreased inhibition (Hahamy et al., 2017)].

Multivoxel pattern analysis allows us to decipher the information content underlying changed activity, or even in the absence of activity changes (Haynes and Rees, 2005; Kamitani and Tong, 2005). As this analysis is also able to identify consistencies in representational structure when activity levels are different (Arbuckle et al., 2019; Diedrichsen et al., 2013) it provides a measure dissociated from univariate activity, and is arguably better suited to identify representational changes. As such, it can uncover persistent or changed brain organisation, which might be buried under the net activity changes producing remapping, or even non-functional activity changes (see

previous section). This approach allowed us to determine whether the deprived brain area (whether undergoing clear remapping or not) actually contains representational features that may be relevant for the enhanced foot use repertoire of the artists.

Our multivoxel patterns analysis revealed that the missing hand area contralateral to the dextrous foot shares representational features with a canonical hand representation, beyond what is found in controls. We previously speculated that representations in the missing-hand territory of congenital one-handers can be flexibly distributed to body parts that share the same functional utility as the missing hand (Hahamy et al., 2017) (though others have argued against the role of altered bodily experience in shaping topography (Striem-Amit et al., 2018)). According to our adaptive-usage account, synergistic inputs that more closely mimic the missing hand's function across body parts and sensory systems (e.g. mouth-foot interaction in feeding with the feet; visuomotor interactions when manipulating objects) may consolidate preferentially in the missing hand territory, due to large-scale connectivity architectural constraints (Graziano & Aflalo, 2007; B. Mahon & Caramazza, 2011). Our current results lend empirical support for the relationship between compensatory behaviour and brain reorganisation, as demonstrated by the correlation between activity patterns in the missing hand area and the artists' ability to move their toes independently in motor action. This may indicate the (typical) hand territory need not necessarily represent the hand per se, but rather any other body part that can mimic the missing hand's functionality.

### 5.5.5 Conclusions

We identified key features of canonical hand representation in the foot representation of handless individuals who use their feet to substitute missing hand function that considerably exceeds that seen in two-handed controls. Given that it has not yet been possible to improve foot dexterity with training in two-handed adults (Friedman and

Goodman, 2016), it remains an outstanding challenge to delineate the competing roles of genetics, behaviour and developmental plasticity in shaping this distinct functional organisation.

# Chapter 6

# Localised input loss

This is adapted from:

Sanders, Z.-B., Wesselink, D.B., Dempsey-Jones, H. and Makin, T.R. (2019) Similar somatotopy for active and passive digit representation in primary somatosensory cortex, bioRxiv, 754648.

&

Wesselink D.B., Sanders, Z.-B., Edmondson, L.R., Dempsey-Jones, H., Kieliba, P., Themistocleous, A.C., Kikkert, S., Emir. U., Diedrichsen, J., Saal, H.P. and Makin, T.R. (In prep). Malleability of the cortical hand map following a single digit nerve block.

## 6.1 Abstract

Classical primate studies demonstrate that following single digit amputation, the deprived cortical territory becomes responsive to passive input from its neighbouring digits, demonstrating the capacity of the primary somatosensory cortex (SI) to reorganise. Yet, little research has been carried to characterise the impact of such local reorganisation on the entire hand map, known to comprise of lateral inhibitory circuitry. Here we investigated the malleability of the SI hand map in the acute phase of deprivation. 15 participants attended two 7T MRI scanning sessions involving both active and passive stimulation of single digits. approx. 2 hours prior to one session, participants received a localised pharmacological nerve block of digit 2 (D2). Contrary to classical findings, on this short timescale, no significant activity increase was found for the neighbouring digits in the blocked territory, using both passive and active stimulation. Instead, we identified a significant decrease in digit selectivity across the entire hand map with passive stimulation, i.e. in the non-blocked territory. With active stimulation, no selectivity changes were found in the digit map. This indicates that in the acute phase of input loss, activity changes for passive stimulation extend well beyond the deprived cortical region, but additional input associated with the active task can offset this change. To further characterise larger-scale effects to local input loss, we interrogated inter-digit similarity using multivariate pattern analyses, extensively used to characterise human hand representation. Our results demonstrate that local deprivation triggers rapid large-scale activity changes, while inter-digit relationship are maintained.

## 6.2 Introduction

In the preceding chapters, we have seen that hand representation in S1 does not fundamentally change after upper limb amputation or other impactful forms of input

change. This is in contrast with many studies in the animal literature that show apparent adult sensorimotor plasticity following input change (see chapter 3). We have argued that the stability in human amputees is because they can be instructed to move their phantom hand (provided their percept is vivid and kinaesthetic ability good enough), that if animal subjects were to move their phantom limbs, they would also show stable hand representation, but one may offer an alternative explanation. Given the stability shown in this thesis so far, across multiple populations, one may doubt it is possible to affect hand representation at all in humans.

In order to test whether targeted input deprivation in adulthood would affect hand representation, we deprived participant of the (somatosensory) afferent input from one digit. 15 participants attended two MRI scanning sessions involving both active and passive stimulation of single digits. Approx. 1 hour prior to one session, participants received a localised pharmacological nerve block of digit 2 (D2), resulting in abolished tactile perception to D2 (Figure 6.2B). We predicted that mechanisms of plasticity discovered in animal models would affect S1 at this timescale, i.e. that it is indeed possible to measure representational change in adulthood using fMRI. Simultaneously, however, we also predicted that certain aspects of hand representation would stay preserved. Preliminary results are presented below.

## 6.3 Methods

### 6.3.1 Participants

Fifteen healthy volunteers (6 female, age = 26.44 $\pm$ 1.04) were recruited for this study. All participants except one were right handed and all experimental tasks were performed using the right hand. All participants gave written informed consent and ethical approval for the study was obtained from the Health Research Authority UK (13/SC/0502).

One participant was excluded as an outlier from the passive multivariate task analysis (>3$\sigma$ below group mean during injection session). This participant was included in the active condition where their results were within normal group variance (0.3$\sigma$ above group mean).

### 6.3.2 Experimental procedures

Participants attended two near-identical sessions. A pharmacological finger nerve block was carried out during one of the two sessions (in counter-balanced order). In both scan sessions, the participants completed an active and a passive task, resting-state and spectroscopy scans. In the baseline session, data was collected using an (active) functional localiser task, which was used to define the region of interest with.




Figure 6.1: Experimental timeline. Time is indicated in mins (total time 3.5 hours for baseline session, 4 hours for injection session). Testing sessions were counterbalanced. In the baseline scan the phase-encoding always preceded the active task, however the order of the passive and the phase-encoding + active task was counterbalanced. The red line indicates time spent inside the scanner and the blue line indicates time spent outside the scanner. The green circles and yellow squares indicate tasks in and out of the scanner

### Pharmacological nerve block

Half the participants received the nerve block in the first session and half received it in the second session. The pharmacological nerve block consisted of a mixture of 2 mL of lidocaine 2% and 2 mL of Bupivacaine hydrochloride 0.5%. Both anaesthetics are commonly used for minor surgeries or in dental practise. This combination allowed for both a rapid onset of the anaesthetic effect, as well as a long lasting effect of 5 - 8 hours (depending on blood circulation). The solution was injected around the base of the right index finger forming a ring block, with approximately half of the solution injected on each side of the finger.

### Sensitivity testing

In order to verify the effectiveness of the pharmacological nerve block, measures of tactile sensitivity were carried out. A plastic domed grating with a grating width of 3.5mm was briefly applied to the glabrous surface of the distal index finger of the right hand by the experimenter. The participants were asked to indicate via mouse click (with their left hand) whether the grating was oriented vertically or horizontally over 20 trials. Accuracy below 70% was considered indicative of a successful nerve block. This was the primary measure of sensitivity used in this experiment and was carried out at four time points: an initial test shortly after the injection, immediately prior to scanning start, immediately after scanning finish and at the end of the behavioural session (see figure 6.1). During the first test the adjacent, middle finger was also tested in order to check for any spill-over effect of the anaesthetics or for any effects that the nerve block may be having on general concentration or attention. Tactile sensitivity was also assessed using Von Frey hairs. Two hairs of different forces (2.0 mN and 8.0 mN) were applied to the glabrous surface of the distal index finger. Participants were asked to indicate whether the pressure they felt was high or low over 20 trials. Accuracy below 70% was considered indicative of successful nerve block. Sensitivity

measures were also carried out during the baseline testing session in order to check for normal tactile sensitivity without nerve block.

### Active task

During the active task, participants were required to move individual digits by making button presses on a MRI-safe keyboard with five keys (Berlot et al., 2019). The digit to be moved in the upcoming block was indicated by a visual display of five grey bars, with one highlighted green  indicating the digit to be moved during the upcoming block. In each trial participants were required to move a cursor from the starting position (inside a grey box at the lower part of the screen) into a green box that appeared above the grey box by pressing the relevant keyboard key. After hovering the cursor inside the box for 400ms they received a point for successful completion, and were instructed to release the force on the keyboard key  allowing the cursor to fall back into the starting position grey box, ready for the next trial. Participants completed 12 trials per digit before receiving instructions for the next digit. The keys required force application to activate, though the actual displacement of the digit was low (approx. 10mm).

### Passive task

In the passive stimulation task, participants were asked to rest their right hand in a comfortable, supine position on a foam support. The experimenter used a plastic probe to stimulate each digit by tapping the probe against the distal pad of the digit at a 1Hz rate for twelve seconds, before moving on to the next digit. During the task participants were shown five white dots on the screen, corresponding to each of the five digits. The dots flashed individually at a rate of 1/second whilst the digit was being stimulated. To promote engagement across the duration of the task, double taps would be administered randomly (one double-tap per digit condition in

each session). Participants were asked to indicate when they felt the double taps by pressing a button on a button-box placed in their left hand.

#### Digit-selective clusters localiser

A travelling wave task was used as an independent functional localizer for digit-specific regions-of-interest (ROIs). The travelling wave protocol involves a set digit conditions cycle. This approach is particularly useful to selectively locate voxels that show an enhanced response to one digit compared to all other digits, and has previously been used to identify SI digit somatotopy (for example: (Kikkert et al., 2016; Kolasinski, Makin, Jbabdi, et al., 2016; Sanchez-Panchuelo et al., 2010).

Participants used the same keyboard and visual display as in the active task. Two separate scans with reverse orders (forward and backward cycles) were used to overcome potential order-related biases due to the sluggish haemodynamic response. In the forward scan, the order of digit blocks cycled from digit 1 to digit 5 (D1-D2-D3-D4-D5) whereas the reverse order was used in the backward scan (D5-D4-D3-D2-D1). In each scan, the cycle was repeated five times continuously with no rest periods in between. During the cycles, each digit was moved 8 times (at 1Hz) before the instructions for the next digit were shown. As in the active task, at the start of each block, the digit to be used in the upcoming block was visually cued, then 8 digit presses were made, before receiving the cue for the next digit.

### 6.3.3 MRI acquisition, pre-processing and low-level analysis

All MRI measurements were acquired using a Siemens 7 Tesla Magnetom scanner with a 32-channel head coil. Task fMRI data was acquired using a multiband EPI sequence with an acceleration factor of 2 (Moeller et al., 2010; Uurbil et al., 2013). A limited field-of-view was used consisting of 56 slices each 1mm thick over the primary somatosensory cortex with a 192x192mm in-plane FOV (TR 2000ms, TE 25ms, FA

85deg, GRAPPA 3). This resulted in spatial resolution of 1mm isotropic.

A whole brain anatomical T1-weighted image was also collected with a 1mm isotropic spatial resolution (TR 2200ms, TE 2.82ms, FA 7deg, TI 1050ms).

1H magnetic resonance spectroscopy (MRS) data was acquired and preprocessed as described in Lunghi, Emir, Morrone, and Bridge (2015). A 2 x 1 x 1 voxel was placed manually over the hand knob in S1, using the collected T1-weighted anatomical scan. Three guidelines were followed to motivate correct placement (in order of importance): 1) the voxel avoided the dura matter, to prevent signal issues; 2) the voxel was placed posterior to the central sulcus, to limit the influence of M1; and 3) the voxel was placed as far superior as possible, to focus on the hand region. Because these guidelines could not be followed in all participants and sessions, some participants' data could not be used. In the end, in only 10 participants, the placement was good enough in both sessions to produce reliable spectra.

### MRI pre-processing

All MRI data pre-processing and analysis was carried out using FMRIB Software Library (FSL; version 6.0) as well as Matlab scripts (version R2014b) which were developed in-house. Surface reconstruction was carried out using Freesurfer (Dale et al., 1999; www.freesurfer.net) and results from the task and travelling wave analysis were projected onto the cortical surface for visualization purposes using Connectome Workbench software (www.humanconnectome.org).

### Pre-processing

Standard pre-processing steps were carried out using FSL (Jenkinson, Beckmann, Behrens, Woolrich, & Smith, 2012). FSL's Expert Analysis Tool (FEAT) was used to carry out motion correction (using MCFLIRT; Jenkinson, Bannister, Brady, & Smith, 2002) brain extraction (BET; (Smith, 2002) spatial smoothing using a 1mm

full width at half maximum (FWHM) Gaussian kernel and high pass filtering using a cut-off of 100s. The output from the MCFLIRT analysis were visually inspected for excessive motion (defined as $>$ 1mm absolute mean displacement). No participants had an absolute mean displacement greater than 1mm.

#### Image registration

in order not to bias any analysis to a particular session or task, registration was done using midspaces, i.e. average spaces in which the images are minimally reoriented. For each participant, a midspace was calculated between the four active and four passive scans, i.e. the average space in which the images are minimally reoriented. Each scan was then aligned to this session-midspace using FMRIB's Linear Image Registration Tool linear registration (FLIRT; Jenkinson et al., 2002; Jenkinson & Smith, 2001).

Midspaces for both sessions were aligned to each other to create one midspace for all sessions. Manual adjustments were made when needed to ensure an accurate co-registration of the hand-knob. All scans were aligned to this midspace. Registration was run separately for the functional localiser scans and consequently registered to the study midspace using FLIRT.

Each participant's (functional) midspace was manually coregistered to their native anatomical scan.

### 6.3.4 fMRI analysis

#### Active and passive tasks

A voxel-based general linear model (GLM) analysis was carried out on each of the 8 scans (4 active and 4 passive) using FEAT, to identify activity patterns for each digit condition. The design was convolved with the double-gamma haemodynamic response function, as well as its temporal derivative. Eleven contrasts were set up: each digit

versus rest, each digit versus all other digits and all digits versus rest. The estimates from the four active/passive scans were then averaged voxel-wise using a fixed effects model with a cluster forming z-threshold of 3.1 and family-wise error corrected cluster significance threshold of $p < .05$, creating eleven main activity patterns for each task. These contrasts were used for the key analyses described below.

### Localiser & Regions of interest definition

The travelling wave task described above was used in order to identify digit-specific voxel clusters. The analysis was carried out as in Kikkert et al. (2016). In short, a reference model was first created using a convolved hemodynamic response function to account for the hemodynamic delay. This model consisted of an 8 second 'on' period followed by a 32 second 'off' period to model the movement block of one digit for one cycle. The model was shifted 20 times by one lag of 2 seconds (runs were acquired with a TR of 2s) in order to model one entire movement cycle (which lasted 40s), thus resulting in 20 reference models, this was repeated five times to model the five cycles in each scan. Following this the pre-processed BOLD signal time course for each voxel was correlated with each of the reference models. This resulted in cross correlation r-values, which were standardized using the Fisher's r-to-z transformation. Lags were assigned to each digit (four lags per digit) in order to average the r-values across scans for each voxel. This resulted in a r-value for each digit which was further averaged across the forward and backward runs. To define digit specificity, each voxel was assigned to one digit using a 'winner-takes-all' approach. This was done by finding the maximum correlation for each voxel across the five averaged values, and assigning the voxel to the corresponding digit.

To correct for multiple comparisons, a false discovery rate (Benjamini & Hochberg, 1995) threshold ($q < 0.01$) was applied to each digit individually (as in Kikkert et al., 2016 ; see supplementary materials for average cluster size, and results from the same

analysis using a more conservative threshold). The resulting FDR corrected digit-specific voxels were then used to create digit-specific clusters showing strong digit selectivity for each of the digits. This was done by using an anatomically defined mask of the hand region which was defined for each participant based on a Freesurfer structural segmentation of SI subdivisions. Broadmann Areas 3a, 3b and 1, spanning a 2cm strip medial/lateral to the anatomical hand knob was included the mask (see Chapter 3). The digit specific activity under this mask was used to create digit-specific clusters (see figure 6.2A for example). This approach allowed us to identify digit-specific clusters on an individual participant basis, which were used for further analysis of the active and passive tasks.

**Representational similarity analysis**

We used representational similarity analysis (Kriegeskorte, Mur, & Bandettini, 2008) in order to assess the multivariate relationships between the activity patterns generated across digits and tasks. The (dis)similarity between activity patterns within the entire SI hand mask was measured for each digit pair using the cross-validated squared Mahalanobis distance (see chapter 2). First, the activity patterns were pre-whitened using the residuals from the GLM and then cross-nobis distances were calculated for each task (active/passive) separately, using each pair of imaging runs and averaging those results. Due to cross-validations, the distance value is expected to be zero (but can go below) if two patterns are not statistically different from each other. Otherwise, greater distances indicate larger differences in multivariate representation.

The above analysis produced 10 distance values (one for each digit pair) per task, forming a representational dissimilarity matrix (RDM) per participant. Strength of representation was assessed by calculating the average value of the distances in an RDM (i.e., averaging across the values in the RDM, discounting values on the diagonal). Shape of representation was assessed by calculating the Spearman's rho

correlation between a measured RDM and the groups' RDM (for each of the two tasks; mean excluding participant-of-interest; and RDMs were normalised prior to averaging not to bias the mean towards more dissimilar RDMs).

As an aid to visualise the RDMs (and not used in any statistical analysis), we also performed multidimensional scaling (MDS). This analysis projects the higher-dimensional RDM into a lower-dimensional space while preserving the inter-digit distances as accurately as possible (Borg & Groenen, 2003). MDS was performed on individual RDMs and averaged after Procrustes alignment (without scaling) to remove any arbitrary rotations introduced by MDS. Alignment was based on RDMs including both active and passive conditions (as well as a rest condition) as not to bias the visualisation. Dimensions were sorted on the basis of high variance between digits to demonstrate hand representation at the expense of non-digit-specific variation from rest.

#### Magnetic resonance spectroscopy

Absolute neurochemical concentrations of GABA and Glutamate were extracted from the spectra of the greater S1 hand area while correcting for voxel tissue content. The metabolite ratios for all participants were compared across sessions using a t-test. These results are not discussed in this thesis for sake of simplicity.

## 6.4 Preliminary Results & Discussion

The following results and discussion are preliminary findings. We first confirmed that the participants' index finger (D2) was effectively blocked during the injection session using a grating orientation test. Participants performed consistently at (near-)ceiling during the baseline session and at chance level during the injection session (see figure 6.2A). This effect remained for the duration of the session and the sensitivity of a

neighbouring digit (D3) was unaffected.

In order to follow traditional fMRI analysis for characterising digit representation in SI, we identified 5 clusters showing strong selectivity to each of the digits. Within each cluster, we examined activity levels across digits. As expected, after the nerve block, passive stimulation of D2 no longer induced activity in its corresponding digit cluster. Contrary to classical findings in amputation, on this short timescale, we found no significant activity increase for the neighbouring digits in the (blocked) D2 cluster, for either passive or active stimulation (Figure 6.2C). Instead, with passive stimulation, we identified a significant decrease in digit selectivity (defined as each cluster's selected digit minus the mean of the remaining three digits, excluding D2) across the whole hand map, i.e. in the non-blocked digit clusters (p=.002). In the active task, digit selectivity was not significantly affected in the non-blocked territory (p=.172), presumably due to additional input associated with the active task which can offset changes.

We next interrogated digit representation in a larger cortical area extending the entire hand region, using representational similarity analysis (Figure 6.3A). At first, one may notice the similarities between the actively and passively probed representations. This has been examined in depth in Sanders et al. (2019). Regarding the effect of the nerve block, akin to the selectivity reduction mentioned above, we found that both active and passive stimulation resulted in significant reduction of inter-digit dissimilarity across the 4 non-blocked digits (active: -19%, p=.001; passive: -25%, p=.033). This indicates individuated digit representation became less distinct across the hand area. Importantly, despite the marked reduction of activity for D2 observed in the highly selective digit clusters, the representation of D2 was stable relative to the other digits, even in the passive condition: there was no significant interaction between digit (D2, neighbours, non-neighbours) and effect of injection on the distance between each digit and rest ($F(1,84)=1.03$, p=.361). This result demonstrates that

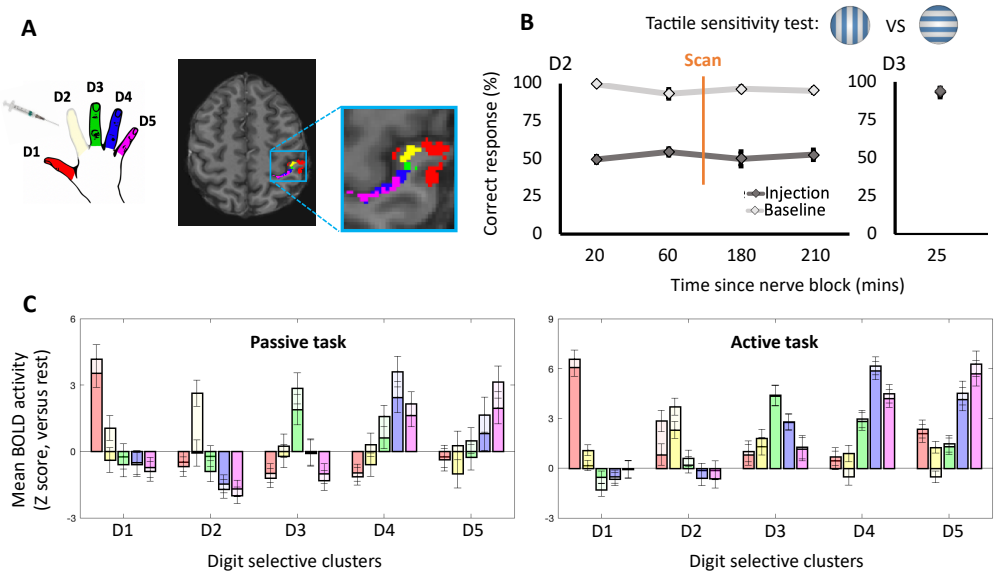



Figure 6.2: Univariate analysis. A Participants were test with and without local anaesthetics of D2. In the baseline session, a localiser task was used to identify clusters showing strong selectivity for each of the five digits. These clusters were used as regions of interest for further analysis. B Tactile sensitivity test (two alternative forced choice between horizontal vs vertical tactile probes) demonstrated ceiling level performance during the baseline session and chance performance during the injection session, for injected D2. No change was found for D3. C Classical univariate analysis of digit activity versus rest (left: passive stimulation; right: active movement), showed decreased selectivity within digit clusters (mean difference between selected and other digits). Pale colours indicate baseline session, full colours the injection session. In non-deprived clusters (D1, D3-5), selectivity is reduced during passive, but not active digit stimulation.

the representational change following local deprivation are truly hand-wide.

We confirmed there were no differences between sessions for (active) task performance, press force, GLM error and task-unspecific suppression of S1 (measured using resting-state signal variance). We further confirmed that the observed reduction in inter-digit dissimilarity could be ascribed to overall excitability by comparing this reduction to the reduction in average (i.e. non-digit-specific) distance to rest (Figure 6.3B): although the latter was reduced, inter-digit dissimilarity decreased more than expected based on previously reported ratios between the two measures (Arbuckle et al., 2019). Local deprivation may have large hand-wide effects because digit information is relatively distributed across the hand map. Even in clusters that are not selective to a particular digit, the relationship between its activity pattern and that of the other digits remains present. To conclude, our findings suggest the presence of a mechanism that can rapidly down-scale S1 organisation following an extreme change in input, while inter-digit relationships are preserved.

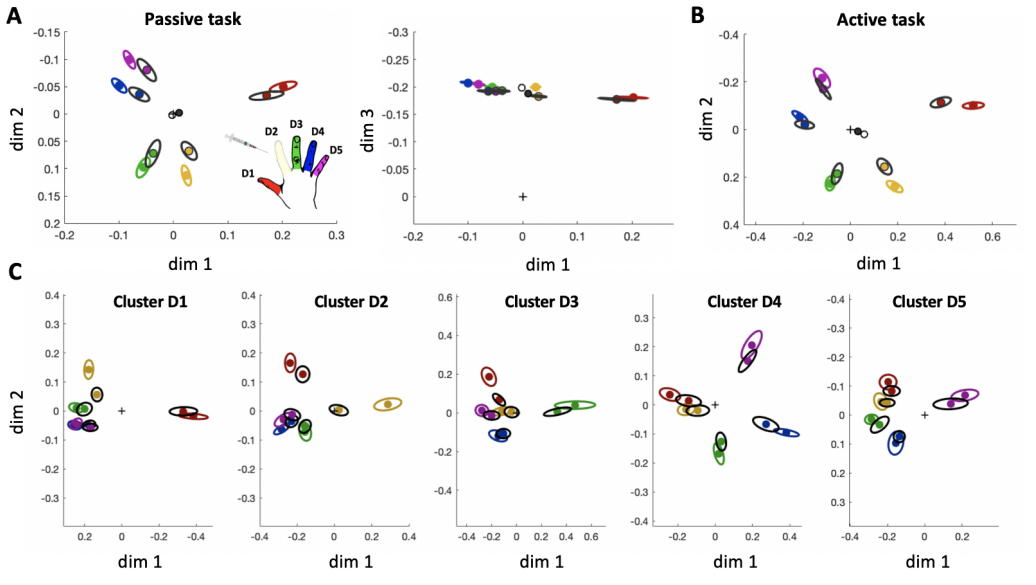



Figure 6.3: Global rescaling of hand representation in the SI hand area. A) Visualisation of hand representation across entire hand area. Both passive and active task show reduced inter-digit dissimilarity, yet a stable representational structure. Ellipses reflect inter-subject variance; black ellipses indicate the injection session. The baseline session mean is indicated by a white dot, the injection session mean by a black dot, and rest by a plus sign. B) Non-digit-specific distinctiveness of the hand map was calculated by mean distance to rest. This was slightly reduced but not enough to explain the shrunk inter-digit representational structure. C) Digit activity consistent with organisational structure, even within digit-selective clusters. Passive task, all symbols as in A. This suggest digit information is distributed to some extent across the hand map.

# Chapter 7

# Discussion

## 7.1 Overview

This thesis comprised of a number of experiments designed to study plasticity in the primary somatosensory cortex in humans. Specially, I've examined individuals for whom input to the hand area was altered at some point during their life, for varying reasons. Together, these studies sketch out the role of behaviour in shaping neural representation of the hand (and feet). In chapter 3, congenital one-handers did not show any hand representation. In chapter 5, foot representation was starkly altered concurrently with different foot behaviour from birth. Thus, in both cases, extreme changes in input to S1 from birth onwards, results in alternative development.

The studies included in this thesis also indicate that, later in life, body representation no longer requires typical behaviour to be maintained. In chapter 3, amputees showed preserved hand representation for their missing hand. In chapter 6, local anaesthesia rapidly affected hand representation, but the overall inter-digit relationships were preserved. Thus, in both cases, once hand representation was established, loss of sensory input did not affect gross characteristics of hand representation.

Finally, in chapter 4, I have argued that, in the primary somatosensory cortex, blind individuals do not show different hand representation from controls. Whichever manner in which blind individuals use their hands differently is not sufficient to drive representational plasticity in the hand area. This is consistent with general stable hand representation across an increasing number of population.

## 7.2 Persistence and plasticity

The conclusion that sensorimotor representations are relatively stable after a critical period is not the predominant view in the field or common in neuroscientific textbooks. Indeed, there is an abundance of evidence - mainly from model systems such as rodents' whisker map in the barrel cortex - that somatosensory neurons can adapt

their behaviour into adulthood (Feldman & Brecht, 2005; Kole, Scheenen, Tiesinga, & Celikel, 2018). Still, even in the barrel cortex, some features are stable in adulthood. For instance, thalamocortical connections to layer IV, where the dissimilarity between whisker representations is clearest, experience a clear critical period. After the first postnatal week, they exhibit little to no plasticity (Glazewski et al., 1996; Polley et al., 2004). Similarly, the development of anatomical parcellation between barrels can only be arrested in newborns (Van der Loos & Woolsey, 1973). Layer II/III, on the other hand, remains relatively plastic throughout life and is affected by e.g. deprivation (Feldman & Brecht, 2005). Although a direct comparison between the human S1 hand area and either barrel layer IV or other more plastic layers is not meaningful, these results suggests that even in rodents the prevalent idea of life-long malleability should be nuanced. Furthermore, even if we assume all microlevel mechanisms translate between species and brain area (Fox & Wong, 2005), the findings discussed in this thesis suggest that these mechanisms of axonal and synaptic plasticity (Feldman, 2009) are not sufficient, at the macrolevel, to erase e.g. the representation of a missing hand. In other words, even if new sensory representations are formed, they do not supplant the old ones. Potential reasons for this will be discussed below.

The stability of low-level presentation fits the pattern that behaviourally instigated plasticity preferentially occurs in higher-order cortical areas (Huxlin, 2008; Dhruv & Carandini, 2014; Striem-Amit et al., 2018b). Even if representational changes are needed and the brain retains mechanisms for plasticity well into adulthood, it is more difficult to adapt low-level representations. Any change would trickle down, i.e. require compensatory adaptations in higher order areas. In many cases, therefore, it would be easier to adapt the downstream areas and/or their connectivity directly. For instance, Beukema et al. (2019) argued that training on motor sequences with particular digit relationships do not affect low-level representations (in adulthood), but rather premotor areas' recruitment and chunking of these low-level representations.

Only at an early developmental stage, it may be more efficient to alter low-level representations and all their downstream dependencies to increase computational efficiency (Law & Gold, 2008). Either because the entire sensorimotor is still in the process of fine-tuning, or because the potential benefit will compound over many years of life.

The conclusions of this thesis do not extend beyond the primary cortical areas. Given studies showing reorganisation at the microlevel and reorganisation in higher-order and association cortex, one should not conclude the brain is incapable of plasticity inf adulthood. What, then, makes primary cortex different? Some argue a shift in the neurochemical profile of a brain area marks the end of its critical period (e.g. Filbin, 2003; Hensch, 2005) and with that, its propensity for plasticity. If so, would it be possible to bring S1 back in such a juvenile state? This is a topic of ongoing research (Zeiler et al., 2016), but given the microlevel mechanics, this is not straightforward. If additional mechanisms that facilitate plasticity are available solely during the critical period, this can either be an integral part of development or an addition to it. For the former, one may imagine a more-or-less pluripotent brain area whose development can be guided by behaviour into several directions, but once developed a certain way, its initial pluripotency cannot be regained (compare Waddington's "epigenetic landscape"; Mitchell, 2018). Such a mechanism may be at play in the development of higher-order cortex (Bedny, 2017). Although the results in this thesis do not require anything beyond alternative development, i.e. the alternative representations presented in chapter 3-5 could have manifested itself during the critical period, it is unlikely such these mechanisms are the only factor in primary cortex. Since rudimentary somatotopy is seen long before the critical period typically ends (DallOrso et al., 2018; Arcaro et al., 2019), the successful adaptation within the critical period after nerve reinnervation (Lundborg & Rosén, 2001) suggest plasticity mechanisms beyond development. It is unclear, however, where the necessary plasticity takes place: if the bulk of it indeed occurs sub-cortically (Kambi et al.,

2014) - before finger information enters S1 - then even this result may be consistent with stable representation in S1.

When no plasticity is observed, it may simply be the case that input loss was not sufficiently extreme to drive change. Specifically, when examining amputees in chapter 3 and the participants with a nerve block in chapter 6, one may argue that efference could be unaffected. Indeed, both groups of participant could activate S1 using their motor system. As such, input from the motor system may have been sufficient information to prevent the somatosensory cortex from reorganising. While this is possible and the involvement of the motor system should be studied further (see section 7.4), the general stability shown in this thesis demonstrates at least independence from the periphery. If completely isolating a brain area from the rest of the brain is required to trigger plasticity, then for all practical purposes, the primary somatosensory area would not reorganise in adulthood. Also, considering similar conclusions are being drawn for the primary areas in other modalities (see chapter 1), which arguably are less closely connected with the motor system, adult stability is more parsimonious. Finally, amputees who had little to no perceived control over their phantom hand, still had signs of missing hand representation (when activated with their intact hand). If efferent output is the main factor in keeping missing hand representation stable, one may wonder whether these individuals' phantom motor behaviours are as similar to each other as their representations.

## 7.3 Spatiotemporal detail of representations

The proxy for hand representation that was used in this thesis is by no means all encompassing, nor is our measure of behaviour. Because the dimensionality of neural representation can only be measured as richly as the dimensionality of the behaviour it probed with, our measure of behaviour has actually been a fundamental bottleneck.

Hand representation in S1 is used for more than separating five regularly tapping digits  understanding finer details of behaviour (Overduin et al., 2012) would allow more complicated encoding models, more complicated than our current more-or-less 2-dimensional representational structure. There have been studies going in this direction. Locations along the same digit have been shown to be separable using fMRI (Sanchez-Panchuelo et al., 2012b). Also, different actions may recruit S1 in slightly different ways. In M1, flexion and extension have been shown to produce distinct somatotopic digit representations (L. Huber et al., 2019). Granted, the same study only exhibited a single digit map in S1 and compared to M1, S1 may be relatively more constrained by somatotopy than action representation, but it is not inconceivable multiple overlapping digit maps exist in S1. If so, different actions would likely be sparsely encoded, because large-scale clustering is already mostly based on somatotopy. Sparse encoding can easily be averaged out at the resolution of a typical voxel, even at sub-millimetre resolution of L. Huber et al. (2019). It should be noted, however, that currently, a number of the order of magnitude of 10,000 voxels can be summarised reasonably well using 10 numbers. Most developments should therefore be expected from behaviourally more complex tasks, rather than from a reduced voxel size, e.g. studying flexion and extension separately as above. More specific ideas will be discussed in section 7.4.

It is not unlikely that more advanced reflections of hand representation, both in behaviour and neural representation, will indicate group differences where the experiments in this thesis did not. Here, we focussed on the fundamental hallmarks of hand representations. Chapter 6 already showed that in the event of rapid input loss, it is possible for some aspects of hand representation to change while other remain relatively persistent. Research to increase the complexity of our models could be as large as a step forward as going from using average activity to using representational structure, as described explicitly in chapter 4. Here, we argued to be careful inter-

preting too much into average activity and proposed to use representational models to identify representational content (see e.g. Mattioni et al., 2019) Still, because finer precision can only increase dissimilarity between two conditions - never decrease - the specific aspects of hand representation (and its relation to behaviour) that have been shown to be different between groups in this thesis, will remain different even if further details about hand representation are discovered. As stated before, the robustness of the RSA measure, i.e. it can be probed using many different types of design (see chapter 6), suggests these aspects are fundamental, albeit simple, hallmarks of sensorimotor representation. Future research will tell whether they are relevant and sufficient for any practical applications and understanding as well.

## 7.4 Future directions

In this thesis, we have examined the brains and behaviour of individuals from special populations. Together, amputees, congenital one-handers, congenitally blind individuals and foot artists indicate the influence of early life behaviour on the development of neural representation. The dichotomy between one-handers and foot painters, who received alternative input early in life and show extensive change, and adult amputees is a coarse one, i.e. the two groups are very different. Future research can build upon this finding in a number of ways.

First of all, future research should further specify the developmental time window in which organisation is guided by behaviour. Given ethical constraints, however, it is difficult to design a study involving the extreme input changes that may be needed to induce reorganisation. Fortunately, the measures of hand presentation used in this thesis can still be informative with a small number of participants, as noted by the experiments presented here. As such, in time, the small number of young amputees that can participate in a study may span the entire range, from infantile to adolescent.

On the basis of their results, one can study whether there is any non-congenital time in which the primary somatosensory cortex either arrests its development, or undergoes considerable changes.

As discussed in chapter 5, foot artists use their feet differently than two-handed controls, but it was difficult to assess precisely how. Many standardized tests in the lab do not capture everyday behaviour very well. Better tracking equipment based on automatic visual capture may allow for more naturalistic, freely moving experiments. Such experiments already exist (Ingram et al., 2008; Haar et al., 2019), but they are currently hard to do and require complex equipment. When such technologies become more widely available, the study of behaviour can lead the study of the mapping of behaviour (Krakauer et al., 2017).

The primary measurement tool in this thesis was ultra-high field fMRI, complemented by psychophysics and MR spectroscopy. Without a resolution of 1 $mm^3$, some of the findings in chapter 4 and 5 would arguably not have been discovered. Certainly, the ability to distinguish activity patterns for individual digits has been a step forward compared to previous work relying on area-wide activity changes (e.g. Makin, Scholz, et al., 2013; Raffin, Mattout, et al., 2012 and others) Further technological improvements will allow for new questions to be studied building upon this thesis. I will discuss a number of recent developments that are promising. First, higher resolution allows more detailed assessment of hand representation as described in section 7.3. Particularly interesting, however, is that ultra-high field fMRI has reached the necessary resolution to image cortical layers separately. Neurons at different depths of sensory cortex are involved with different stages of processing, e.g. superficial layers mostly receive and send out cortico-cortical projections, whereas afferent input from the thalamus primarily enters in deeper layers (Friston, 2010; Thomson & Bannister, 2003; Y. Yu et al., 2019). Although 1 $mm^3$ is theoretically sufficient to separately measure these two categories of cortex, typical fMRI sequences suffer from distortions

due to blood drainage that make this difficult in practice (Goense et al., 2012). By using MRI acquisition protocols that measure cerebral blood flow more directly and a slight increase in resolution, groups have recently acquired reliable signals from independent layers (e.g. L. Huber et al., 2019; Y. Yu et al., 2019). This technological advance invites follow-up questions about the findings presented in this thesis. The ability to separate input from M1 from afferent input would allow experiments to test whether missing hand representation in amputees' S1 is stable without input or kept intact by digit information from M1. Also, this would allow us to study better how active tasks engage the somatosensory representations, such as in chapter 6.

Behaviour of the phantom limb in chapter 3 has not been measured directly. Instead, we relied on self-report, both inside the scanner and during the assessment of phantom kinaesthesia, where the participants mimicked the movement skill of their phantom hand with their intact one. Although erroneous movement was not an issue in our study as all amputees recruited S1 in a manner resembling the hand of controls, further research would be improved by better tracking of phantom movement. Because phantom movement is accompanied by stump muscle involvement, it is possible to measure it using EMG technology. Currently, conventional EMG electrodes cannot distinguish individual digits, but new systems that are capable of doing that are actively being developed (Gailey et al., 2017; Krasoulis et al., 2018). When it is possible to track the movement of the phantom hand using stump EMG, the role between behaviour and brain representation in amputees can be studied at more detail. For instance, in chapter 3, I presented a relationship between phantom kinaesthesia and the representational typicality of the deprived hand area, but it was unclear whether those participants who had poor control over phantom movements did not activate S1 as well due to misperformed movement, or whether a less well preserved sensorimotor cortex could not facilitate individualised movement. By tracking phantom hand motion online, mistakes in task performance may be more clearly

identifiable (for digits that can be moved). Furthermore, online tracking would allow (phantom) motor training studies, which, while unlikely to affect hand representation directly (Beukema et al., 2019), may improve motor capabilities, and consequently our ability to stimulate the brain.

# Personal contributions

The experimental chapters in this thesis (3-6) are based on work done in collaboration with other authors. Below, my specific contributions are summarised per chapter. Key contributors (in order of appearance): Fiona MZ van den Heiligenberg (FMZvdH), Sanne Kikkert (SK), Harriet Dempsey-Jones (HDJ), Jason Friedman (JF), Tamar R Makin (TRM), and Zeena B Sanders (ZBS). Additional co-authors who primarily contributed to experimental design, recruitment, interpretation of the results and writing of manuscripts beyond the first draft, are not listed here.

### Chapter 3

Data acquisition by FMZvdH. All analysis, initial draft of text. All figures.

### Chapter 4

Data acquisition (with assistance by SK), all analysis, initial draft of text. All figures.

### Chapter 5

Acquisition (with assistance by HDJ) and analysis of imaging data. Behavioural data was collected by HDJ and JF, and analysed by HDJ. Initial draft of text together with HDJ and TRM. All figures except Table S1. Table S1 by HDJ.

### Chapter 6

Imaging data acquisition together with ZBS. Behavioural data was collected and analysed by ZBS and HDJ. Pre-processing of imaging data together with ZBS. All multivariate analysis. All figures except Figure 6.1. Figure 6.1 by ZBS.

# Appendix A

# Supplementary figures and tables

**Table S1**. *Results for the qualitative measures used to assess the artists' complex behavioural repertoire*, related to Figure 1. (Artist 1 = ▼; Artist 2 = ▲). A) The Motor Activity Log is a clinical questionnaire previously validated to assess use of residual limbs and prostheses (e.g., Makin et al., 2013) – here adapted for feet/toes. Both artists reported using their feet/ toes to perform the majority of the 25 listed daily life tasks (very often + sometimes responses: ▼= 80%; ▲= 76%), and that this was typically very easy (not difficult responses: ▼= 80%; ▲= 66%). Please note the wording of some questions has been slightly truncated for presentation reasons. B) Tool use questionnaire assesses how often 42 different tools are used for their typical function with the upper/ lower limbs and mouth. If a tool had not been used for its typical function (i.e., only carried or transported, or not used at all), artists were asked do they think they would be able to use the tool if they had the chance. Results demonstrated both artists had used their lower limbs to use almost all tools for their typical function (▼= 88%; ▲= 90%), and that they reported they would be able to use any unused tools with their lower limbs if they had the chance. C) Adaptation of the Edinburgh Handedness Questionnaire (Oldfield, 1971) to assess preferred foot for performing 10 daily tasks (and one assessing preferred eye). Two squares for one side (left/right) indicates the artists showed full preference for use of that side, where one square for each side indicates equal preference for either the left/ right foot for performing tasks. Results indicated artist 1 was completely left foot dominant (EFI score: -100), and artist 2 was highly right foot dominant (EFI score: +92; this was sub +100 due to preferred use of left eye due to right eye damage). EFI scores range from -100 (complete left preference) to +100 (complete right preference).

| **A** The Motor Activity Log | | | | | | | **B** Tool use | | | | | | **C** Edinburgh footedness inventory | | |
|---|---|---|---|---|---|---|---|---|---|---|---|---|---|---|---|
| | Frequency | | | Difficulty | | | | Used for typical function | | | Never used for typical function | | | Which foot used? | |
| Activity | Never | Some -times | Very often | Not | Med | Very | Tool | Upper limbs | Lower limbs | Mouth | Never used | Would be able | Activity | Left | Right |
| % reported | ▼20%<br>▲24% | ▼20%<br>▲32% | ▼60%<br>▲44% | ▼80%<br>▲66% | ▼0%<br>▲10% | ▼0%<br>▲0% | % reported | NA | ▼88%<br>▲90% | ▼7%<br>▲2% | ▼5%<br>▲7% | ▼5%<br>▲7% | EFI ▼ -100<br>EFI ▲ 83 | ▼100%<br>▲ 8% | ▼ 0%<br>▲92% |
| Money from wallet | | ▲ | ▼ | ▼▲ | | | Bowl scraper | | ▼▲ | | | | Writing | ▼▼ | ▲▲ |
| Open envelope | | | ▼▲ | ▼▲ | | | Calculator | | ▼▲ | | | | Drawing | ▼▼ | ▲▲ |
| Pick up/ lift glasses | | | ▼▲ | ▼▲ | | | Can opener | | ▼▲ | | | | Throwing | ▼▼ | ▲▲ |
| Pick up/ hold up phone | | | ▼▲ | ▼▲ | | | Cards | | ▼▲ | | | | Scissors | ▼▼ | ▲▲ |
| Wipe counter | | ▲ | ▼ | ▼▲ | | | Chess pawn | | ▲ | | ▼ | ▼ | Toothbrush | ▼▼ | ▲▲ |
| Get out of a car | | | ▼▲ | ▼▲ | | | Comb | | | | ▼▲ | ▼▲ | Knife (alone) | ▼▼ | ▲▲ |
| Stabilize paper | | | ▼▲ | ▼▲ | | | Computer mouse | | ▼▲ | | | | Spoon | ▼▼ | ▲▲ |
| Carrying cup/ can | ▼▲ | | | | | | Cooking strainer | | ▲ | ▼ | | | Broom (upper foot) | ▼▼ | ▲▲ |

| | | | | | | | | | | | | | | | |
|---|---|---|---|---|---|---|---|---|---|---|---|---|---|---|---|
| Carry bags | ▼▲ | | | | | | Correction pen | | ▼▲ | | | | Striking match | ▼▼ | ▲▲ |
| Pull chair out | | ▲ | ▼ | ▼▲ | | | Elastic band | | ▼▲ | | | | Opening box (lid) | ▼▼ | ▲▲ |
| Hold book/ turn pages | | ▲ | ▼ | ▼▲ | | | Erasing gum | | ▼▲ | | | | Kick (preferred) | ▼▼ | ▲▲ |
| Keyboard/ mouse buttons | | | ▼▲ | ▼▲ | | | File | | ▼▲ | | | | Eye (if using one) | ▼▼ ▲▲ | |
| Move mouse | | | ▼▲ | ▼▲ | | | Frisbee | | ▼▲ | | | | | | |
| Put on socks | | ▼▲ | | ▼▲ | | | Garlic Press | | ▼▲ | | | | | | |
| Put on shoes | ▲ | | ▼ | ▼ | | | Glue stick | | ▼▲ | | | | | | |
| Tie shoelaces | ▼▲ | | | | | | Hair brush | | ▼▲ | | | | | | |
| Put on trousers | ▲ | | ▼ | ▼ | | | Hairdryer | | ▼▲ | | | | | | |
| Lotion/crea m on face | | ▼ | ▲ | ▼▲ | | | Hand fan | | ▼ | | ▲ | ▲ | | | |
| Wash face | | | ▼▲ | ▼▲ | | | Hold punch | | ▼▲ | | | | | | |
| Dry face | | | ▼▲ | ▼▲ | | | Iron | | ▼▲ | | | | | | |
| Comb hair | ▼▲ | | | | | | Kettle | | ▲ | ▼ | | | | | |
| Button shirt | ▼ | ▲ | | ▲ (undo) | ▲ (do up) | | Kitchen sponge | | ▼▲ | | | | | | |
| Zip up coat | | ▼▲ | | ▼ | ▲ | | Match | | ▼▲ | | | | | | |
| Peel fruit skin | | ▼▲ | | ▼ | ▲ | | Nail | | ▼▲ | | | | | | |
| Use fork/ spoon | | ▼ | ▲ | ▼▲ | | | Nail polish | | ▼▲ | | | | | | |

| | | | | | | | | | | | | | | | |
|---|---|---|---|---|---|---|---|---|---|---|---|---|---|---|---|
| | | | | | | | Paper clip | | ▼▲ | | | | | | |
| | | | | | | | Pencil sharpener | | ▼▲ | | | | | | |
| | | | | | | | Protractor | | ▼ | | ▲ | ▲ | | | |
| | | | | | | | Razor | | ▼▲ | | | | | | |
| | | | | | | | Rolling pin | | ▼▲ | | | | | | |
| | | | | | | | Scissors | | ▼▲ | | | | | | |
| | | | | | | | Screw | | ▼▲ | | | | | | |
| | | | | | | | Sewing needle | | ▼▲ | | | | | | |
| | | | | | | | Spinning top | | ▼▲ | | | | | | |
| | | | | | | | Stapler | | ▼▲ | | | | | | |
| | | | | | | | Syringe | | ▼▲ | | | | | | |
| | | | | | | | Tambourine | | ▼▲ | | | | | | |
| | | | | | | | Thermometer | | ▼ | ▲ | | | | | |
| | | | | | | | Toaster | | ▲ | ▼ | | | | | |
| | | | | | | | Tooth-brush | | ▼▲ | | | | | | |
| | | | | | | | Vegetable peeler | | ▼▲ | | | | | | |
| | | | | | | | Yo-yo | | ▼▲ | | | | | | |
| | | | | | | | | | | | | | | | |

**Table S2**, *Representational similarity analysis in control regions of interest (ROIs)*, related to Figure 3. A) Controlling for Artist 2's enlarged Foot area ROI. The individually defined ROI for the Foot area (see STAR Methods) was significantly larger for both feet than controls (dextrous foot, size=1262, t(8)=3.97, p=.003, stabilising foot, size=1330, t(8)=4.31, p=.002). Artist 1's ROI was not larger (dextrous foot, size=591, t(8)=0.58, p=.575; stabilising foot, size=737, t(8)=1.32, p=.219). To confirm that this didn't impact our main findings, we repeated our analysis using an ROI of the mean controls' ROI size (dextrous: 474 $mm^2$, stabilising: 475 $mm^2$, mean control: 476±70 $mm^2$). Considering all of our findings were observed with the adjusted ROI size, we retained our original analysis as constraining the size was not specified a priori. B) No increased foot representation in the artists' lip area (defined using a group average activity mask for mouth movement from a different dataset (see Hamamy et al., 2017). This suggests that more 'hand-like' representation is not universal across the entire primary sensorimotor strip, but more specific to the foot and (deprived) hand area. Abbrev: A: Artist; Ctr: Control; Corr.: Correlation.

| | | ***A1 VS CTR (T)*** | ***A1 VS CTR (P)*** | ***A2 VS CTR (T)*** | ***A2 VS CTR (P)*** |
|---|---|---|---|---|---|
| **A** | Artist 2's Foot area ROI (reduced): | | | | |
| | *Dextrous foot* | | | | |
| | Mean dissimilarity | x | x | 2.33 | 0.047 |
| | Corr. with canonical hand | x | x | 3.44 | 0.008 |
| | *Stabilising foot* | | | | |
| | Mean dissimilarity | x | x | 2.33 | 0.047 |
| | Corr. with canonical hand | x | x | 3.44 | 0.008 |
| **B** | Lip area ROI: | | | | |
| | *Dextrous foot* | | | | |
| | Mean dissimilarity | 0.24 | 0.815 | -0.09 | 0.93 |
| | Corr. with canonical hand | -0.78 | 0.459 | 2.1 | 0.07 |
| | *Stabilising foot* | | | | |
| | Mean dissimilarity | -0.34 | 0.745 | -0.4 | 0.701 |
| | Corr. with canonical hand | -0.17 | 0.866 | -0.41 | 0.696 |

**Table S3**, *FDR thresholds*, related to Figure 2. FDR thresholds for individual digit contrasts for the artists' dexterous foot shown in Figure 1 (Z-statistic).

| | Artist 1 | Artist 2 |
|---|---|---|
| Whole-brain contrast: q(FDR)<.05 | 3.98 | 5.28 |
| S1/M1 contrast D1 vs Others : q(FDR)<.05 | 3.83 | 3.06 |
| D2 vs Others: q(FDR)<.05 | 3.43 | 3.68 |
| D3 vs Others: q(FDR)<.05 | 2.75 | 3.36 |
| D4 vs Others: q(FDR)<.05 | 3.41 | 3.17 |
| D5 vs Others: q(FDR)<.05 | 3.84 | 3.45 |

**Table S4**, *Demographic details*, related to STAR Methods. Demographic details of participants including age, gender and dextrous foot (for the artists). Please note that not all participants performed all tests: an 'x' indicates participation in either the tactile, motor or fMRI testing protocols.

| ID Code | Age | Gender | Dextrous foot | Tactile testing | Motor testing | fMRI testing |
|---|---|---|---|---|---|---|
| Artist 1 | 55 | M | L | x | x | x |
| Artist 2 | 56 | M | R | x | x | x |
| C1 | 53 | F | R | x | x | x |
| C2 | 60 | M | R | x | x | x |
| C3 | 48 | F | R | x | x | x |
| C4 | 45 | M | R | x | x | x |
| C5 | 52 | F | R | x | x | x |
| C6 | 39 | F | R | x | x | x |
| C7 | 75 | M | R | x | x | x |
| C8 | 69 | M | R | x | x | x |
| C9 | 51 | F | L | x | x | x |
| C10 | 50 | M | R | x | x | |
| C11 | 60 | M | R | x | x | |
| C12 | 70 | M | R | x | x | |
| C13 | 53 | F | R | x | x | |
| C14 | 71 | M | R | x | x | |
| C15 | 40 | M | R | x | x | |
| C16 | 46 | M | R | x | | |
| C17 | 52 | F | R | x | | |
| C18 | 53 | M | R | x | | |
| C19 | 50 | F | L | x | | |
| C20 | 54 | M | R | x | | |
| C21 | 49 | F | R | x | | |

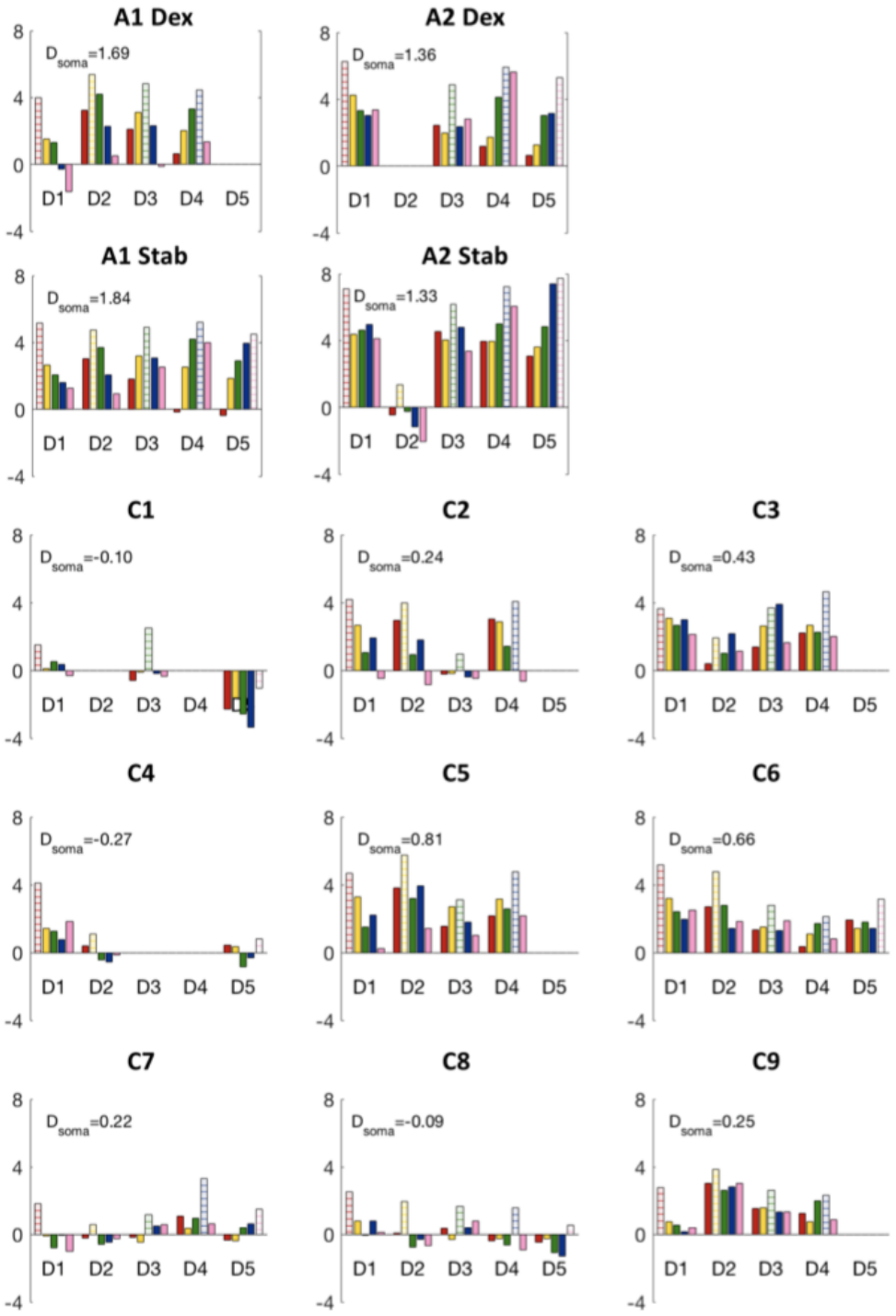



Figure S1: Related to Figure 5.3. Selectivity graphs in Foot area (activity versus rest, in digit-specific clusters) illustrating somatotopic organisation (higher activity in digits neighbouring each clusters strongest digit, than in digits further away; indicated by $D_{soma}$ score). Somatotopy was more pronounced for artists stabilising foot as compared to controls (artist 1 vs. controls, $t(8)=4.26$, $p=.003$; artist 2 vs. controls, $t(8)=2.90$, $p=.019$).Abbreviations: Dex: dextrous foot; Stab: stabilising foot. All other annotation as in Figure 5.3D.

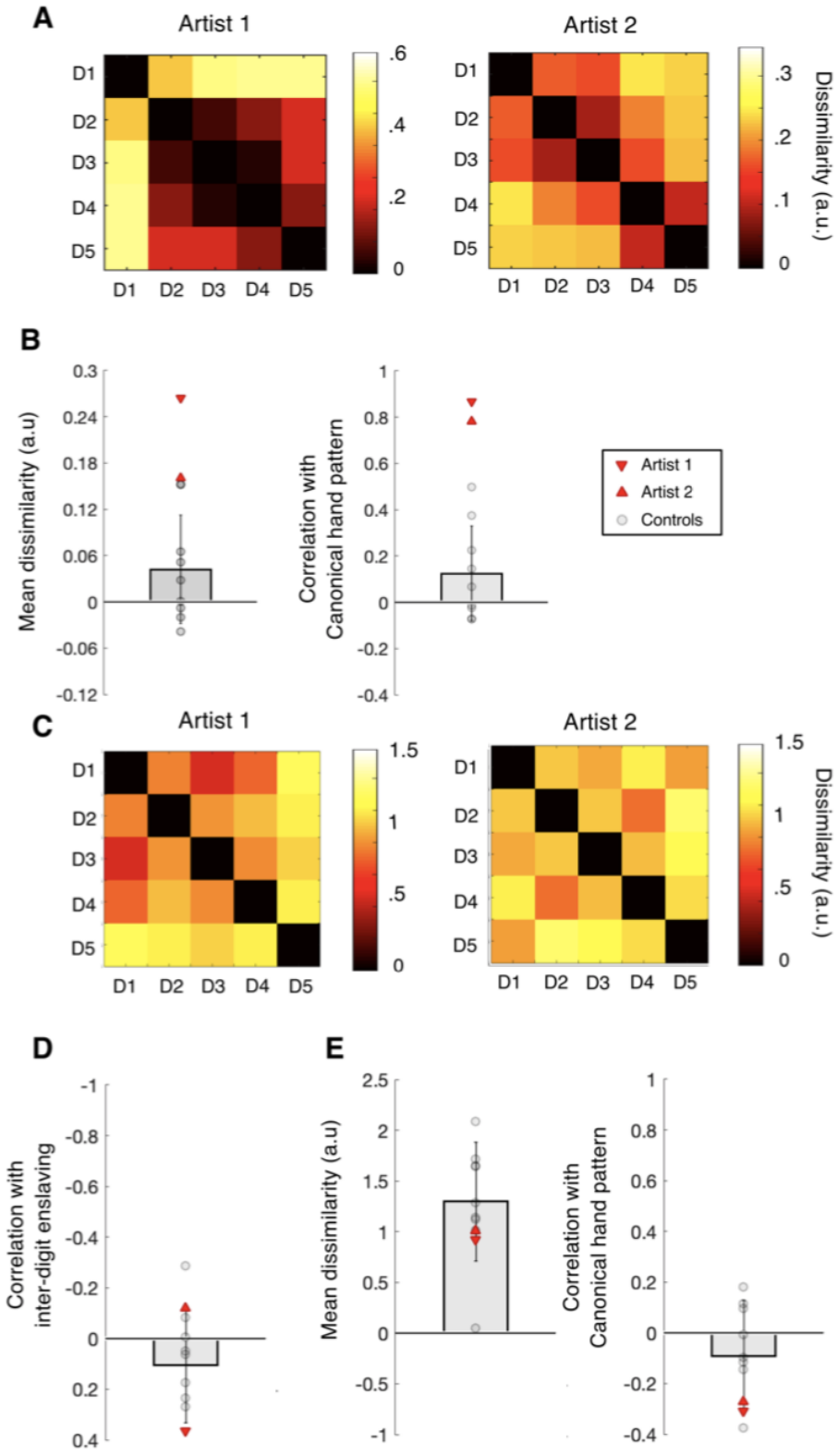



Figure S2: (See next page)

(See previous page.) Stabilising foot representation, related to Figures 5.6 and 5.7. Foot Area: A) Representational dissimilarity matrices (RDM) B) RSA results. Mean dissimilarity (across the RDM) was greater for artist 1 versus controls ($t(8)=2.99$, $p=.017$), but this was not significant for artist 2 versus controls ($t(8)=1.60$, $p=.149$). Correlation with the canonical hand RDM was greater than controls for both artists (control rho, $M=.125$, $SD=.20$; artist 1 versus controls, $t(8)=3.44$, $p=.009$; artist 2 versus controls, $t(8)=3.05$, $p=.015$). Hand Area: C) RDMs. D) Correlation between the kinematics and the hand RDM was not different in the artists versus controls (artist 1: rho=.364, $t(8)=1.08$, $p=.312$; artist 2: rho=-.121, $t(8)=-.93$, $p=.381$). E) RSA results. Mean dissimilarity was not different for artists and controls (artist 1: $t(8)=-.618$, $p=.554$; artist 2:, $t(8)=-.472$, $p=.650$). Correlation with the canonical hand RDM was not greater than controls (artist 1: $t(8)=-.929$, $p=.380$; artist 2: $t(8)=-.774$, $p=.461$).

# References


Adams, R. A., Shipp, S., & Friston, K. J. (2013). Predictions not commands: active inference in the motor system. *Brain Structure and Function*, *218*(3), 611–643.

Ajina, S., & Bridge, H. (2018). Blindsight relies on a functional connection between hmt+ and the lateral geniculate nucleus, not the pulvinar. *PLoS Biol*, *16*(7), e2005769.

Ajina, S., Kennard, C., Rees, G., & Bridge, H. (2015). Motion area v5/mt+ response to global motion in the absence of v1 resembles early visual cortex. *Brain*, *138*(Pt 1), 164-78.

Ajina, S., Pestilli, F., Rokem, A., Kennard, C., & Bridge, H. (2015). Human blindsight is mediated by an intact geniculo-extrastriate pathway. *Elife*, *4*.

Akselrod, M., Martuzzi, R., Serino, A., van der Zwaag, W., Gassert, R., & Blanke, O. (2017). Anatomical and functional properties of the foot and leg representation in areas 3b, 1 and 2 of primary somatosensory cortex in humans: A 7t fmri study. *Neuroimage*, *159*, 473-487.

Alary, F., Duquette, M., Goldstein, R., Elaine Chapman, C., Voss, P., La Buissonniere-Ariza, V., & Lepore, F. (2009). Tactile acuity in the blind: a closer look reveals superiority over the sighted in some but not all cutaneous tasks. *Neuropsychologia*, *47*(10), 2037-43.

Allard, T., Clark, S. A., Jenkins, W. M., & Merzenich, M. M. (1991). Reorganization of somatosensory area 3b representations in adult owl monkeys after digital syndactyly. *Journal of Neurophysiology*, *66*(3), 1048-1058.

Amedi, A., Jacobson, G., Hendler, T., Malach, R., & Zohary, E. (2002). Convergence of visual and tactile shape processing in the human lateral occipital complex. *Cereb Cortex*, *12*(11), 1202-12.

Amedi, A., Raz, N., Azulay, H., Malach, R., & Zohary, E. (2010). Cortical activity during tactile exploration of objects in blind and sighted humans. *Restor Neurol Neurosci*, *28*(2), 143-56.

Amedi, A., Stern, W. M., Camprodon, J. A., Bermpohl, F., Merabet, L., Rotman, S., ... Pascual-Leone, A. (2007). Shape conveyed by visual-to-auditory sensory substitution activates the lateral occipital complex. *Nat Neurosci*, *10*(6), 687-9.

Andersen, R. A., Snyder, L. H., Bradley, D. C., & Xing, J. (1997). Multimodal

representation of space in the posterior parietal cortex and its use in planning movements. *Annual review of neuroscience*, *20*(1), 303–330.

Andoh, J., Milde, C., Tsao, J. W., & Flor, H. (2017). Cortical plasticity as a basis of phantom limb pain: Fact or fiction? *Neuroscience*.

Arbuckle, S. A., Yokoi, A., Pruszynski, J. A., & Diedrichsen, J. (2019). Stability of representational geometry across a wide range of fmri activity levels. *Neuroimage*, *186*, 155-163.

Arcaro, M. J., & Livingstone, M. S. (2017). A hierarchical, retinotopic proto-organization of the primate visual system at birth. *Elife*, *6*.

Arcaro, M. J., Schade, P., & Livingstone, M. S. (2019). Body-map proto-organization in newborn macaques. *bioRxiv*, *565390*.

Astafiev, S. V., Stanley, C. M., Shulman, G. L., & Corbetta, M. (2004). Extrastriate body area in human occipital cortex responds to the performance of motor actions. *Nat Neurosci*, *7*(5), 542-8.

Baker, C. I., Peli, E., Knouf, N., & Kanwisher, N. G. (2005). Reorganization of visual processing in macular degeneration. *Journal of Neuroscience*, *25*(3), 614–618.

Barnsley, R. H., & Rabinovitch, M. S. (1970). Handedness: proficiency versus stated preference. *Percept Mot Skills*, *30*(2), 343-62.

Baseler, H. A., Gouws, A., Haak, K. V., Racey, C., Crossland, M. D., Tufail, A., ... Morland, A. B. (2011). Large-scale remapping of visual cortex is absent in adult humans with macular degeneration. *Nat Neurosci*, *14*(5), 649-55.

Bavelier, D., & Neville, H. J. (2002). Cross-modal plasticity: where and how? *Nat Rev Neurosci*, *3*(6), 443-52.

Beauchamp, M. S., Laconte, S., & Yasar, N. (2009). Distributed representation of single touches in somatosensory and visual cortex. *Hum Brain Mapp*, *30*(10), 3163-71.

Beauchamp, M. S., Yasar, N. E., Kishan, N., & Ro, T. (2007). Human mst but not mt responds to tactile stimulation. *J Neurosci*, *27*(31), 8261-7.

Bechtel, W. (1998). Representations and cognitive explanations: Assessing the dynamicist's challenge in cognitive science. *Cognitive Science*, *22*(3), 295–317.

Bedny, M. (2017). Evidence from blindness for a cognitively pluripotent cortex. *Trends Cogn Sci*.

Bedny, M., Pascual-Leone, A., Dodell-Feder, D., Fedorenko, E., & Saxe, R. (2011). Language processing in the occipital cortex of congenitally blind adults. *Proc Natl Acad Sci U S A*, *108*(11), 4429-34.

Berardi, N., Pizzorusso, T., & Maffei, L. (2000). Critical periods during sensory development. *Current opinion in neurobiology*, *10*(1), 138–145.

Berlot, E., Prichard, G., OReilly, J., Ejaz, N., & Diedrichsen, J. (2018). Ipsilateral

finger representations in the sensorimotor cortex are driven by active movement processes, not passive sensory input. *Journal of neurophysiology*, *121*(2), 418-426.

Besle, J., Sanchez-Panchuelo, R. M., Bowtell, R., Francis, S., & Schluppeck, D. (2013). Single-subject fmri mapping at 7 t of the representation of fingertips in s1: a comparison of event-related and phase-encoding designs. *J Neurophysiol*, *109*(9), 2293-305.

Besle, J., Sanchez-Panchuelo, R. M., Bowtell, R., Francis, S., & Schluppeck, D. (2014). Event-related fmri at 7t reveals overlapping cortical representations for adjacent fingertips in s1 of individual subjects. *Hum Brain Mapp*, *35*(5), 2027-43.

Beukema, P., Diedrichsen, J., & Verstynen, T. D. (2019). Binding during sequence learning does not alter cortical representations of individual actions. *J Neurosci*, *39*(35), 6968-6977.

Bishara, A. J., & Hittner, J. B. (2012). Testing the significance of a correlation with nonnormal data: comparison of pearson, spearman, transformation, and resampling approaches. *Psychological methods*, *17*(3), 399.

Boakye, M., Huckins, S. C., Szeverenyi, N. M., Taskey, B. I., & Hodge, J., C. J. (2000). Functional magnetic resonance imaging of somatosensory cortex activity produced by electrical stimulation of the median nerve or tactile stimulation of the index finger. *J Neurosurg*, *93*(5), 774-83.

Bogdanov, S., Smith, J., & Frey, S. H. (2012). Former hand territory activity increases after amputation during intact hand movements, but is unaffected by illusory visual feedback. *Neurorehabil Neural Repair*, *26*(6), 604-15.

Borg, I., & Groenen, P. J. F. (2005). *Modern multidimensional scaling: Theory and applications*. Springer Science & Business Media.

Branscheidt, M., Ejaz, N., Xu, J., Widmer, M., Harran, M. D., Cortés, J. C., ... others (2019). No evidence for motor recovery-related cortical reorganization after stroke using resting-state fmri. *bioRxiv*, 681320.

Bruurmijn, M., Pereboom, I. P. L., Vansteensel, M. J., Raemaekers, M. A. H., & Ramsey, N. F. (2017). Preservation of hand movement representation in the sensorimotor areas of amputees. *Brain*, *140*(12), 3166-3178.

Burton, H. (2003). Visual cortex activity in early and late blind people. *J Neurosci*, *23*(10), 4005-11.

Burton, H., Sinclair, R. J., & McLaren, D. G. (2004). Cortical activity to vibrotactile stimulation: an fmri study in blind and sighted individuals. *Hum Brain Mapp*, *23*(4), 210-28.

Burton, H., Snyder, A. Z., Conturo, T. E., Akbudak, E., Ollinger, J. M., & Raichle, M. E. (2002). Adaptive changes in early and late blind: a fmri study of braille reading. *J Neurophysiol*, *87*(1), 589-607.

Butterworth, S., Francis, S., Kelly, E., McGlone, F., Bowtell, R., & Sawle, G. V. (2003). Abnormal cortical sensory activation in dystonia: an fmri study. *Movement disorders*, *18*(6), 673–682.

Campi, K. L., & Krubitzer, L. (2010). Comparative studies of diurnal and nocturnal rodents: differences in lifestyle result in alterations in cortical field size and number. *Journal of Comparative Neurology*, *518*(22), 4491–4512.

Catania, K. C., Leitch, D. B., & Gauthier, D. (2011). A star in the brainstem reveals the first step of cortical magnification. *PloS one*, *6*(7), e22406.

Chen, L. M., Friedman, R. M., & Roe, A. W. (2005). Optical imaging of si topography in anesthetized and awake squirrel monkeys. *Journal of Neuroscience*, *25*(33), 7648–7659.

Cirstea, C. M., Choi, I. Y., Lee, P., Peng, H., Kaufman, C. L., & Frey, S. H. (2017). Magnetic resonance spectroscopy of current hand amputees reveals evidence for neuronal-level changes in former sensorimotor cortex. *J Neurophysiol*, *117*(4), 1821-1830.

Clark, S. A., Allard, T., Jenkins, W. M., & Merzenich, M. M. (1988). Receptive fields in the body-surface map in adult cortex defined by temporally correlated inputs. *Nature*, *332*(6163), 444–445.

Collignon, O., Dormal, G., Albouy, G., Vandewalle, G., Voss, P., Phillips, C., & Lepore, F. (2013). Impact of blindness onset on the functional organization and the connectivity of the occipital cortex. *Brain*, *136*, 2769-2783.

Coq, J.-O., & Xerri, C. (1999). Tactile impoverishment and sensorimotor restriction deteriorate the forepaw cutaneous map in the primary somatosensory cortex of adult rats. *Experimental brain research*, *129*(4), 518–531.

Crawford, J., & Howell, D. (1998). Comparing an individual's test score against norms derived from small samples. *The Clinical Neuropsychologist*, *12*(4), 482-486.

Dale, A. M., Fischl, B., & Sereno, M. I. (1999). Cortical surface-based analysis: I. segmentation and surface reconstruction. *Neuroimage*, *9*(2), 179-194.

DallOrso, S., Steinweg, J., Allievi, A., Edwards, A., Burdet, E., & Arichi, T. (2018). Somatotopic mapping of the developing sensorimotor cortex in the preterm human brain. *Cerebral Cortex*, *28*(7), 2507–2515.

Davis, K. D., Kiss, Z. H. T., Luo, L., Tasker, R. R., Lozano, A. M., & Dostrovsky, J. O. (1998). Phantom sensations generated by thalamic microstimulation. *Nature*, *391*(6665), 385-387.

Dempsey-Jones, H., Harrar, V., Oliver, J., Johansen-Berg, H., Spence, C., & Makin, T. R. (2016). Transfer of tactile perceptual learning to untrained neighboring fingers reflects natural use relationships. *J Neurophysiol*, *115*(3), 1088-97.

Dempsey-Jones, H., Themistocleous, A. C., Carone, D., Ng, T. W. C., Harrar, V., & Makin, T. R. (2019). Blocking tactile input to one finger using anaesthetic

enhances touch perception and learning in other fingers. *J Exp Psychol Gen*, *148*(4), 713-727.

Dempsey-Jones, H., Wesselink, D. B., Friedman, J., & Makin, T. R. (2019). Organized toe maps in extreme foot users. *Cell Reports*, *28*, 19.

Dhillon, G. S., Lawrence, S. M., Hutchinson, D. T., & Horch, K. W. (2004). Residual function in peripheral nerve stumps of amputees: implications for neural control of artificial limbs. *The Journal of hand surgery*, *29*(4), 605–615.

Dhruv, N. T., & Carandini, M. (2014). Cascaded effects of spatial adaptation in the early visual system. *Neuron*, *81*(3), 529–535.

Diedrichsen, J., Provost, S., & Zareamoghaddam, H. (2016). On the distribution of cross-validated mahalanobis distances. *arXiv preprint arXiv:1607.01371*.

Diedrichsen, J., & Shadmehr, R. (2005). Detecting and adjusting for artifacts in fmri time series data. *Neuroimage*, *27*(3), 624-634.

Diedrichsen, J., Wiestler, T., & Krakauer, J. W. (2013). Two distinct ipsilateral cortical representations for individuated finger movements. *Cereb Cortex*, *23*(6), 1362-77.

Diedrichsen, J., Yokoi, A., & Arbuckle, S. A. (2018). Pattern component modeling: A flexible approach for understanding the representational structure of brain activity patterns. *Neuroimage*, *180*(Pt A), 119-133.

Dienes, Z. (2014). Using bayes to get the most out of non-significant results. *Front Psychol*, *5*, 781.

Dilks, D. D., Serences, J. T., Rosenau, B. J., Yantis, S., & McCloskey, M. (2007). Human adult cortical reorganization and consequent visual distortion. *Journal of Neuroscience*, *27*(36), 9585–9594.

Disbrow, E., Litinas, E., Recanzone, G. H., Padberg, J., & Krubitzer, L. (2003). Cortical connections of the second somatosensory area and the parietal ventral area in macaque monkeys. *Journal of Comparative Neurology*, *462*(4), 382–399.

Disbrow, E., Roberts, T., & Krubitzer, L. (2000). Somatotopic organization of cortical fields in the lateral sulcus of homo sapiens: evidence for sii and pv. *Journal of Comparative Neurology*, *418*(1), 1–21.

Dormal, G., Rezk, M., Yakobov, E., Lepore, F., & Collignon, O. (2016). Auditory motion in the sighted and blind: Early visual deprivation triggers a large-scale imbalance between auditory and "visual" brain regions. *Neuroimage*, *134*, 630-644.

Downing, P. E., Jiang, Y., Shuman, M., & Kanwisher, N. (2001). A cortical area selective for visual processing of the human body. *Science*, *293*(5539), 2470-3.

Duda, R. O., Hart, P. E., & Stork, D. G. (2012). *Pattern classification*. John Wiley & Sons.

Dumoulin, S. O., Bittar, R. G., Kabani, N. J., Baker, J., C. L., Le Goualher, G., Bruce Pike, G., & Evans, A. C. (2000). A new anatomical landmark for reliable identification of human area v5/mt: a quantitative analysis of sulcal patterning. *Cereb Cortex*, *10*(5), 454-63.

Dumoulin, S. O., & Wandell, B. A. (2008). Population receptive field estimates in human visual cortex. *Neuroimage*, *39*(2), 647–660.

Ehrsson, H. H., Rosén, B., Stockselius, A., Ragnö, C., Köhler, P., & Lundborg, G. (2008). Upper limb amputees can be induced to experience a rubber hand as their own. *Brain*, *131*(12), 3443–3452.

Ejaz, N., Hamada, M., & Diedrichsen, J. (2015). Hand use predicts the structure of representations in sensorimotor cortex. *Nat Neurosci*, *18*(7), 1034-40.

Ejaz, N., Sadnicka, A., Wiestler, T., Butler, K., Edwards, M., & Diedrichsen, J. (2016). Finger representations in sensorimotor cortex are not disrupted in musicians dystonia. In *Society for neuroscience annual meeting, san diego, usa.*

Elbert, T., Candia, V., Altenmüller, E., Rau, H., Sterr, A., Rockstroh, B., ... Taub, E. (1998). Alteration of digital representations in somatosensory cortex in focal hand dystonia. *Neuroreport*, *9*(16), 3571–3575.

Elbert, T., Pantev, C., Wienbruch, C., Rockstroh, B., & Taub, E. (1995). Increased cortical representation of the fingers of the left hand in string players. *Science*, *270*(5234), 305-7.

Feldman, D. E. (2009). Synaptic mechanisms for plasticity in neocortex. *Annual review of neuroscience*, *32*, 33–55.

Feldman, D. E., & Brecht, M. (2005). Map plasticity in somatosensory cortex. *Science*, *310*(5749), 810-5.

Felleman, D. J., & Van Essen, D. C. (1991). Distributed hierarchical processing in the primate cerebral cortex. *Cereb Cortex*, *1*(1), 1-47.

Filbin, M. T. (2003). Myelin-associated inhibitors of axonal regeneration in the adult mammalian cns. *Nature Reviews Neuroscience*, *4*(9), 703.

Fischl, B., Rajendran, N., Busa, E., Augustinack, J., Hinds, O., Yeo, B. T., ... Zilles, K. (2008). Cortical folding patterns and predicting cytoarchitecture. *Cereb Cortex*, *18*(8), 1973-80.

Flesher, S. N., Collinger, J. L., Foldes, S. T., Weiss, J. M., Downey, J. E., Tyler-kabara, E. C., ... Gaunt, R. (2016). Intracortical microstimulation of human somatosensory cortex intracortical microstimulation of human somatosensory cortex. *Science Translational Medicine*(December), 1-11.

Flor, H., Elbert, T., Knecht, S., Wienbruch, C., Pantev, C., Birbaumer, N., ... Taub, E. (1995). Phantom-limb pain as a perceptual correlate of cortical reorganization following arm amputation. *Nature*, *375*(6531), 482-4.

Flor, H., Nikolajsen, L., & Staehelin Jensen, T. (2006). Phantom limb pain: a case

of maladaptive cns plasticity? *Nat Rev Neurosci*, *7*(11), 873-81.

Fox, K., & Wong, R. O. (2005). A comparison of experience-dependent plasticity in the visual and somatosensory systems. *Neuron*, *48*(3), 465–477.

Frey, S. H., Bogdanov, S., Smith, J. C., Watrous, S., & Breidenbach, W. C. (2008). Chronically deafferented sensory cortex recovers a grossly typical organization after allogenic hand transplantation. *Curr Biol*, *18*(19), 1530-4.

Friedman, J., & Goodman, M. (2016). Can healthy individuals learn to individuate toe movements? a pilot study. *Proceedings of Motor Control 2016 - Bridging motor control and biomechanics*.

Friedman, R. M., Chen, L. M., & Roe, A. W. (2008). Responses of areas 3b and 1 in anesthetized squirrel monkeys to single-and dual-site stimulation of the digits. *Journal of neurophysiology*, *100*(6), 3185–3196.

Friston, K. (2010). The free-energy principle: a unified brain theory? *Nature reviews neuroscience*, *11*(2), 127.

Fulton, J. F., & Dusser de Barenne, J. (1933). The representation of the tail in the motor cortex of primates, with special reference to spider monkeys. *Journal of Cellular & Comparative Physiology*.

Gaglianese, A., Costagli, M., Ueno, K., Ricciardi, E., Bernardi, G., Pietrini, P., & Cheng, K. (2015). The direct, not v1-mediated, functional influence between the thalamus and middle temporal complex in the human brain is modulated by the speed of visual motion. *Neuroscience*, *284*, 833-44.

Gailey, A., Artemiadis, P., & Santello, M. (2017). Proof of concept of an online emg-based decoding of hand postures and individual digit forces for prosthetic hand control. *Frontiers in neurology*, *8*, 7.

Gallivan, J. P. (2014). A motor-oriented organization of human ventral visual cortex? *J Neurosci*, *34*(9), 3119-21.

Garbarini, F., Bisio, A., Biggio, M., Pia, L., & Bove, M. (2018). Motor sequence learning and intermanual transfer with a phantom limb. *Cortex*.

Gindrat, A. D., Chytiris, M., Balerna, M., Rouiller, E. M., & Ghosh, A. (2015). Use-dependent cortical processing from fingertips in touchscreen phone users. *Curr Biol*, *25*(1), 109-16.

Giriyappa, D., Subrahmanyam, R. M., Rangashetty, S., & Sharma, R. (2009). Index finger somatosensory evoked potentials in blind braille readers. *Neurol Neurochir Pol*, *43*(5), 439-45.

Gizewski, E. R., Gasser, T., de Greiff, A., Boehm, A., & Forsting, M. (2003). Cross-modal plasticity for sensory and motor activation patterns in blind subjects. *Neuroimage*, *19*(3), 968-75.

Glasser, M. F., Smith, S. M., Marcus, D. S., Andersson, J. L., Auerbach, E. J., Behrens, T. E., ... Van Essen, D. C. (2016). The human connectome project's

neuroimaging approach. *Nat Neurosci*, *19*(9), 1175-87.

Glazewski, S., Chen, C.-M., Silva, A., & Fox, K. (1996). Requirement for $\alpha$-camkii in experience-dependent plasticity of the barrel cortex. *Science*, *272*(5260), 421–423.

Goense, J., Merkle, H., & Logothetis, N. K. (2012). High-resolution fmri reveals laminar differences in neurovascular coupling between positive and negative bold responses. *Neuron*, *76*(3), 629–639.

Goldreich, D., & Kanics, I. M. (2003). Tactile acuity is enhanced in blindness. *J Neurosci*, *23*(8), 3439-45.

Grant, A. C., Thiagarajah, M. C., & Sathian, K. (2000). Tactile perception in blind braille readers: a psychophysical study of acuity and hyperacuity using gratings and dot patterns. *Percept Psychophys*, *62*(2), 301-12.

Graziano, M. S. (2016). Ethological action maps: a paradigm shift for the motor cortex. *Trends in cognitive sciences*, *20*(2), 121–132.

Graziano, M. S., & Aflalo, T. N. (2007). Mapping behavioral repertoire onto the cortex. *Neuron*, *56*(2), 239-51.

Haak, K. V., Langers, D. R., Renken, R., van Dijk, P., Borgstein, J., & Cornelissen, F. W. (2014). Abnormal visual field maps in human cortex: a mini-review and a case report. *Cortex*, *56*, 14–25.

Haar, S., van Assel, C. M., & Faisal, A. A. (2019). Neurobehavioural signatures of learning that emerge in a real-world motor skill task. *bioRxiv*, 612218.

Hahamy, A., Macdonald, S. N., van den Heiligenberg, F., Kieliba, P., Emir, U., Malach, R., ... Makin, T. R. (2017). Representation of multiple body parts in the missing-hand territory of congenital one-handers. *Curr Biol*, *27*(9), 1350-1355.

Hahamy, A., & Makin, T. R. (2019). Reorganization in cerebral and cerebellar cortices is not restricted by proximity between body-part representations. *bioRxiv*, *439356*.

Hahamy, A., Sotiropoulos, S. N., Henderson Slater, D., Malach, R., Johansen-Berg, H., & Makin, T. R. (2015). Normalisation of brain connectivity through compensatory behaviour, despite congenital hand absence. *eLife*, *4*, 1-12.

Hamilton, R., Keenan, J. P., Catala, M., & Pascual-Leone, A. (2000). Alexia for braille following bilateral occipital stroke in an early blind woman. *Neuroreport*, *11*(2), 237-40.

Harrar, V., Spence, C., & Makin, T. R. (2014). Topographic generalization of tactile perceptual learning. *Journal of experimental psychology. Human perception and performance*, *40*(1), 15-23.

Hashimoto, T., Ueno, K., Ogawa, A., Asamizuya, T., Suzuki, C., Cheng, K., ... Iriki, A. (2013). Hand before foot? cortical somatotopy suggests manual dexterity is

primitive and evolved independently of bipedalism. *Philos Trans R Soc Lond B Biol Sci*, *368*(1630), 20120417.

Heller, M. A. (1989). Texture perception in sighted and blind observers. *Percept Psychophys*, *45*(1), 49-54.

Henderson, W. R., & Smyth, G. E. (1948). Phantom limbs. *Journal of neurology, neurosurgery, and psychiatry*, *11*(2), 88-112.

Hendriks, M. H. A., Daniels, N., Pegado, F., & Op de Beeck, H. P. (2017). The effect of spatial smoothing on representational similarity in a simple motor paradigm. *Front Neurol*, *8*, 222.

Hensch, T. K. (2004). Critical period regulation. *Annu. Rev. Neurosci.*, *27*, 549–579.

Hensch, T. K. (2005). Critical period plasticity in local cortical circuits. *Nature Reviews Neuroscience*, *6*(11), 877.

Hoffmann, M. B., Tolhurst, D. J., Moore, A. T., & Morland, A. B. (2003). Organization of the visual cortex in human albinism. *Journal of Neuroscience*, *23*(26), 8921–8930.

Huber, E., Jiang, F., & Fine, I. (2019). Responses in area hmt+ reflect tuning for both auditory frequency and motion after blindness early in life. *Proc Natl Acad Sci U S A*, *116*(20), 10081-10086.

Huber, L., Finn, E. S., Handwerker, D. A., Boenstrup, M., Glen, D., Kashyap, S., ... others (2019). Sub-millimeter fmri reveals multiple topographical digit representations that form action maps in human motor cortex. *BioRxiv*, 457002.

Huxlin, K. R. (2008). Perceptual plasticity in damaged adult visual systems. *Vision research*, *48*(20), 2154–2166.

Ingram, J. N., Kording, K. P., Howard, I. S., & Wolpert, D. M. (2008). The statistics of natural hand movements. *Experimental Brain Research*, *188*(2), 223-236.

Institute, J. (2009). *The braille literacy crisis in america: Facing the truth, reversing the trend, empowering the blind* (Tech. Rep.). .: National Federation of the Blind.

Jain, N., Qi, H.-X., Collins, C. E., & Kaas, J. H. (2008). Large-scale reorganization in the somatosensory cortex and thalamus after sensory loss in macaque monkeys. *Journal of Neuroscience*, *28*(43), 11042–11060.

Jenkins, W., Merzenich, M. M., & Recanzone, G. H. (1990). Neocortical representational dynamics in adult primates - implications for neuropsychology. *Neuropsychologia*, *28*(6), 573-584.

Jenkins, W. M., Merzenich, M. M., Ochs, M. T., Allard, T., & Guic-Robles, E. (1990). Functional reorganization of primary somatosensory cortex in adult owl monkeys after behaviorally controlled tactile stimulation. *J Neurophysiol*, *63*(1), 82-104.

Jenkinson, M., Bannister, P., Brady, M., & Smith, S. (2002). Improved optimization for the robust and accurate linear registration and motion correction of brain images. *Neuroimage*, *17*(2), 825-41.

Jenkinson, M., Beckmann, C. F., Behrens, T. E. J., Woolrich, M. W., & Smith, S. M. (2012). Fsl. *Neuroimage*, *62*(2), 782-790.

Jones, E. G., & Pons, T. P. (1998). Thalamic and brainstem contributions to large-scale plasticity of primate somatosensory cortex. *Science*, *282*(5391), 1121–1125.

Kaas, J. H. (1993). The functional organization of somatosensory cortex in primates. *Annals of Anatomy-Anatomischer Anzeiger*, *175*(6), 509–518.

Kaas, J. H., Merzenich, M. M., & Killackey, H. P. (1983). The reorganization of somatosensory cortex following peripheral nerve damage in adult and developing mammals. *Annu Rev Neurosci*, *6*, 325-56.

Kaas, J. H., Nelson, R. J., Sur, M., Lin, C.-S., & Merzenich, M. M. (1979). Multiple representations of the body within the primary somatosensory cortex of primates. *Science*, *204*(4392), 521-523.

Kambi, N., Halder, P., Rajan, R., Arora, V., Chand, P., Arora, M., & Jain, N. (2014). Large-scale reorganization of the somatosensory cortex following spinal cord injuries is due to brainstem plasticity. *Nature Communications*, *5*, 1-10.

Kaschube, M., Wolf, F., Geisel, T., & Löwel, S. (2002). Genetic influence on quantitative features of neocortical architecture. *Journal of Neuroscience*, *22*(16), 7206–7217.

Kass, R., & Raftery, A. (1995). Bayes factors. *Journal of the American Statistical Association*, *90*(430), 773-795.

Kelly, C., & Castellanos, F. X. (2014). Strengthening connections: functional connectivity and brain plasticity. *Neuropsychology review*, *24*(1), 63–76.

Kikkert, S., Kolasinski, J., Jbabdi, S., Tracey, I., Beckmann, C. F., Johansen-Berg, H., & Makin, T. R. (2016). Revealing the neural fingerprints of a missing hand. *Elife*, *5*.

Kitada, R., Yoshihara, K., Sasaki, A. T., Hashiguchi, M., Kochiyama, T., & Sadato, N. (2014). The brain network underlying the recognition of hand gestures in the blind: the supramodal role of the extrastriate body area. *J Neurosci*, *34*(30), 10096-108.

Kleinfeld, D., Ahissar, E., & Diamond, M. E. (2006). Active sensation: insights from the rodent vibrissa sensorimotor system. *Current opinion in neurobiology*, *16*(4), 435–444.

Kline, P. (2000). *The handbook of psychological testing (2nd ed.)*. London: Routledge.

Kokotilo, K. J., Eng, J. J., & Curt, A. (2009). Reorganization and preservation of motor control of the brain in spinal cord injury: a systematic review. *J*

*Neurotrauma*, *26*(11), 2113-26.

Kolasinski, J., Makin, T. R., Jbabdi, S., Clare, S., Stagg, C. J., & Johansen-Berg, H. (2016). Investigating the stability of fine-grain digit somatotopy in individual human participants. *J Neurosci*, *36*(4), 1113-27.

Kolasinski, J., Makin, T. R., Logan, J. P., Jbabdi, S., Clare, S., Stagg, C. J., & Johansen-Berg, H. (2016). Perceptually relevant remapping of human somatotopy in 24 hours. *Elife*, *5*.

Kole, K., Scheenen, W., Tiesinga, P., & Celikel, T. (2018). Cellular diversity of the somatosensory cortical map plasticity. *Neuroscience & Biobehavioral Reviews*, *84*, 100–115.

Kontaris, I., Wiggett, A. J., & Downing, P. E. (2009). Dissociation of extrastriate body and biological-motion selective areas by manipulation of visual-motor congruency. *Neuropsychologia*, *47*(14), 3118–3124.

Krakauer, J. W., Ghazanfar, A. A., Gomez-Marin, A., MacIver, M. A., & Poeppel, D. (2017). Neuroscience needs behavior: correcting a reductionist bias. *Neuron*, *93*(3), 480–490.

Krasoulis, A., Vijayakumar, S., & Nazarpour, K. (2018). Continuous versus discrete simultaneous control of prosthetic fingers. In *2018 40th annual international conference of the ieee engineering in medicine and biology society (embc)* (pp. 3774–3777).

Kriegeskorte, N., Mur, M., & Bandettini, P. A. (2008). Representational similarity analysis-connecting the branches of systems neuroscience. *Frontiers in systems neuroscience*, *2*, 4.

Krubitzer, L., Clarey, J., Tweedale, R., Elston, G., & Calford, M. (1995). A redefinition of somatosensory areas in the lateral sulcus of macaque monkeys. *Journal of Neuroscience*, *15*(5), 3821–3839.

Krubitzer, L. A., & Prescott, T. J. (2018). The combinatorial creature: Cortical phenotypes within and across lifetimes. *Trends Neurosci*, *41*(10), 744-762.

Kuehn, E., Haggard, P., Villringer, A., Pleger, B., & Sereno, M. I. (2018). Visually-driven maps in area 3b. *J Neurosci*, *38*(5), 1295-1310.

Kuner, R., & Flor, H. (2017). Structural plasticity and reorganisation in chronic pain. *Nat Rev Neurosci*, *18*(2), 113.

Kupers, R., & Ptito, M. (2014). Compensatory plasticity and cross-modal reorganization following early visual deprivation. *Neurosci Biobehav Rev*, *41*, 36-52.

Kurth, R., Villringer, K., Mackert, B. M., Schwiemann, J., Braun, J., Curio, G., ... Wolf, K. J. (1998). fmri assessment of somatotopy in human brodmann area 3b by electrical finger stimulation. *Neuroreport*, *9*(2), 207-12.

Lara, A. H., Cunningham, J. P., & Churchland, M. M. (2018). Different population dynamics in the supplementary motor area and motor cortex during reaching.

*Nature communications*, *9*(1), 2754.

Law, C.-T., & Gold, J. I. (2008). Neural correlates of perceptual learning in a sensory-motor, but not a sensory, cortical area. *Nature neuroscience*, *11*(4), 505.

Lee, S., Carvell, G. E., & Simons, D. J. (2008). Motor modulation of afferent somatosensory circuits. *Nature neuroscience*, *11*(12), 1430.

Legge, G. E., Madison, C., Vaughn, B. N., Cheong, A. M., & Miller, J. C. (2008). Retention of high tactile acuity throughout the life span in blindness. *Percept Psychophys*, *70*(8), 1471-88.

Levin, N., Dumoulin, S. O., Winawer, J., Dougherty, R. F., & Wandell, B. A. (2010). Cortical maps and white matter tracts following long period of visual deprivation and retinal image restoration. *Neuron*, *65*(1), 21–31.

Liao, C. C., Qi, H. X., Reed, J. L., Miller, D. J., & Kaas, J. H. (2016). Congenital foot deformation alters the topographic organization in the primate somatosensory system. *Brain Struct Funct*, *221*(1), 383-406.

Lipton, M. L., Liszewski, M. C., O'Connell, M. N., Mills, A., Smiley, J. F., Branch, C. A., ... Schroeder, C. E. (2010). Interactions within the hand representation in primary somatosensory cortex of primates. *Journal of Neuroscience*, *30*(47), 15895–15903.

Lissek, S., Wilimzig, C., Stude, P., Pleger, B., Kalisch, T., Maier, C., ... Dinse, H. R. (2009). Immobilization impairs tactile perception and shrinks somatosensory cortical maps. *Curr Biol*, *19*(10), 837-42.

Liu, Y., & Rouiller, E. M. (1999). Mechanisms of recovery of dexterity following unilateral lesion of the sensorimotor cortex in adult monkeys. *Experimental brain research*, *128*(1-2), 149–159.

London, B. M., & Miller, L. E. (2013). Responses of somatosensory area 2 neurons to actively and passively generated limb movements. *Journal of neurophysiology*, *109*(6), 1505-13.

Lundborg, G., & Rosén, B. (2001). Sensory relearning after nerve repair. *The Lancet*, *358*(9284), 809–810.

Lunghi, C., Emir, U. E., Morrone, M. C., & Bridge, H. (2015). Short-term monocular deprivation alters gaba in the adult human visual cortex. *Current Biology*, *25*(11), 1496–1501.

Mahon, B., & Caramazza, A. (2011). What drives the organization of object knowledge in the brain? *Trends Cogn Sci*, *15*(3), 97-103.

Mahon, B. Z., Anzellotti, S., Schwarzbach, J., Zampini, M., & Caramazza, A. (2009). Category-specific organization in the human brain does not require visual experience. *Neuron*, *63*(3), 397-405.

Maidenbaum, S., Abboud, S., & Amedi, A. (2014). Sensory substitution: closing

the gap between basic research and widespread practical visual rehabilitation. *Neurosci Biobehav Rev*, *41*, 3-15.

Makin, T. R., & Bensmaia, S. J. (2017). Stability of sensory topographies in adult cortex. *Trends in Cognitive Sciences*.

Makin, T. R., Cramer, A. O., Scholz, J., Hahamy, A., Slater, D. H., Tracey, I., & Johansen-Berg, H. (2013). Deprivation-related and use-dependent plasticity go hand in hand. *Elife*, *2*, e01273-e01273.

Makin, T. R., Scholz, J., Filippini, N., Slater, D. H., Tracey, I., & Johansen-Berg, H. (2013). Phantom pain is associated with preserved structure and function in the former hand area. *Nature communications*, *4*, 1570-1570.

Makin, T. R., Scholz, J., Henderson Slater, D., Johansen-Berg, H., & Tracey, I. (2015). Reassessing cortical reorganization in the primary sensorimotor cortex following arm amputation. *Brain*, *138*(8), 2140-2146.

Matteau, I., Kupers, R., Ricciardi, E., Pietrini, P., & Ptito, M. (2010). Beyond visual, aural and haptic movement perception: hmt+ is activated by electrotactile motion stimulation of the tongue in sighted and in congenitally blind individuals. *Brain Res Bull*, *82*(5-6), 264-70.

Mattioni, S., Rezk, M., Battal, C., Bottini, R., Mendoza, K. E. C., Oosterhof, N. N., & Collignon, O. (2019). Similar categorical representation from sound and sight in the occipito-temporal cortex of sighted and blind. *bioRxiv*, 719690.

Mehring, C., Akselrod, M., Bashford, L., Mace, M., Choi, H., Blüher, M., ... others (2019). Augmented manipulation ability in humans with six-fingered hands. *Nature communications*, *10*(1), 2401.

Merabet, L. B., & Pascual-Leone, A. (2010). Neural reorganization following sensory loss: the opportunity of change. *Nat Rev Neurosci*, *11*(1), 44-52.

Mercier, C., Reilly, K. T., Vargas, C. D., Aballea, A., & Sirigu, A. (2006). Mapping phantom movement representations in the motor cortex of amputees. *Brain*, *129*(8), 2202-2210.

Merzenich, M. M., Kaas, J. H., Wall, J., Nelson, R. J., Sur, M., & Felleman, D. (1983). Topographic reorganization of somatosensory cortical areas 3b and 1 in adult monkeys following restricted deafferentation. *Neuroscience*, *8*(1), 33-55.

Merzenich, M. M., Nelson, R. J., Stryker, M. P., Cynader, M. S., Schoppmann, A., & Zook, J. M. (1984). Somatosensory cortical map changes following digit amputation in adult monkeys. *Journal of Comparative Neurology*, *224*(4), 591-605.

Meyer, G. (1987). Forms and spatial arrangement of neurons in the primary motor cortex of man. *Journal of Comparative Neurology*, *262*(3), 402–428.

Michel, G. F., Campbell, J. M., Marcinowski, E. C., Nelson, E. L., & Babik, I. (2016). Infant hand preference and the development of cognitive abilities. *Front*

*Psychol*, *7*, 410.

Mitchell, K. J. (2018). *Innate: How the wiring of our brains shapes who we are.* Princeton University Press.

Miyashita-Lin, E. M., Hevner, R., Wassarman, K. M., Martinez, S., & Rubenstein, J. L. R. (1999). Early neocortical regionalization in the absence of thalamic innervation. *Science*, *285*(5429), 906-909.

Moeller, S., Yacoub, E., Olman, C. A., Auerbach, E., Strupp, J., Harel, N., & Uğurbil, K. (2010). Multiband multislice ge-epi at 7 tesla, with 16-fold acceleration using partial parallel imaging with application to high spatial and temporal whole-brain fmri. *Magnetic resonance in medicine*, *63*(5), 1144–1153.

Mogilner, A., Grossman, J. A., Ribary, U., Joliot, M., Volkmann, J., Rapaport, D., ... Llinas, R. R. (1993). Somatosensory cortical plasticity in adult humans revealed by magnetoencephalography. *Proc Natl Acad Sci U S A*, *90*(8), 3593-7.

Muckli, L., Naumer, M. J., & Singer, W. (2009). Bilateral visual field maps in a patient with only one hemisphere. *Proceedings of the National Academy of Sciences*, *106*(31), 13034–13039.

Nakamura, A., Yamada, T., Goto, A., Kato, T., Ito, K., Abe, Y., ... Kakigi, R. (1998). Somatosensory homunculus as drawn by meg. *Neuroimage*, *7*(4), 377–386.

Nelson, R. J., Sur, M., Felleman, D. J., & Kaas, J. H. (1980). Representations of the body surface in postcentral parietal cortex of macaca fascicularis. *J Comp Neurol*, *192*(4), 611-43.

Nijboer, T. C., Buma, F. E., Winters, C., Vansteensel, M. J., Kwakkel, G., Ramsey, N. F., & Raemaekers, M. (2017). No changes in functional connectivity during motor recovery beyond 5 weeks after stroke; a longitudinal resting-state fmri study. *PloS one*, *12*(6), e0178017.

Nili, H., Wingfield, C., Walther, A., Su, L., Marslen-Wilson, W., & Kriegeskorte, N. (2014). A toolbox for representational similarity analysis. *PLoS computational biology*, *10*(4), e1003553-e1003553.

Norman, J. F., & Bartholomew, A. N. (2011). Blindness enhances tactile acuity and haptic 3-d shape discrimination. *Atten Percept Psychophys*, *73*(7), 2323-31.

Ogawa, K., Mitsui, K., Imai, F., & Nishida, S. (2019). Long-term training-dependent representation of individual finger movements in the primary motor cortex. *Neuroimage*, 116051.

Ojemann, J. O., & Silbergeld, D. L. (1995). Cortical stimulation mapping of phantom limb rolandic cortex: case report. *Journal of neurosurgery*, *82*(4), 641–644.

Oldfield, R. C., et al. (1971). The assessment and analysis of handedness: the edinburgh inventory. *Neuropsychologia*, *9*(1), 97–113.

Orlov, T., Makin, T. R., & Zohary, E. (2010). Topographic representation of the

human body in the occipitotemporal cortex. *Neuron*, *68*(3), 586-600.

Ostry, D. J., Darainy, M., Mattar, A. A., Wong, J., & Gribble, P. L. (2010). Somatosensory plasticity and motor learning. *Journal of Neuroscience*, *30*(15), 5384–5393.

Overduin, S. A., d'Avella, A., Carmena, J. M., & Bizzi, E. (2012). Microstimulation activates a handful of muscle synergies. *Neuron*, *76*(6), 1071-7.

Pascual-Leone, A., Cammarota, A., Wassermann, E. M., Brasil-Neto, J. P., Cohen, L. G., & Hallett, M. (1993). Modulation of motor cortical outputs to the reading hand of braille readers. *Ann Neurol*, *34*(1), 33-7.

Pascual-Leone, A., & Hamilton, R. (2001). The metamodal organization of the brain. *Prog Brain Res*, *134*, 427-45.

Pascual-Leone, A., & Torres, F. (1993). Plasticity of the sensorimotor cortex representation of the reading finger in braille readers. *Brain*, *116 ( Pt 1)*, 39-52.

Pascual-Leone, A., Wassermann, E. M., Sadato, N., & Hallett, M. (1995). The role of reading activity on the modulation of motor cortical outputs to the reading hand in braille readers. *Ann Neurol*, *38*(6), 910-5.

Peelen, M. V., Bracci, S., Lu, X., He, C., Caramazza, A., & Bi, Y. (2013). Tool selectivity in left occipitotemporal cortex develops without vision. *J Cogn Neurosci*, *25*(8), 1225-34.

Peelen, M. V., & Downing, P. E. (2005). Is the extrastriate body area involved in motor actions? *Nat Neurosci*, *8*(2), 125; author reply 125-6.

Penfield, W., & Boldrey, E. (1937). Somatic motor and sensory representation in the cerebral cortex of man as studied by electrical stimulation. *Brain*, *60*(4), 389–443.

Penfield, W., & Rasmussen, T. (1950). *The cerebral cortex of man; a clinical study of localization of function*. Macmillan.

Philip, B. A., & Frey, S. H. (2014). Compensatory changes accompanying chronic forced use of the nondominant hand by unilateral amputees. *Journal of Neuroscience*, *34*(10), 3622-3631.

Pleger, B., Foerster, A. F., Ragert, P., Dinse, H. R., Schwenkreis, P., Malin, J. P., ... Tegenthoff, M. (2003). Functional imaging of perceptual learning in human primary and secondary somatosensory cortex. *Neuron*, *40*(3), 643-53.

Poirier, C., Collignon, O., Devolder, A. G., Renier, L., Vanlierde, A., Tranduy, D., & Scheiber, C. (2005). Specific activation of the v5 brain area by auditory motion processing: an fmri study. *Brain Res Cogn Brain Res*, *25*(3), 650-8.

Polley, D. B., Kvašňák, E., & Frostig, R. D. (2004). Naturalistic experience transforms sensory maps in the adult cortex of caged animals. *Nature*, *429*(6987), 67.

Pons, T. P., Garraghty, P. E., Ommaya, A. K., Kaas, J. H., Taub, E., & Mishkin, M.

(1991). Massive cortical reorganization after sensory deafferentation in adult macaques. *Science*, *252*(5014), 1857-60.

Puckett, A. M., Bollmann, S., Barth, M., & Cunnington, R. (2017). Measuring the effects of attention to individual fingertips in somatosensory cortex using ultra-high field (7t) fmri. *Neuroimage*, *161*, 179-187.

Raffin, E., Giraux, P., & Reilly, K. T. (2012). The moving phantom: motor execution or motor imagery? *Cortex*, *48*(6), 746-757.

Raffin, E., Mattout, J., Reilly, K. T., & Giraux, P. (2012). Disentangling motor execution from motor imagery with the phantom limb. *Brain*, 582-595.

Raffin, E., Pellegrino, G., Di Lazzaro, V., Thielscher, A., & Siebner, H. R. (2015). Bringing transcranial mapping into shape: sulcus-aligned mapping captures motor somatotopy in human primary motor hand area. *Neuroimage*, *120*, 164–175.

Raffin, E., Richard, N., Giraux, P., & Reilly, K. T. (2016). Primary motor cortex changes after amputation correlate with phantom limb pain and the ability to move the phantom limb. *NeuroImage*, 1-11.

Rathelot, J.-A., Dum, R. P., & Strick, P. L. (2017). Posterior parietal cortex contains a command apparatus for hand movements. *Proceedings of the National Academy of Sciences*, *114*(16), 4255–4260.

Rauschecker, J. P., Tian, B., Korte, M., & Egert, U. (1992). Crossmodal changes in the somatosensory vibrissa/barrel system of visually deprived animals. *Proc Natl Acad Sci U S A*, *89*(11), 5063-7.

Recanzone, G. H., Merzenich, M. M., & Jenkins, W. M. (1992). Frequency discrimination training engaging a restricted skin surface results in an emergence of a cutaneous response zone in cortical area 3a. *J Neurophysiol*, *67*(5), 1057-70.

Recanzone, G. H., Merzenich, M. M., Jenkins, W. M., Grajski, K. A., & Dinse, H. R. (1992). Topographic reorganization of the hand representation in cortical area 3b owl monkeys trained in a frequency-discrimination task. *J Neurophysiol*, *67*(5), 1031-56.

Reed, J. L., Pouget, P., Qi, H.-X., Zhou, Z., Bernard, M. R., Burish, M. J., ... Kaas, J. H. (2008). Widespread spatial integration in primary somatosensory cortex. *Proceedings of the National Academy of Sciences*, *105*(29), 10233–10237.

Reilly, K. T., Mercier, C., Schieber, M. H., & Sirigu, A. (2006). Persistent hand motor commands in the amputees brain. *Brain*, *129*(8), 2211-2223.

Reitsma, D. C., Mathis, J., Ulmer, J. L., Mueller, W., Maciejewski, M. J., & DeYoe, E. A. (2013). Atypical retinotopic organization of visual cortex in patients with central brain damage: congenital and adult onset. *Journal of Neuroscience*, *33*(32), 13010–13024.

Ricciardi, E., Bonino, D., Pellegrini, S., & Pietrini, P. (2014). Mind the blind

brain to understand the sighted one! is there a supramodal cortical functional architecture? *Neurosci Biobehav Rev*, *41*, 64-77.

Romo, R., & Salinas, E. (2001). Touch and go: decision-making mechanisms in somatosensation. *Annu Rev Neurosci*, *24*, 107-37.

Rubenstein, J. L. R., Anderson, S., Shi, L., Miyashita-Lin, E., Bulfone, A., & Hevner, R. (1999). Genetic control of cortical regionalization and connectivity. *Cerebral Cortex*, *9*(6), 524-532.

Ruiz, S., Crespo, P., & Romo, R. (1995). Representation of moving tactile stimuli in the somatic sensory cortex of awake monkeys. *Journal of neurophysiology*, *73*(2), 525–537.

Sadato, N., Okada, T., Kubota, K., & Yonekura, Y. (2004). Tactile discrimination activates the visual cortex of the recently blind naive to braille: a functional magnetic resonance imaging study in humans. *Neurosci Lett*, *359*(1-2), 49-52.

Sadato, N., Pascual-Leone, A., Grafman, J., Ibanez, V., Deiber, M. P., Dold, G., & Hallett, M. (1996). Activation of the primary visual cortex by braille reading in blind subjects. *Nature*, *380*(6574), 526-8.

Sanchez-Panchuelo, R. M., Besle, J., Beckett, A., Bowtell, R., Schluppeck, D., & Francis, S. (2012a). Within-digit functional parcellation of brodmann areas of the human primary somatosensory cortex using functional magnetic resonance imaging at 7 tesla. *J Neurosci*, *32*(45), 15815-22.

Sanchez-Panchuelo, R. M., Besle, J., Beckett, A., Bowtell, R., Schluppeck, D., & Francis, S. (2012b). Within-digit functional parcellation of brodmann areas of the human primary somatosensory cortex using functional magnetic resonance imaging at 7 tesla. *Journal of Neuroscience*, *32*(45), 15815–15822.

Sanchez-Panchuelo, R. M., Francis, S., Bowtell, R., & Schluppeck, D. (2010). Mapping human somatosensory cortex in individual subjects with 7t functional mri. *J Neurophysiol*, *103*(5), 2544-56.

Sanders, Z.-B., Wesselink, D. B., Dempsey-Jones, H., & Makin, T. R. (2019). Similar somatotopy for active and passive digit representation in primary somatosensory cortex. *bioRxiv*.

Sathian, K., Deshpande, G., & Stilla, R. (2013). Neural changes with tactile learning reflect decision-level reweighting of perceptual readout. *J Neurosci*, *33*(12), 5387-98.

Sathian, K., & Stilla, R. (2010). Cross-modal plasticity of tactile perception in blindness. *Restor Neurol Neurosci*, *28*(2), 271-81.

Schellekens, W., Petridou, N., & Ramsey, N. F. (2018). Detailed somatotopy in primary motor and somatosensory cortex revealed by gaussian population receptive fields. *Neuroimage*, *179*, 337–347.

Schieber, M. H., & Hibbard, L. S. (1993). How somatotopic is the motor cortex hand

area? *Science*, *261*(5120), 489–492.

Serino, A., Akselrod, M., Salomon, R., Martuzzi, R., Blefari, M. L., Canzoneri, E., ... Blanke, O. (2017). Upper limb cortical maps in amputees with targeted muscle and sensory reinnervation. *Brain*, *140*(11), 2993-3011.

Shatz, C. J., & Stryker, M. P. (1978). Ocular dominance in layer iv of the cat's visual cortex and the effects of monocular deprivation. *The Journal of physiology*, *281*(1), 267–283.

Shenoy, K. V., Sahani, M., & Churchland, M. M. (2013). Cortical control of arm movements: a dynamical systems perspective. *Annual review of neuroscience*, *36*, 337–359.

Shiell, M. M. (2014). Tonotopic organization of v5/mt+ in congenital anopthalmia: implications for auditory motion processing and metamodal cross-modal reorganization. *J Neurosci*, *34*(11), 3807-9.

Sirigu, A., Duhamel, J.-R., Cohen, L., Pillon, B., Dubois, B., & Agid, Y. (1996). The mental representation of hand movements after parietal cortex damage. *Science*, *273*(5281), 1564–1568.

Smirnakis, S. M., Brewer, A. A., Schmid, M. C., Tolias, A. S., Schüz, A., Augath, M., ... Logothetis, N. K. (2005). Lack of long-term cortical reorganization after macaque retinal lesions. *Nature*, *435*(7040), 300.

Smith, S. M. (2002). Fast robust automated brain extraction. *Hum Brain Mapp*, *17*(3), 143-55.

Smith, S. M., Jenkinson, M., Woolrich, M. W., Beckmann, C. F., Behrens, T. E. J., Johansen-Berg, H., ... Matthews, P. M. (2004). Advances in functional and structural mr image analysis and implementation as fsl. *Neuroimage*, *23*, S208-S219.

Song, W., & Semework, M. (2015). Tactile representation in somatosensory thalamus (vpl) and cortex (s1) of awake primate and the plasticity induced by vpl neuroprosthetic stimulation. *Brain research*, *1625*, 301–313.

Stagg, C., Bestmann, S., Constantinescu, A., Moreno Moreno, L., Allman, C., Mekle, R., ... Rothwell, J. (2011). Relationship between physiological measures of excitability and levels of glutamate and gaba in the human motor cortex. *The Journal of physiology*, *589*(23), 5845–5855.

Steenhuis, R. E. (1999). The relation between hand preference and hand performance: what you get depends on what you measure. *Laterality*, *4*(1), 3-26.

Sterr, A., Muller, M. M., Elbert, T., Rockstroh, B., Pantev, C., & Taub, E. (1998). Perceptual correlates of changes in cortical representation of fingers in blind multifinger braille readers. *J Neurosci*, *18*(11), 4417-23.

Stilla, R., Deshpande, G., LaConte, S., Hu, X., & Sathian, K. (2007). Posteromedial parietal cortical activity and inputs predict tactile spatial acuity. *J Neurosci*,

*27*(41), 11091-102.

Stoeckel, M. C., Pollok, B., Schnitzler, A., Witte, O. W., & Seitz, R. J. (2004). Use-dependent cortical plasticity in thalidomide-induced upper extremity dysplasia: evidence from somaesthesia and neuroimaging. *Exp Brain Res*, *156*(3), 333-41.

Stoeckel, M. C., Seitz, R. J., & Buetefisch, C. M. (2009). Congenitally altered motor experience alters somatotopic organization of human primary motor cortex. *Proc Natl Acad Sci U S A*, *106*(7), 2395-400.

Striem-Amit, E., & Amedi, A. (2014). Visual cortex extrastriate body-selective area activation in congenitally blind people "seeing" by using sounds. *Curr Biol*, *24*(6), 687-92.

Striem-Amit, E., Cohen, L., Dehaene, S., & Amedi, A. (2012). Reading with sounds: sensory substitution selectively activates the visual word form area in the blind. *Neuron*, *76*(3), 640-52.

Striem-Amit, E., Ovadia-Caro, S., Caramazza, A., Margulies, D. S., Villringer, A., & Amedi, A. (2015). Functional connectivity of visual cortex in the blind follows retinotopic organization principles. *Brain*, *138*(Pt 6), 1679-95.

Striem-Amit, E., Vannuscorps, G., & Caramazza, A. (2018a). Limitations of compensatory plasticity: the organization of the primary sensorimotor cortex in foot-using bilateral upper limb dysplasics. *bioRxiv*, 190462.

Striem-Amit, E., Vannuscorps, G., & Caramazza, A. (2018b). Plasticity based on compensatory effector use in the association but not primary sensorimotor cortex of people born without hands. *Proceedings of the National Academy of Sciences*, *115*(30), 7801–7806.

Sur, M., Merzenich, M. M., & Kaas, J. H. (1980). Magnification, receptive-field area, and" hypercolumn" size in areas 3b and 1 of somatosensory cortex in owl monkeys. *Journal of neurophysiology*, *44*(2), 295–311.

Tan, D. W., Schiefer, M. A., Keith, M. W., Anderson, J. R., Tyler, J., & Tyler, D. J. (2014). A neural interface provides long-term stable natural touch perception. *Science translational medicine*, *6*(257), 257ra138–257ra138.

Thakur, P. H., Fitzgerald, P. J., & Hsiao, S. S. (2012). Second-order receptive fields reveal multidigit interactions in area 3b of the macaque monkey. *Journal of Neurophysiology*, *108*(1), 243-262.

Thompson, B. (1995). Exploring the replicability of a study's results: Bootstrap statistics for the multivariate case. *Educational Psychological Measurement*, *55*(1), 84-94.

Thomson, A. M., & Bannister, A. P. (2003). Interlaminar connections in the neocortex. *Cerebral cortex*, *13*(1), 5–14.

Toldi, J., Farkas, T., & Volgyi, B. (1994). Neonatal enucleation induces cross-modal changes in the barrel cortex of rat. a behavioural and electrophysiological study.

*Neurosci Lett*, *167*(1-2), 1-4.

Tommerdahl, M., Favorov, O. V., & Whitsel, B. L. (2010). Dynamic representations of the somatosensory cortex. *Neuroscience & Biobehavioral Reviews*, *34*(2), 160–170.

Van Boven, R. W., Hamilton, R. H., Kauffman, T., Keenan, J. P., & Pascual-Leone, A. (2000). Tactile spatial resolution in blind braille readers. *Neurology*, *54*(12), 2230-6.

van den Heiligenberg, F. M. Z., Yeung, N., Brugger, P., Culham, J. C., & Makin, T. R. (2017). Adaptable categorization of hands and tools in prosthesis users. *Psychological science*, *28*(3), 395-398.

Van der Loos, H., & Woolsey, T. A. (1973). Somatosensory cortex: structural alterations following early injury to sense organs. *Science*, *179*(4071), 395–398.

van der Zwaag, W., Kusters, R., Magill, A., Gruetter, R., Martuzzi, R., Blanke, O., & Marques, J. P. (2013). Digit somatotopy in the human cerebellum: a 7t fmri study. *Neuroimage*, *67*, 354-62.

Vaso, A., Adahan, H. M., Gjika, A., Zahaj, S., Zhurda, T., Vyshka, G., & Devor, M. (2014). Peripheral nervous system origin of phantom limb pain. *Pain*, *155*(7), 1384-91.

Vaughan, J. T., Garwood, M., Collins, C., Liu, W., DelaBarre, L., Adriany, G., ... others (2001). 7t vs. 4t: Rf power, homogeneity, and signal-to-noise comparison in head images. *Magnetic Resonance in Medicine: An Official Journal of the International Society for Magnetic Resonance in Medicine*, *46*(1), 24–30.

Vidyasagar, R., Folger, S. E., & Parkes, L. M. (2014). Re-wiring the brain: increased functional connectivity within primary somatosensory cortex following synchronous co-activation. *Neuroimage*, *92*, 19-26.

Wallace, H., Glazewski, S., Liming, K., & Fox, K. (2001). The role of cortical activity in experience-dependent potentiation and depression of sensory responses in rat barrel cortex. *Journal of Neuroscience*, *21*(11), 3881–3894.

Walther, A., Nili, H., Ejaz, N., Alink, A., Kriegeskorte, N., & Diedrichsen, J. (2016). Reliability of dissimilarity measures for multi-voxel pattern analysis. *Neuroimage*, *137*, 188-200.

Wandell, B. A., & Smirnakis, S. M. (2009). Plasticity and stability of visual field maps in adult primary visual cortex. *Nature Reviews Neuroscience*, *10*(12), 873.

Wang, L., Uhrig, L., Jarraya, B., & Dehaene, S. (2015). Representation of numerical and sequential patterns in macaque and human brains. *Current Biology*, *25*(15), 1966–1974.

Wang, X., Merzenich, M. M., Sameshima, K., & Jenkins, W. M. (1995). Remodelling of hand representation in adult cortex determined by timing of tactile

stimulation. *Nature*, *378*(6552), 71-75.

Watkins, K. E., Shakespeare, T. J., O'Donoghue, M. C., Alexander, I., Ragge, N., Cowey, A., & Bridge, H. (2013). Early auditory processing in area v5/mt+ of the congenitally blind brain. *J Neurosci*, *33*(46), 18242-6.

Wesselink, D., Kikkert, S., Bridge, H., & Makin, T. R. (2018). Sensorimotor finger-specific information in the cortex of the congenitally blind. *Journal of Vision*, *18*(10), 1.

Wesselink, D. B., van den Heiligenberg, F. M., Ejaz, N., Dempsey-Jones, H., Cardinali, L., Tarall-Jozwiak, A., ... Makin, T. R. (2019). Obtaining and maintaining cortical hand representation as evidenced from acquired and congenital handlessness. *Elife*, *8*.

Wetzels, R., Matzke, D., Lee, M. D., Rouder, J. N., Iverson, G. J., & Wagenmakers, E. J. (2011). Statistical evidence in experimental psychology: An empirical comparison using 855 t tests. *Perspect Psychol Sci*, *6*(3), 291-8.

White, L. E., Andrews, T. J., Hulette, C., Richards, A., Groelle, M., Paydarfar, J., & Purves, D. (1997). Structure of the human sensorimotor system. ii: Lateral symmetry. *Cereb Cortex*, *7*(1), 31-47.

Wiesel, T. N., & Hubel, D. H. (1963). Single-cell responses in striate cortex of kittens deprived of vision in one eye. *Journal of neurophysiology*, *26*(6), 1003–1017.

Wiesel, T. N., & Hubel, D. H. (1965a). Comparison of the effects of unilateral and bilateral eye closure on cortical unit responses in kittens. *J Neurophysiol*, *28*(6), 1029-40.

Wiesel, T. N., & Hubel, D. H. (1965b). Extent of recovery from the effects of visual deprivation in kittens. *J Neurophysiol*, *28*(6), 1060-72.

Wiestler, T., & Diedrichsen, J. (2013). Skill learning strengthens cortical representations of motor sequences. *Elife*, *2*, e00801-e00801.

Wiestler, T., McGonigle, D. J., & Diedrichsen, J. (2011). Integration of sensory and motor representations of single fingers in the human cerebellum. *Journal of neurophysiology*, *105*(6), 3042–3053.

Wolbers, T., Klatzky, R. L., Loomis, J. M., Wutte, M. G., & Giudice, N. A. (2011). Modality-independent coding of spatial layout in the human brain. *Curr Biol*, *21*(11), 984-9.

Wolpert, D. M., & Ghahramani, Z. (2000). Computational principles of movement neuroscience. *Nature neuroscience*, *3*(11s), 1212.

Wong, M., Gnanakumaran, V., & Goldreich, D. (2011). Tactile spatial acuity enhancement in blindness: evidence for experience-dependent mechanisms. *J Neurosci*, *31*(19), 7028-37.

Xerri, C., Merzenich, M. M., Jenkins, W., & Santucci, S. (1999). Representational plasticity in cortical area 3b paralleling tactual-motor skill acquisition in adult

monkeys. *Cerebral cortex*, *9*(3), 264–276.

Yinon, U., Shemesh, R., Arda, H., Dobin, G., & Jaros, P. (1993). Physiological studies in deafferented visual cortex cells of cats following transplantation of fetal xenografts from the rat's cortex. *Experimental neurology*, *122*(2), 335–341.

Yousry, T. A., Schmid, U. D., Alkadhi, H., Schmidt, D., Peraud, A., Buettner, A., & Winkler, P. (1997). Localization of the motor hand area to a knob on the precentral gyrus. a new landmark. *Brain*, *120 ( Pt 1)*, 141-57.

Yu, X., He, H. J., Zhang, Q. W., Zhao, F., Zee, C. S., Zhang, S. Z., & Gong, X. Y. (2014). Somatotopic reorganization of hand representation in bilateral arm amputees with or without special foot movement skill. *Brain Res*, *1546*, 9-17.

Yu, X., Zhang, S., Liu, H., & Chen, Y. (2006). The activation of the cortical hand area by toe tapping in two bilateral upper-extremities amputees with extraordinary foot movement skill. *Magn Reson Imaging*, *24*(1), 45-50.

Yu, Y., Huber, L., Yang, J., Jangraw, D. C., Handwerker, D. A., Molfese, P. J., ... Bandettini, P. A. (2019). Layer-specific activation of sensory input and predictive feedback in the human primary somatosensory cortex. *Science advances*, *5*(5), eaav9053.

Zangaladze, A., Epstein, C. M., Grafton, S. T., & Sathian, K. (1999). Involvement of visual cortex in tactile discrimination of orientation. *Nature*, *401*(6753), 587-90.

Zangenehpour, S., & Zatorre, R. J. (2010). Crossmodal recruitment of primary visual cortex following brief exposure to bimodal audiovisual stimuli. *Neuropsychologia*, *48*(2), 591-600.

Zeharia, N., Hertz, U., Flash, T., & Amedi, A. (2015). New whole-body sensory-motor gradients revealed using phase-locked analysis and verified using multivoxel pattern analysis and functional connectivity. *J Neurosci*, *35*(7), 2845-59.

Zeharia, N., Hofstetter, S., Flash, T., & Amedi, A. (2019). A whole-body sensory-motor gradient is revealed in the medial wall of the parietal lobe. *Journal of Neuroscience*, *39*(40), 7882–7892.

Zeiler, S. R., Hubbard, R., Gibson, E. M., Zheng, T., Ng, K., OBrien, R., & Krakauer, J. W. (2016). Paradoxical motor recovery from a first stroke after induction of a second stroke: reopening a postischemic sensitive period. *Neurorehabilitation and neural repair*, *30*(8), 794–800.

Zuiderbaan, W., Harvey, B. M., & Dumoulin, S. O. (2012). Modeling center–surround configurations in population receptive fields using fmri. *Journal of vision*, *12*(3), 10–10.